Microscopic modeling of Personal Mobility Devices (PMDs), in mixed traffic and share space conditions

Yeltsin Valero Camarena

Université Gustave Eiffel

Modélisation microscopique des engins de déplacement personnel (EDP), dans des conditions de trafic mixte et d'espaces partagés.

Thèse de doctorat de l'Université Gustave Eiffel

Ecole doctorale Ville, Transports et Territoires (VTT) Spécialité de doctorat: Transport
Unité de recherche : COSYS/GRETTIA

Thèse présentée et soutenue à l'Université Gustave Eiffel, le xx/xx/2023, par :

Yeltsin VALERO

Composition du Jury:

Directrise	Mme. Zoi CHRISTOFOROU	University of Patras
Co-Directeur	M. Nadir Farhi	Gustave Eiffel University
Rapporteur	M. George YANNIS	National Technical University of Athens
Rapporteur	Mme. Amalia POLYDOROPOULOU	University of the Aegean
Examinateur	M. Pierre Argoul	Gustave Eiffel University
Examinateur	M. Rosaldo ROSSETTI	University of Porto

Acknowledgment

I would like to express my sincere gratitude to each of you for your unwavering support and guidance throughout my doctoral journey. Your wisdom, encouragement and guidance helped me overcome many obstacles and enabled me to successfully complete my thesis.

I am deeply grateful to Zoi CHRISTOFOROU, for your mentorship and for taking the time to guide me through every step of my research. Your invaluable insights and expertise helped me to develop a stronger understanding of my field, and I am forever grateful for your unwavering support, your patient in helping me find the errors in my work and correcting them.

Nadir FARHI, thank you for your help that you gave me in order finish my work and for your valuable contributions to my research. Your expertise and guidance were instrumental in helping me to achieve my goals.

I would also like to express my gratitude to the reviewers who agreed to evaluate my thesis, Professor George YANNIS, Amalia POLYDOROPOULOU, Pierre ARGOUL and Rosaldo ROSETTI.

Jean-Patrick LEBACQUE, Regine SEIDOWSKY, Latifa OUKHELLOU and Mahdi ZARGAYOUNA; I am also grateful for your support and for providing me with the resources I needed to complete my thesis. Your commitment to excellence has been an inspiration to me, and I am proud to have worked under your leadership.

I want to extend my heartfelt thanks to my parents for their unwavering love, support, and encouragement throughout my life. Your belief in me has given me the strength to pursue my dreams, and I am forever grateful for the sacrifices you have made on my behalf.

Thank you again for your support and guidance. I am proud to have had the opportunity to work with each of you, and I will never forget the lessons I have learned along the way.

This project was supported by Eiffage and ISITE in the framework of the E3S project https://www.programme-e3s.com/en/. Its contents are solely the responsibility of the author and do not necessarily represent the official views of the Eiffage. The project was also supported by La Fondation Maif. The author would like to particularly thank Mr. Marc Rigolot.

Sincerely,

Yeltsin VALERO

”To my mother Epifania, my father Teodoro,
To my family”

Abstract

PhD thesis on microscopic modeling of Personal Mobility Devices (PMDs) under mixed traffic and share space conditions is proposed in the context of the implementation of an eco-district LaVallée in Châtenay-Malabry, Île de France, France. LaVallée is an eco-district where the implementation of micromobility services will generate spaces where vehicles, pedestrians and PMDs can interact with each other. In order to ensure harmony and road security among the different users of the eco-district, the interactions of the different users are studied at a microscopic level in this thesis. The first chapter includes a comprehensive review of the existing literature review with emphasis on microscopic-level traffic simulation models of pedestrians, bicycles and cars. Both classical traffic models such as the Social Force Model (SFM) for pedestrians and the Car Following Model (CFM) for cars, as well as recent machine learning models such as the use of neural networks for microscopic traffic simulation. The second chapter focuses on the database, where the data was collected, and the development of a software based on advanced computer vision techniques (µ-scope) and which has been the subject of previous research. The methodology of data collection was thoroughly explained, and the locations where the data was collected were identified. In the third chapter, a process of calibrating existing traffic models is performed. Calibration allows to determine the parameters corresponding to the PMDs for both the SFM and the CFM, and therefore to make the first conclusions on the hybrid behavior of the PMDs. In view of the low performance of the existing models in Chapter 4, two new models based on Long-Short Term Memory (LSTM) recurrent deep neural networks are proposed. These models aim to improve the accuracy of traffic simulation by incorporating advanced machine learning techniques. The results of the simulation and the effectiveness of the proposed models are discussed and evaluated. The overall aim of the thesis is to advance the understanding of traffic behavior of PMDs and to contribute to the development of more effective traffic management under mixed traffic conditions.

It is important to emphasize that this thesis includes a large part of informatics development, code development and algorithms that are accessible through the following link https://github.com/yeltsinvc/THESIS_DOCTORAT and µ-scope software developed during this thesis https://github.com/yeltsinvc/THESIS_DOCTORAT/tree/main/u-scope_sofware.

Keywords: Microscopic traffic simulation, Personal Mobility Devices, Shared space, Mixed Traffic, Long-Short Term Memory, Computer vision data collection.

Résumé

La thèse de doctorat sur la Modélisation microscopique des engins de déplacement personnel (EDP), dans des conditions de trafic mixte et d'espaces partagés est proposée dans le contexte de la mise en place d'un éco-quartier LaVallée à Châtenay-Malabry, Île de France, France. LaVallée est un éco-quartier où la mise en place de services de micromobilité va générer des espaces où les véhicules, les piétons et les EDP interagissent entre eux. Afin d'assurer l'harmonie et la sécurité de la circulation entre les différents utilisateurs de l'éco-quartier, les interactions des différents utilisateurs sont étudiées à un niveau microscopique dans cette thèse. Le premier chapitre comprend une revue complète de la littérature existante en se focalisant sur les modèles de simulation de trafic au niveau microscopique des piétons et des voitures. Il s'agit aussi bien de modèles de trafic classiques tels que le Social Force Model (SFM) pour les piétons et le Car Following Model (CFM) pour les voitures, que de modèles récents d'apprentissage automatique tels que l'utilisation de réseaux neuronaux pour la simulation de trafic microscopique. Le deuxième chapitre se concentre sur la base de données, où les données ont été recueillies, et sur le développement d'un logiciel basé sur des techniques avancées de vision par ordinateur (µ-scope) et qui a fait l'objet de recherches précédentes. La méthodologie de recueil des données est expliquée en détail, et les endroits où les données ont été recueillies sont identifiés. Dans le troisième chapitre, un processus de calibrage des modèles de trafic existants est effectué. Le calibrage permet de déterminer les paramètres correspondant aux EDP pour le SFM et le CFM, et donc de réaliser les premières conclusions sur le comportement hybride des EDP. En raison de la performance insuffisante des modèles existants, le chapitre 4 propose deux nouveaux modèles basés sur des réseaux neuronaux profonds récurrents à mémoire à long terme (LSTM). Ces modèles ont pour but d'améliorer la performance de la simulation du trafic en incorporant des techniques avancées d'apprentissage automatique. Les résultats de la simulation et la performance des modèles proposés sont discutés et évalués. L'objectif global de la thèse est de faire avancer la compréhension du comportement du trafic des PMD et de contribuer au développement d'une gestion plus efficace du trafic dans des conditions de trafic mixte.

Il est important de préciser que cette thèse comprend une grande partie de développement informatique, de développement de code et d'algorithmes qui sont accessibles via le lien suivant https://github.com/yeltsinvc/THESIS_DOCTORAT ainsi que le logiciel µ-scope développé lors de la thèse https://github.com/yeltsinvc/THESIS_DOCTORAT/tree/main/u-scope_sofware.

Mots-clés: Simulation microscopique du trafic, Engis de déplacement personnel, Espaces partagés, trafic mixte, Long-Short Term Memory, Vision par ordinateur recueil de données.

Contents

List of Figures

List of Tables

List of Acronyms

ANN	:	Artificial Neuronal Network
CFM	:	Car Following Model
CNN	:	Convolution Neural Network
CEM	:	Cross-Entropy Metod
IDM	:	Intelligent Driver Model
LSTM	:	Long-Short Term Memory
MAPE	:	Mean Absolute Percentage Error
PMDs	:	Personal Mobility Devices
RMES	:	Root Mean Square Error
RNN	:	Recurrent Neuronal Network
SD	:	Standard Deviation
SFM	:	Social Force Model
SUMO	:	Simulation of Urban Mobility
TTC	:	Time To Collision
YOLO	:	You Only Look Once

Publications

1. Christoforou, Z., Farhi, N., & Valero, Y. (2020). Is the car-following model appropriate for the simulation of mixed traffic considering e-scooters?. In *Transport Research Arena 2020 (Conference accepted)*

2. Valero, Y., Antonelli, A., Christoforou, Z., Farhi, N., Kabalan, B., Gioldasis, C., & Foissaud, N. (2020, September). Adaptation and calibration of a social force based model to study interactions between electric scooters and pedestrians. In *2020 IEEE 23rd International Conference on Intelligent Transportation Systems (ITSC)* (pp. 1-7). IEEE.

3. Valero, Y., Gioldasis, C., Christoforou, Z.(2022). Generalization of the Social Force Model for Mixed Traffic Contexts including Personal Mobility Devices. 10th symposium of the European Association for Research in Transportation (hEART) 2022.

4. Zhao, L., Farhi, N., Valero, Y., & Christoforou, Z.(2022). Long Short-Time Memory Neural Networks for Human Driving Behavior Modeling. Transport Research Arena Conference dedicated to European Research and Technology on Transport and Mobility TRA 2022.

5. Valero, Y., Gioldasis, C., & Christoforou, Z.(2022). Modeling Personal Mobility Device movement under mixed traffic conditions. Transport Research Arena Conference dedicated to European Research and Technology on Transport and Mobility TRA 2022,.

6. Christoforou, Z., Gioldasis, C., Valero, Y., & Vasileiou-Voudouris, G. (2022). Smart traffic data for the analysis of sustainable travel modes. *Sustainability*, *14*(18), 11150 .

Introduction

1. Motivation

A personal transporter (also powered transporter, electric rideable, personal light electric vehicle, personal mobility device, etc.) is any of a class of compact, mostly recent (21st century), motorized micromobility vehicle for transporting an individual at speeds that do not normally exceed 25 km/h (16 mph)[1]. The use of Personal Mobility Devices (PMDs) has drastically increased in dense urban areas over the last years because it offers an interesting alternative for both door-to-door and first/ last mile trips. According to [1], passenger trips of less than 8 kilometers (5 miles) represent between 50% and 60% of current total passenger kilometers traveled in China, the European Union and the United States. For instance, about 60% of car trips are less than 8 kilometers and could benefit from PMDs solutions. The intensive use of these vehicles can be confirmed with the revenue of the e-scooter sharing market segment presented by [1] and which can be seen in Figure 1 a progressive increase in revenue worldwide.

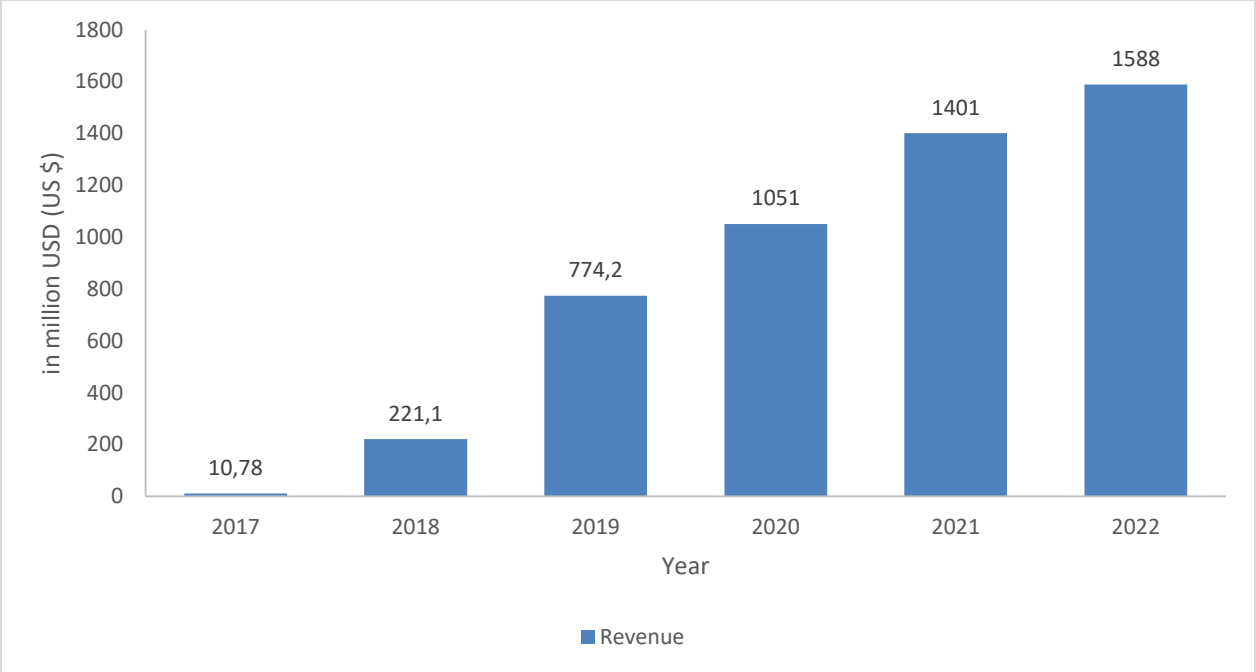

Figure 1. Revenue of the E-scooter sharing segment in worldwide (Source: [1])

[1] https://en.wikipedia.org/wiki/Personal_transporter

This increase is the result of the different advantages that PMD vehicles offer, particularly over short distances of travel. They are low-cost and environmentally friendly solutions (i.e. compared to private cars) offering increased flexibility and comfort (i.e. compared to mass transit) as discussed in [2]. Furthermore; they take up a small space both for circulation and parking. As a result, they can contribute to congestion mitigation and can be easily stored in apartments or offices in dense urban areas or transported in public transport vehicles. PMDs are also flexible in their usage as they can be privately owned or part of sharing fleets while driving has no specific prerequisites in terms of age or driving license. Evidence from surveys suggests that they are used for all travel purposes: work, studies, tourism, shopping, day and night and leisure activities [2]. In all cases, playfulness is found to be one of the key drivers for choosing PMDs over other transportation modes.

PMDs usage comes, of course, with certain shortcomings. First and foremost, the number of accidents involving PMDs has significantly increased as their number increases. PMD users are vulnerable road users and the severity of collisions with private cars is high. Also, in case of collisions with pedestrians, the latter may suffer from severe injuries [3]. The problem of "co-existence" with other road users is accentuated by the fact that relevant traffic rules are not well defined in various cities and the legislative framework presents certain gaps, ambiguities, or inconsistencies. Overall, it remains an open research question whether PMDs are over- or under-represented in traffic accidents and if they represent an important accident risk compared to other modes. Furthermore, PMDs often use Li-ion batteries and their environmental footprint is far from being negligible [4]. Especially when substituting public transport or walking, PMDs may have an important impact on the environment and contribute to climate change.

Besides, those shortcomings have led Paris mayor to call for a referendum on April 2nd 2023 in order for Parisians to decide whether they want to keep the operations of e-scooter free-floating companies or not[2]. The Parisian case is important as PMDs are extremely popular and Paris is often cited as the showcase of micromobility for free-floating bicycles and e-scooters. Free-floating e-scooters made their first appearance in 2018 and by the end of 2019 a dozen companies were competing totalizing almost 40,000 vehicles. The covid outbreak in 2020 and the curfew that followed reduced significantly their usage while local Authorities decided to limit the number of companies to 3, with the authorization to deploy a maximum of 5,000 devices for each operator, in order to better regulate their usage. 15,000 e-scooters free-floating are offered every day in Paris by the three operators (Dott, Lime and TIER) with a total of 55,000 trips per day in October 2022. The contract with the 3 operators will be terminated on March 23th, 2023 for this reason the Mayor of Paris started to put in question the continuity of the service on both safety and environmental

[2]https://www.lemonde.fr/en/france/article/2023/01/15/paris-to-hold-referendum-on-e-scooter-rental-services_6011644_7.html

grounds. Nevertheless, privately-owned PMDs are not included in the eventual prohibition and their usage is expected to grow in the coming years. In parallel, the French central government was among the first to vote a law defining the rights and obligations of PMD drivers in 2019[3].

PMDs have the right to use cycling infrastructure, such as bike paths and lanes, for their movement. They also have the right to use normal traffic lanes when bicycle infrastructure is not available. The use of sidewalks is prohibited unless indicated otherwise. The speed limit is fixed at 25km/h. Consequently, PMDs do have a footprint on city traffic and level of road safety. As their movement is made on different types of urban infrastructure, their footprint concerns car traffic, bicycle traffic and, also, pedestrian movements. Their presence may have a direct impact upon other road users' choices (for example driving speed, lateral and longitudinal safety distance) and accident risk. Their presence is naturally influencing macroscopic flow characteristics such as average speed, traffic density or travel time. However, this impact has not been quantified so far and their movement has not been integrated in current urban traffic simulators. A first reason for this is certainly their rapidly growing popularity that made it difficult for engineers and decision-makers to follow up. A second reason is also the lack of knowledge and evidence regarding the dynamics of their movement and their safety performance.

In [5], a strategic framework for evaluating if neighborhoods are suitable for different micromobility modes was proposed to help local authorities, planners and mobility operators in their decision making. However, this framework remains macroscopic and does not integrate the modeling part of PMDs and their interactions with other modes of transport, either with existing models used for the simulation of vehicles or pedestrians, or with new models that allow a more detailed representation. The main motivation of this research is thus to contribute in the description of the movement of PMDs in urban contexts in order to be able to better understand and analyze their proprieties, to quantify their impact on traffic flow and safety as well as on the environment. This knowledge is expected to be useful to researchers, engineers and decision-makers who wish to integrate PMDs in urban models, perform socio-economic assessments, and make evidence-based decisions.

2. Research questions and thesis objectives

In view of the above, the thesis research questions are formulated as follows:

RQ1: To what extent are current traffic models capable of reproducing the movement of PMDs?

RQ2: How can the performance of existing models be ameliorated?

[3] https://www.legifrance.gouv.fr/loda/id/JORFTEXT000039272656

The objective of the present thesis is to develop and test a microscopic modeling framework suitable for PMD particular characteristics. Specific objectives include:

O1. Perform a literature review of previous PMD modeling efforts

O2. Comparatively assess existing microscopic traffic models as to their suitability for PMDs

O3. Calibrate the most prominent existing models for the PMD case

O4. Propose ways to improve model performance, going from new data acquisition techniques to new model formulations

3. Research perimeter

This paragraph describes the perimeter in which the research questions will be addressed. The perimeter is defined in terms of (i) PMD vehicles considered, (ii) geographical space and type of road infrastructure analyzed, and (iii) travel patterns, trips and usage included in the analysis.

3.1. Vehicles

Personal Mobility Devices (PMDs) are easy-to-carry or easy-to-push vehicles. They may range from lighter rollers and skis to heaviest two-wheeled self-balancing personal transporters and include bikes, e-bikes, e-scooters among others. They may be motorized or not, shared or privately-owned and they allow their users to make a 'hybrid usage' at their convenience. Thus, they behave either as a pedestrian or a vehicle [2] when riders use at their convenience different types of infrastructure. Figure 2 shows indicatively some types of PMDs. The present thesis focuses on e-scooters and regular bikes.

Figure 2. Different types of PMDs

3.2. Area and infrastructure

As micromobility has mainly emerged in metropolitan areas, the main emphasis of the thesis will be placed on urban contexts where interrupted vehicular flows are observed. The scope of the analysis covers all urban infrastructure used, legally or illegally according to national legislation and local prohibitions. In that sense, the developed models will address pedestrian areas and shared spaces where interactions between pedestrians and PMDs are observed. They will also address road traffic lanes where interactions with private cars mostly occur. PMD specific infrastructure, such as bike lanes and paths, are also in the scope of the thesis.

3.3. Trips and usage

PMDs can be used for door-to-door trips or to cover the first/last mile in a multimodal context, combined with private cars or public transport vehicles. They also serve leisure and tourism-related travel purposes or, in some cases, physical activity and sports. PMDs can be either privately owned by the user or part of a shared vehicle scheme. In the latter case, the PMD service operates either with specific drop off points (docks) or dockless using GPS information to find available vehicles. All of the aforementioned cases are included in the analysis with no distinction. However, recent

evidence suggests that there may exist differences in the driving behavior according to the user profiles and travel purpose. For example, tourists seem to travel at lower speeds compared to locals [6].

4. Context

The thesis is part of the E3S program, a "living lab" of micro-mobility, i.e. to test the implementation of PMDs. In this context, the creation of "pilot" applications of reduced size are necessary, with the objective of highlighting the possible difficulties and the obstacles to a wider deployment. This very ambitious program has a budget of 2 million €, financed 50/50 by Eiffage and I-SITE Future This paragraph provides key information on the project. For further details, the reader can refer to the project's official website: https://www.programme-e3s.com/en/

4.1. LaVallée Eco neighbourhood

The LaVallée eco-neighborhood in Châtenay-Malabry (in Southern Paris) is designed as an innovative eco-neighborhood with a surface area of 213,000 m^2 that provides a connection between downtown Châtenay-Malabry, the green corridor and the Sceaux park. The eco-neighborhood will include 2,200 houses, 8,000 inhabitants and numerous services. Transportation accessibility is currently moderate for the RER B and buses; however, it is planned in the route of the future T10 tramway, which will improve the public transportation offer in the area.

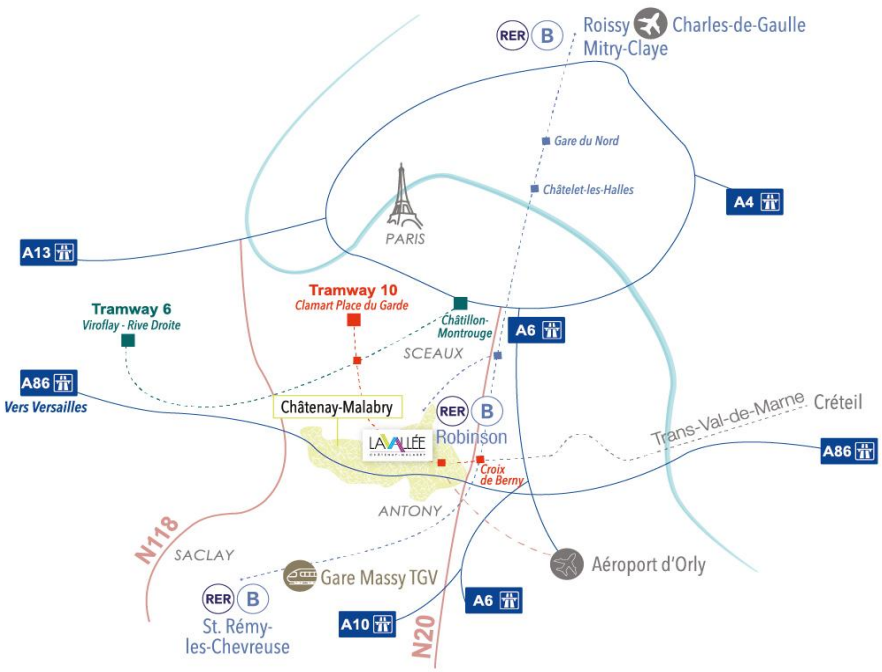

Figure 3. Localisation of eco-neighborhood Source : https://lavallee-chatenay-malabry.com/

In Figure 4 we can observe the future configuration of the eco-neighborhood as follow:

Public Transportation

- RER B that is located between 5-8 minutes walking time from the La Croix de Berny station.
- Future Tramway T10, which will include a station in front of the neighborhood entrance, on the Division-Leclerc side (in 2023).
- Numerous bus lines

Road

- Several automobile access points
- The A86 motorway is 5 minutes away
- Underground parking

Soft Mobility

- Numerous pedestrian paths
- Wide sidewalks in the avenue where the shops will be installed
- New bicycle paths along Avenue de la Division-Leclerc

As a consequence, numerous trips will be generated, in particular to ensure connections. In this perspective PMDs appear as a mobility solution perfectly adapted to the future mobility needs of the eco-district.

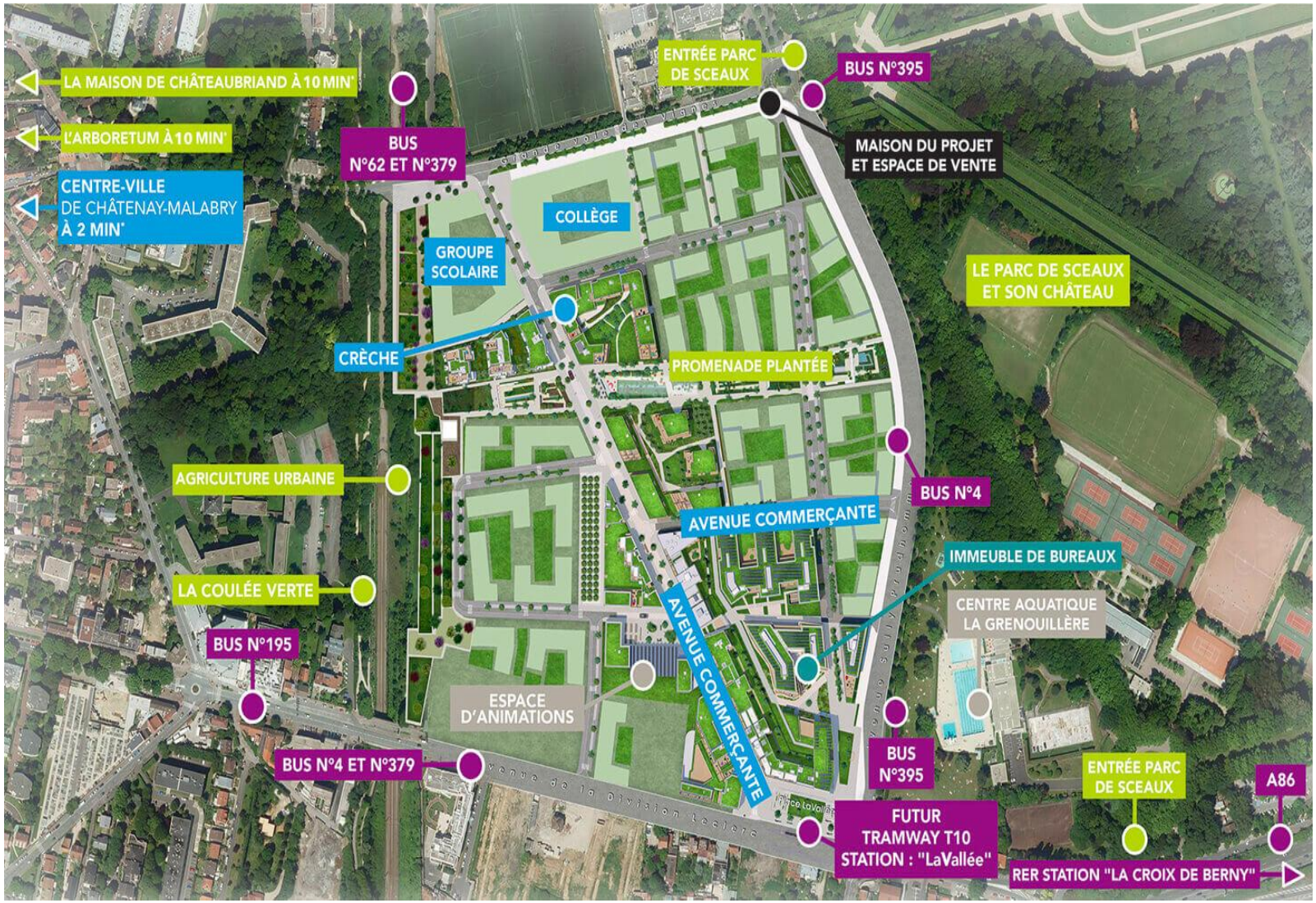

Figure 4. Configuration of eco-neighborhood Source : https://lavallee-chatenay-malabry.com/

4.1.1. Project structure and planning

The eco-neighborhood is designed according to the following 5 points:

- Green: LaVallée will promote the development of biodiversity, thanks to the creation of numerous planted spaces, on a site that was originally poor in this area.

Figure 5. Green Point Source : https://lavallee-chatenay-malabry.com/

- Connected: LaVallée will be a new destination for strolling, relaxing and shopping thanks to a new offer of shops. LaVallée will be easily accessible by public transportation but also for motorists who will have an underground parking lot.

Figure 6. Connected Point Source : https://lavallee-chatenay-malabry.com/

- Intense: a new offer of shops, will create a lively place to live.

Figure 7. Intense Point Source : https://lavallee-chatenay-malabry.com/

- Exemplary: The ambition of LaVallée is to be an eco-neighborhood, a demonstrator of sustainable living in the Ile-de-France.

Figure 8. Exemplary Point Source : https://lavallee-chatenay-malabry.com/

- Ideal: ideal to live in regardless of their location, the future homes with their contemporary architecture will take advantage of the omnipresent nature in and around the neighborhood.

Figure 9. Ideal Point Source : https://lavallee-chatenay-malabry.com/

Concerning the planning of the project as shown in Figure 10, the first works of the project started in May 2019, and the opening of the neighborhood to the first people was planned at the beginning of 2022, however due to some inconveniences it was rescheduled to July 2022. This rescheduling of the project did not allow the installation of cameras and data collection at the time of project operation that was previously planned for the thesis.

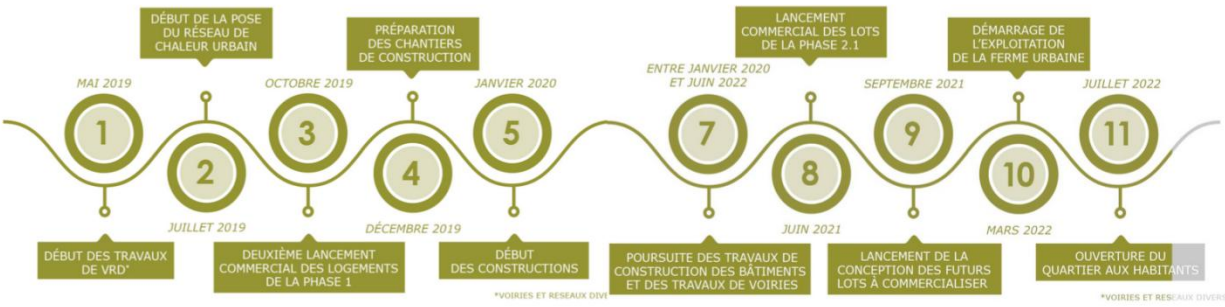

Figure 10. Planning of the project Source : https://lavallee-chatenay-malabry.com/

The contribution of the thesis to the project was to be able to simulate at the microscopic level the interactions between the different modes of transport including the PMDs. In the present thesis different methods were developed to model this interaction, but due to the current state of the

project, which is in the phase of opening to the first residents, it has not been possible to implement during the thesis cameras to analyze the behavior of the PMDs and their interaction with other modes of transport in the eco-neighborhood.

5. Thesis outline

The present PhD dissertation consists of 5 chapters.

Chapter 1 presents the literature review that focuses on microscopic simulation of vehicular and pedestrian traffic.

Chapter 2 describes the methodology used to obtain the data, the scenarios analyzed and the databases generated.

Chapter 3 investigates the performance of existing models for simulating vehicles and pedestrians interacting with PMDs. A calibration of the Car Following Model and the Social Force Model is also realized.

Two new models are proposed in Chapter 4. The first emphasizes on scenarios with vehicle interaction while the second focuses on scenarios with pedestrians and bicycle interactions.

Finally, in the last chapter overall conclusions and future perspectives are provided.

Chapter I

Literature review

This chapter presents a literature review in order to understand the state of the art in the research on the movement and behavior of pedestrians, bicycles, and vehicles. Traffic models can be classified in macro, meso or microscopic according to the level of detail used to represent traffic attributes and characteristics. Macroscopic models are well suited for large-scale applications and provide useful aggregated indicators capable of describing the network performance. Mesoscopic models are an intermediate solution between macro and microscopic models as they describe traffic entities at a high level of detail but, contrarily to microscopic models, the interactions are described at a lower level of detail. Microscopic models need more technical resources and data but provide a finer representation of vehicle dynamics and interactions considering individual moving objects instead of flows [7]. For the needs of our analysis, this research adopts a microscopic approach of the interactions between vehicles, pedestrians, and PMDs. Therefore, the literature review focuses on microscopic modeling approaches for pedestrians, PMDs and private cars and. Figure 11 shows the structure of each of the subchapters analyzed in the literature review and developed throughout this chapter.

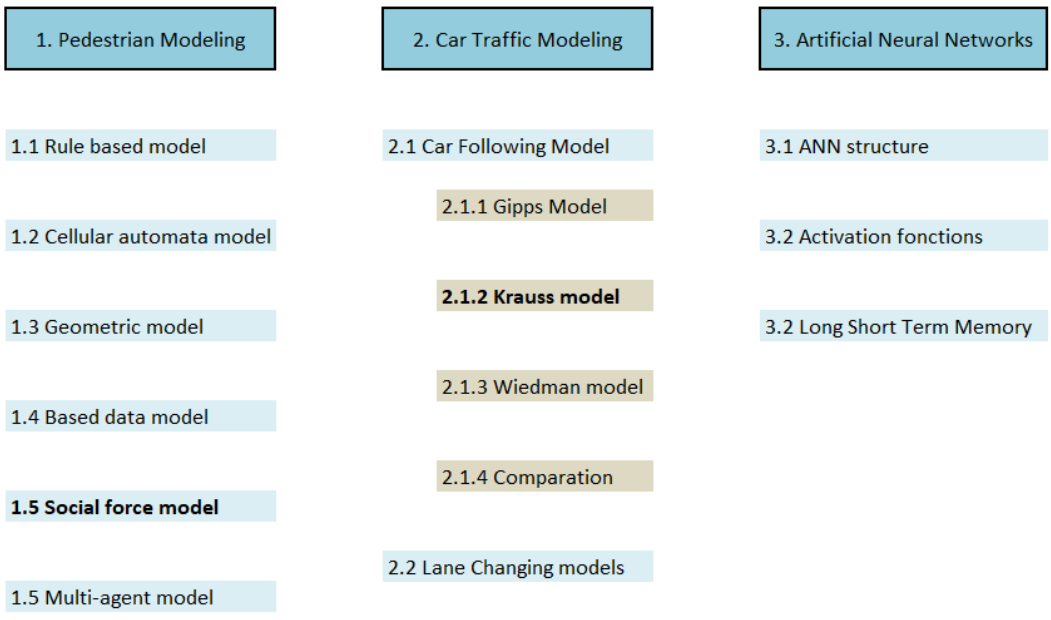

Figure 11. Structure of chapter 1

1.1. Pedestrian modeling

Pedestrian behavior is chaotic, very irregular, difficult and complex to predict. However, there are some situations in which behavior can be considered as predictable. In this context, to model pedestrian interactions, models describing the behavior of objects moving in a two-dimensional environment are required. In the literature review, microscopic and macroscopic models are observed to describe the interactions of pedestrians.

Macroscopic models are based on fluid mechanics (e.g. [8]), perform rather well for high density crowds, but not for mixed traffic with the presence of other road user type like bicycle and PMDs. This is the reason why they were not chosen for the present analysis. Microscopic models simulate the movement at a single-unit level, i.e. the movement of each pedestrian and their interaction with the environment. Microscopic models can be divided into 6 sub-categories: rule-based models, cellular automaton models, geometric models, data-based models, social force models and agent-based models [9]. The most commonly used software tools to simulate the behavior of people when they move (and in particular how the design of a certain infrastructure influences their behavior) are (i) Viswalk which uses the Social Force Model and (ii) Legion which uses the Agent-Based Model. The 6 sub-categories and a comparison between Social Force Model and Agent-Based Model are explained below.

1.1.1. Rule-based model

The rule-based model is a method of simulating the movement of a crowd based on a set of rules that govern the behavior of individuals within the group [10]. Each individual follows rules such as avoiding collisions, adjusting their speed based on their neighbor's speed, and staying with the group. These rules were initially observed in birds and adapted to humans for simulation. The basic idea behind a rule-based model is to define a set of rules that dictate how pedestrians move, interact with each other and their environment, and make decisions based on their perception of the situation. These rules are typically based on real-world observations of pedestrian behavior, and are often fine-tuned to accurately reflect the specific context being simulated. For example, some common rules in a pedestrian simulation might include:

- Pedestrians will walk in the direction of their intended destination.
- Pedestrians will avoid collisions with other pedestrians and objects in their path.
- Pedestrians will slow down or speed up based on the density of the crowd around them.
- Pedestrians will adjust their paths based on perceived obstacles or congestion in their path.
- Pedestrians will make decisions based on the available information and their own preferences, such as choosing a shorter route over a longer one or avoiding stairs if they are carrying heavy bags.

In this model, each pedestrian makes discrete choices while moving [11], and the space is divided into angles and distances to surrounding pedestrians. This model also considers two types of behavior: constrained, which includes collision avoidance and leader tracking, and unconstrained, which is independent of other individuals [12].

The rule-based model produces simulation results that are consistent with real-world observations, but there are limitations due to the possibility of contradictory rules. For example, in the case of personal mobility devices (PMDs), there is a trade-off between safety and travel time savings, and the combination of rules may not always be clear.

1.1.2. Cellular automata model

The Cellular Automata (CA) model is a method of simulating pedestrian movement by discretizing a 2D space into a matrix of cells [13] [14]. The pedestrian moves from cell to cell on this matrix, and obstacles are modeled as inaccessible cells. In this model, each pedestrian has a preferred direction of movement, and a cellular matrix is generated at each time-step containing the probabilities of each pedestrian's movement. Pedestrian movements can be obtained consecutively or simultaneously [15], [16].

One of the early applications of CA to pedestrian simulation was in the work of [14], who developed a CA model to simulate the movement of pedestrians in a panic situation. In their model, the pedestrians had different preferred velocities and tried to move towards their destination while avoiding collisions with other pedestrians and obstacles. The model was able to capture the self-organized behavior of crowds and reproduce some of the features observed in real-world crowd behavior during emergencies.

Since then, many studies have applied CA to simulate various aspects of pedestrian movement. For example, [17] developed a CA model that could reproduce the formation of lanes in crowds, as well as the emergence of congestion and stop-and-go traffic. They used the model to study the impact of different factors, such as the size of the corridor and the speed distribution of the pedestrians, on crowd behavior.

In another study, [18] developed a CA model to simulate the movement of pedestrians in a bottleneck situation. The model included features such as the anticipation of the bottleneck and the different walking speeds of the pedestrians. The simulation results were compared with experimental data, and the model was able to reproduce the observed behavior, such as the formation of arching and the reduction of the flow rate.

More recent studies have further developed CA models for pedestrian simulation, often with a focus on improving the accuracy and realism of the simulation. For example, [19] proposed a CA model that could simulate the walking behavior of individuals with different age and gender characteristics,

as well as the interactions between pedestrians and environmental factors such as weather and lighting conditions.

Overall, CA has been shown to be a useful tool for simulating pedestrian movement in various scenarios. While the accuracy of the simulation results is sometimes limited due to the probabilistic approach applied in CA, these models have provided valuable insights into the mechanisms underlying crowd behavior and have the potential to inform the design of public spaces and transportation systems. Another disadvantage is that the discretization of space results is a discretization of the pedestrian's trajectory, which is not ideal for microscopic analysis.

1.1.3. Geometric model

Geometric models are a type of microscopic model used to predict the speed at which pedestrians can move to avoid obstacles without changing direction. They have been adapted to describe pedestrian movement and can take into account the acceleration and speed of other pedestrians in the simulation process [17][18]. One such model allows each pedestrian to explore the space around them and guess the movement of neighboring pedestrians by linear extrapolation [19].

In recent years, geometric models have been adapted to describe pedestrian movement, and have been used to take an increased number of humans into account in the simulation process [23]. The resulting models allow the acceleration and speed of other pedestrians to be taken into consideration, and can simulate the movement of a large number of people in a given area.

One such model proposed by [24] uses a force-based approach to describe the movement of pedestrians. In this model, each pedestrian is assumed to be influenced by a repulsive force from other pedestrians and an attractive force to the desired destination. The model also accounts for obstacles in the environment and allows for the simulation of different pedestrian behaviors.

Another model proposed by [25] uses a differential drive model to simulate the movement of pedestrians. In this model, each pedestrian is represented by a circle and the movement is determined by the position and orientation of the circle. The model takes into account the interaction between pedestrians and can simulate complex pedestrian behaviors, such as avoiding collisions with other pedestrians.

Several studies have explored the use of geometric models in emergency scenarios, such as evacuations from buildings and mass gatherings. For example, one study proposed a geometric model for simulating evacuation scenarios in a shopping mall. The model takes into account the layout of the mall, the location of exits, and the movement of shoppers in response to an emergency situation.

Overall, geometric models provide an effective approach to simulate pedestrian movement and can be used to study a wide range of scenarios. However, these models may not capture the complexities of human behavior in all situations and may require additional calibration to accurately represent real-world scenarios.

1.1.4. Data-based model

Data-based models are developed on the basis of video recording analysis to create databases of pedestrian interactions. They are modeled by drawing similar situations from the database. Several works led by [20] and [21] resulted to the creation of a learning model from observed trajectories. The model decides the movements of each neighbor along with the characteristics of the environment, and store them in a database in order to reconstruct a similar situation later on. These models come up against the lack of data as well as the eventual lack of similarity between two situations. In order for these models to be effective, one of an infinite number of examples should be available and similar enough to the studied situation. As PMD traffic data are relatively few, this method was rejected for the needs of the present thesis.

There is a growing body of research on data-based models for pedestrian simulation that use video recording analysis to create databases of pedestrian interactions. In [22] developed a data-based model for simulating pedestrian movement in crowds. They used video recordings of pedestrian movements to analyze the interactions between individuals and used this information to develop a model that captured the essential features of pedestrian behavior. [29] used video recordings to create a database of pedestrian interactions that was used to inform the behavior of simulated pedestrians. The resulting model was able to reproduce the observed patterns of pedestrian movement in a variety of scenarios, such as walking on sidewalks and crossing streets. [30] developed a model that used video recordings to analyze the behavior of pedestrians at intersections. They used this data to develop a database of pedestrian movements that was used to inform the behavior of simulated pedestrians. The resulting model was able to replicate the observed patterns of pedestrian behavior at intersections. [30] developed a model that used video recordings to analyze the behavior of pedestrians in a shopping center. They used this data to create a database of pedestrian interactions that was used to inform the behavior of simulated pedestrians. The resulting model was able to reproduce the observed patterns of pedestrian movement in the shopping center.

Overall, data-based models that use video recording analysis to create databases of pedestrian interactions have shown promise in improving the accuracy and realism of pedestrian simulation. However, there are also challenges associated with this approach, such as the difficulty of collecting and analyzing video data and the potential for overfitting to specific datasets.

1.1.5. Social force model

The social force model (SFM) is a microscopic model of social forces which utilizes Newtonian physics concepts and allows objects to move continuously inside the environment [22, 23, 24]. In SFM, each pedestrian is subject to (i) propelling forces which direct his/her movement towards his/her goal, and (ii) repulsive forces which are exercised by other individuals and obstacles into himself/herself. The propelling force is expressed with parameters related to free speed and direction of the pedestrian, while the repulsive force depends on the nature of the interaction. The addition of the repulsive and propelling forces leads to the formulation of the model.

Among all microscopic models reviewed above, SFM seems to be the most suitable to use as a starting point for e-scooter modeling. The movement of the pedestrian is expressed by the fundamental principle of dynamics that fragments the forces acting on the pedestrian. When a new individual interacts with the existing individuals, the propelling force and the repulsive force no longer have the same properties. The propelling and repulsive forces get modified by the presence of PMDs. To apply the social force model, an earlier approach is adapted [23], through a special parameter specification, to allow the model to distinguish pedestrians to PMDs.

In the case of high pedestrian density, the initial formulations of SFM generates over-lapping between pedestrians, which is, of course, not realistic. Therefore, [25] propose to take into account an additional body force f_b and a sliding friction force f_t (Figure 12). This adaptation allows for more realistic simulations in high-density conditions such as evacuation in a panic event. Applications of this adaptation can be found in [26, 27, 28].

Figure 12. Body and sliding friction force i (SFM).

Further improvements of the models proposed by [24] and [25] are presented in detail in [29]. Those improvements concern pedestrian attributes such as shape, mass, maximum speed, desired speed. In [24] and [30], the shape of the pedestrian is considered as elliptical (Figure 13 (a)); ie. as if it was projected on a two-dimensional plane. In an effort to improve computational efficiency, [25], replaced the elliptical by a circular shape (Figure 13(b)). The efficiency has been improved, but the simulation error increased. [31] and [32] proposed a three-circle representation (Figure 13(c)). The latter allows for a more realistic modeling of the pedestrian shape (i.e. compared to the circle);

while the computational cost is reasonable. Concluding, in cases of large-scale simulations such as stadiums and stations, it is advisable to use the circular shape for its computational time efficiency. For medium scale pedestrian simulations, such as simulation of sidewalks and walkways, it seems preferable to use the elliptical shape or three-circle [33]. This thesis is focused on the objective of using the model at an eco-neighborhood scale, so it was decided to consider pedestrians in a circular shape.

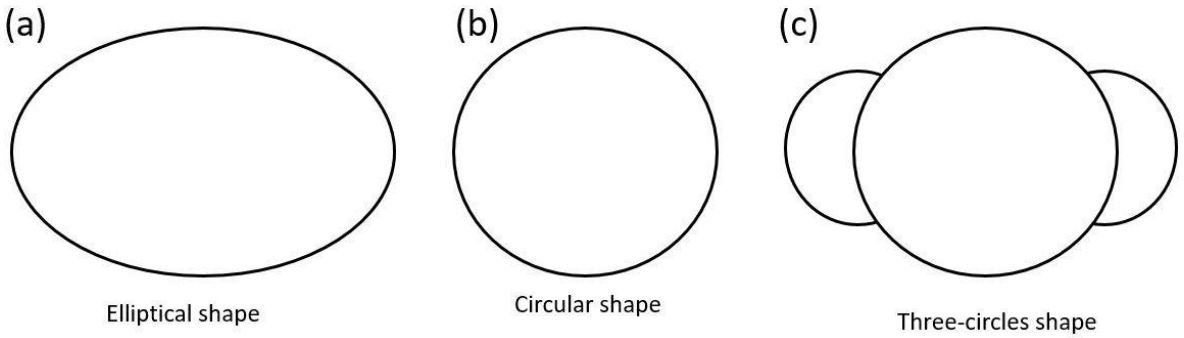

Figure 13. (a) Circular shape, (b) Elliptical shape and (c) Three circles shape of pedestrian i.

Beyond pedestrian interactions, SFM has been extensively used to model the interactions of different agents in spaces shared by pedestrians, bicycles, and vehicles. In [34], the authors introduced the dynamic movement of the motorcycle in the social force theory. A database containing vehicle trajectories obtained from video recordings was used for calibration. Model parameters were obtained with calibration, but they cannot be compared to pedestrian parameters because a different exponential function was used for the repulsion forces.

An adaptation of the social force-based model to simulate mixed car and bicycle traffic was proposed in [35]. This adaptation was used for the purpose of risk analysis. Results suggest that vehicles have a higher strength and period of repulsive force than bicycles. As expected, the collision risk in mixed bicycle-car traffic increases with increasing traffic density. In [36], the authors proposed an extension of SFM to simulate the movements of vehicles on a two-dimensional space. A database containing vehicle trajectories at a T-intersection that was converted to a shared space area was used for calibration. Results show that simulated trajectories provide a good approximation of real trajectories.

Turning to PMDs, a process of calibration of the parameters of SFM to simulate the behavior of a Segway was realized by [22]. Calibration was performed using the cross-entropy method and Root Mean Squared Error (RMSE) was used to assess the measurement error. Results show that the

calibrated model can sufficiently reproduce the movements and interactions of Segway users and pedestrian shared spaces for uncongested scenarios (maximum pedestrian density = 0.5 ped/m2), even without modifying the original social force model. In [37], the parameters of an e-scooter were calculated, based on a database obtained by data image processing. The results of the cited paper are part of the present article and will be discussed in the following Sections.

Overall, SFM is a well-established model that has been extensively used in a variety of applications and has proven to be capable of realistic pedestrian representations. However, its usage remains limited in the case of PMDs even if they act as pedestrians in many contexts.

1.1.6. Agent-based model

The agent based model is based in a multi-agent system, denoted as auto-navigation by [20]. This type of model considers each pedestrian as an autonomous agent with a group of rules that control their movements, providing the agents with artificial intelligence [35]. The concept in the case of pedestrian movement is that each pedestrian performs an evaluation of all feasible options looking for the path with the minimum effort [36]. This is done first at the macro level, looking for the shortest path to the target destination. This macro-level navigation determines path choice. Secondly, the pedestrian evaluates his/her possibilities at the micro level, optimizing the next step. This means that a main path is found at the macro level and then the path is modified at the micro level. The effort, which pedestrians try to minimize, includes three factors:

- Frustration: when traffic jams force you to slow down.
- Inconvenience: when you have to avoid the shortest route
- Discomfort: when your personal space is invaded
- Pedestrians acquire information from their environment, zone of perception, and use it to decide their next step. This decision includes:avoid obstacles
- personal preferences, such as personal zone and desired speed
- collision avoidance
- identifying other pedestrians as "friend or foe", to determine how to interact with them
- learning on the way, accumulating memories
- possibility to configure preferences and characteristics
- commercial sensitive algorithms and parameters, not distributed information.
- parameters have no physical explanation

Due to the previous advantages, the agent-based model was shortlisted for use in the present thesis along with SFM. A detailed comparison between the two models follows.

1.1.7. Comparison between Social Force Model and Agent-based model

In this part we compare the two models that were found to be most suitable for PMD modeling and are also used by the most popular pedestrian simulation software tools. On the one hand, SFM implemented in Viswalk software and, on the other hand, the agent-based model implemented in Legion and Aimsun walk.

Table 1. Comparison of social force and agent-based models.

Social Force Model	Agent-based model
• Pedestrians automatically find their path through the model, from origin to destination.	• Pedestrians automatically find their path through the model, from origin to destination.
• Intermediate points can be constructed to steer pedestrian	• Decision nodes can be used to steer pedestrians
• It is possible modify the parameters on which route choice is based • It is possible modify behavior parameters	• It is possible choose entity profile, but is limited to the available profiles
• Transparent algorithms and parameters, all information available	• Commercial sensitive algorithms and parameters, not distributed information.
• Large number of Python libraries tested	• Few Python libraries and scarce documentation

Social force and agent-based models are both used for pedestrian simulation. In the case of the social force model there is a larger number of libraries in Python to simulate pedestrians compared to the agent-based models. In the case of commercial software, for the social force model all information is available compared to the agent-based model in which commercially sensitive algorithms are not available. That is why social force model was chosen to be used in this thesis.

1.2. Microscopic Car Traffic Modeling

The scientific literature on microscopic car traffic modeling is vast as numerous modeling approaches have been proposed. Two major 'families' of models can be identified: models describing either the lateral or the longitudinal movement. The description of longitudinal behavior

is most commonly made using Car-Following models. In essence, those models use statistical distributions and functions to define maximum, minimum and desired acceleration/deceleration rates, maximum and desired velocity, and other vehicle characteristics [23][37]. Lateral movements have been traditionally described by lane- changing models which are of particular importance in the case of two-wheeled vehicles. In the modeling of two-wheeled vehicles, an important part is the modeling of lateral behavior. This paragraph describes both modeling approaches.

1.1.1. Car Following Model

Car-following model (CFM) is a microscopic simulation model of vehicular traffic, which describes the pairwise interactions between a leading and a following vehicle moving on the same lane (Figure 14). The one-by-one following process of a vehicle called 'follower' is influenced by a vehicle called 'leader' [40]. The CFM initially proposed by General Motors [41] considered that acceleration was proportional to relative velocity. An acceleration/deceleration rate was calculated for the following vehicle depending on the relative speed between the leader and follower. Studies on the calibration and validation of the GM model were undertaken by [42, 43]; and [44], who obtained incoherent parameters between the exponent of the distance headway and the exponent of the velocity. As a result, the GM model stopped being used in the seventies [45].

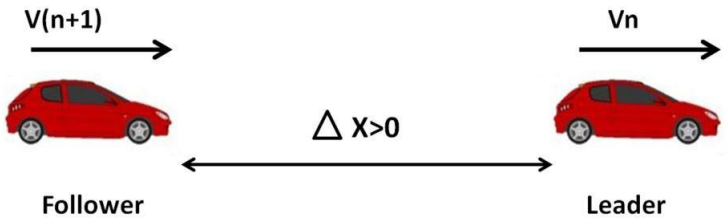

Figure 14. Car Following Model

Different approaches of CFM, based on safety speed, were proposed later by various researchers as [46, 47] and IDM Model [48]. These models assume that the following vehicle will maintain a safety distance from the leading vehicle. The follower chooses a maximum speed allowing him/her to stop safely in the case of an abrupt deceleration and avoid a rear-end collision [49]. In what follows, the most commonmy used CFM are presented and discussed.

1.1.2. Gipps Model

The Gipps model is the most common CFM model and is based on *safety distance*. In each instant of time, a driver plans his speed for the next instant in such way that he/she can stop even if the leading vehicle suddenly stops [41]. The formula used in Gipps' model, allows updating the speed in a time $t + \tau$ [42], as shown below:

$$u_n(t+\tau) = \min\left(G_a(t), G_d(t)\right) \quad \text{Equation 1}$$

$$G_a(t) = u_n(t) + 2.5a_n\tau\left(1 - \frac{u_n(t)}{V_n}\sqrt{0.025 + \frac{u_n(t)}{V_n}}\right) \quad \text{Equation 2}$$

$$G_d(t) = b_n\tau + \sqrt{b_n^2\tau^2 + b_n\left(2\left(x_{n-1}(t) - s_{n-1} - x_n(t)\right)\right) - u_n(t)\tau - u_{n-1}(t)^2/b*}$$

Equation 3

Where:

$u_n(t)$: speed of vehicle n in time t.

a_n: maximum acceleration that the driver of vehicle n wishes to undertake

τ : apparent reaction time

V_n: desired speed of vehicle n

b_n: most severe braking that the driver of vehicle n wishes to undertake.

$x_n(t)$: Location of the front of vehicle n in time t.

s_{n-1}: Effective length of the vehicle n

$b*$: Value of estimated for the driver of vehicle n who cannot know this value by direct observation.

The parameters used in the Gipps car following model are in a microscopic scale and different characteristics are assigned to each vehicle, i.e. each vehicle has its own parameters of the car following model, which results in different maximum accelerations and decelerations due to the fact that some of the parameters correspond to a normal distribution. This model was used in [43], to analyze Time To Collision (TTC), i.e., and assess the risk in mixed traffic conditions. In addition, in [42, 15, 44], the Gipps model was used to simulate the behavior of a two-wheeler and results were satisfactory as the mean absolute percentage error (MAPE) of the speed simulation was small. In our literature review, we found no specific adaptations of CFM for PMDs. On the contrary, some adaptations to two-wheeled vehicles, such as motorcycles and bicycles, have been indeed proposed. [45] modeled the behavior of vehicles in mixed traffic conditions including motorcycles based on [18]. The authors justify their selection on the following grounds: (i) The Gipps model suggests that 'followers' search to avoid rear end collisions and a similar driving strategy is usually adopted by motorcyclists when moving in dense traffic, especially on urban networks, (ii) the equations proposed in [26] allow flexibility to modify kinematic properties.

The main drawback of this model is that it is deterministic but in real life not all PMDs drivers have the same behavior.

1.1.3. Krauss model

The Krauss model is essentially a stochastic version of the Gipps model [48]. The model was implemented in the software Simulation of Urban Mobility - SUMO [54]. Given the possibilities that SUMO offers and the performance of Krauss model, we chose to use it in the present research. The formulation of the model for one lane is given in [47], as shown below:

$$v_{safe} = v_l(t) + \frac{g(t) - v_l(t)\tau_r}{\frac{v_l(t) + v_f(t)}{2b} + \tau_r} \qquad \text{Equation 4}$$

Where :

v_{safe}: is the safety speed (m/s);

$v_l(t)$: is velocity leader vehicle (m/s);

$g(t)$: is the gap (m);

τ_r : is the reaction time s;

$v_f(t)$: is velocity follower vehicle (m/s);

b : is the deceleration capabilities (m/s2).

If the v_{safe} is higher than the maximum speed allowed on the road or higher than the speed the vehicle is able to reach until the next pass owing to its acceleration capabilities, the minimum of these values is calculated as the resultant speed, called ”desired speed” v_{des}.

$$v_{des} = \min\left[v_{max}, v + at, v_{safe}\right] \qquad \text{Equation 5}$$

Where:

v_{max}: is the maximum velocity (m/s);

a: is acceleration capabilities (m/s2);

t: is the step duration of the simulation (s);

Finally, there are two boundary parameters, the minimum gap value g_{min} and the maximum deceleration bemergency under emergency conditions.

This model, is used for the multimodal simulation of traffic, but also because this model is a stochastic adaptation of the Gipps model, we can also analyze the TTC with this model. The advantage of this model is that in [34], they present the simulation of two- wheeled vehicles and bicycle in urban areas, obviously with the help of complementary models such as the lane change model and sub lane model. In addition this, model is the default model of the free software SUMO, which allows to simulate mixed traffic conditions.

1.1.4. IDM model

The Intelligent Driver Model (IDM) is a model that produces realistic acceleration profiles and plausible behavior in virtually all single lane traffic situations.

The equations that describe this model are shown below:

$$\dot{v} = a(1 - \left(\frac{v}{v_0}\right)^{\delta} - \left(\frac{s*(v,\delta v)}{s}\right)^2) \qquad \text{Equation 6}$$

Where the acceleration is given for $a_{mic}(s, v, \delta v)$ consists of two parts, in the first part we compare the current speed v with the desired speed v_0 and the second part, we compare the current distance with the desired distance $s*$.

This expression has an equilibrium term $s_0 + vT$ and dynamic term$\frac{v\delta v}{2\sqrt{ab}}$, which put the 'smart' braking strategy.

IDM gives much better results in terms of the acceleration profile if compared to Gipps model, but its main disadvantage is the high value at the initial acceleration, which would be more realistic if it increased gradually. The same is observed for the braking process, with the exception of the first vehicle which moves in a free-flow regime.

1.1.5. Wiedman model

The Wiedman 74 model uses random numbers to simulate mixed traffic behavior, aiming to model the behavior of different drivers. The Wiedamn model presents 5 areas that represent the state of a vehicle. These are: (1) no reaction area, (2) reaction area, (3) unconscious reaction, (4) deceleration and (5) collision as shown below.

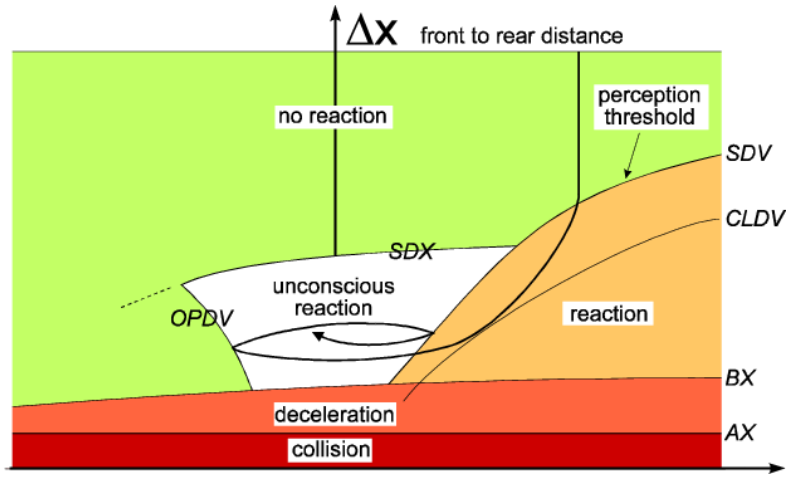

Figure 15. Thresholds and one vehicle trajectory, wiedemann model. Source: Fellendorf, Martin & Ag, Ptv. (2001).

The area of unconscious reaction represents the area of following vehicle. The formulation of the model equation is shown below:

$$AX = \text{VehL} + \text{MinGap} + \text{RND1} * AX_{mult} \quad \text{Equation 7}$$

$$ABX = \text{AX} + \text{BX} * \sqrt{v} \quad \text{Equation 8}$$

Where:

d: safety distance between lead and follower vehicle

AX: Desired distance between the fronts of two successive vehicles in a standing queue

VehL: Length of the leading vehicle

$RND1$: normally distributed N(0.5,0.15);

ABX: Desired minimum following distance;

BX: Safety delta distance

v: speed of vehicles;

In addition to these parameters, for the 5 zones of these models there are different parameters to calibrate. The VISSIM simulator uses the Wiedman model as a following model, which is considered as a psychophysical model of the driver.

1.1.6. Comparison of car following models

In this part, a comparative table of the models has been made, with advantages and disadvantages, this information is the main conclusions of [8, 47, 2]; as shown below:

Table 2. Comparison of car following models

Advantage	Disadvantage

Criteria	Gipps model	Krauss model	IDM model	Wiedeman
Speed results	Relative high values of Mean Absolute Percentage Error (MAPE) of the speed simulation for other vehicles except two-wheelers	Acceptable values for MAPE	Small values of MAPE for speed simulation for cars.	Acceptable values for MAPE
Acceleration results	Low performance for acceleration profile modeling	Improved Gipps model for better performance and more realistic acceleration profiles	High values when estimating the acceleration at the beginning of the vehicle's entry into the network. High deceleration values during braking.	Acceptable values for MAPE
Density results	The MAPE of the density simulation is low	Improved Gipps model for better performance and more realistic density results	Acceptable values for MAPE	Acceptable values for MAPE
Capacity	Acceptable values	May tend to overestimate capacity.	May tend to overestimate capacity	Acceptable values
Calibration	Small number of parameters to	Small number of parameters to	Small number of parameters to	High number of parameters to

	calibrate.	**calibrate.**	**calibrate.**	**calibrate.**
TTC	**Model used to analyze TTC.**	**Model used to analyze TTC.**	**Model used to analyze TTC.**	**Model used to analyze TTC.**
Two-wheeled vehicles	**Small value of MAPE of the speed simulation for two- wheeled vehicles.**	**Small value of MAPE of the speed simulation for two- wheeled vehicles.**	**Small value of MAPE of the speed simulation for two- wheeled vehicles.**	**Small value of MAPE of the speed simulation for two- wheeled vehicles.**
Type of model	**Deterministic**	**Stochastic**	**Stochastic**	**Stochastic**
Software	**Open source**	**Open source**	**Open source**	**Commercial source**

All of the aforementioned models are proven to provide realistic results for private cars. Relative advantages and disadvantages do exist and are considered in the choice of the present thesis along with the particularities of PMDs that present important similarities to powered two-wheelers. The elimination criteria are described below.

- The Gipps model does not have a high performance in the results obtained for two-wheelers with respect to the acceleration profile, so it has not been taken into account.
- Wiedeman model has a high number of parameters where the number of parameters to be calibrated after a sensitivity analysis proposed by [48] is thirteen (13) parameters of calibration. Therefore, in order to avoid high computational costs in the calibration process, the Wiedman model was not selected.
- IDM model performs well in representing the acceleration profile compared to the Gipps model, but has weaknesses in modeling the accelerations at vehicle entry into the network and in the deceleration process. In the present thesis there are certain characteristics of the database, which are explained in chapter 2. The characteristics of the database show that we have a database in which the average time of each vehicle in the network is 5s, i.e. it is an interval in which the vehicle enters the network, therefore, and because the IDM model does not model with high performance in this interval, it was not taken into account.

Considering the disadvantages of the different models analyzed in table 2, the Krauss model was chosen, because it is an improved version of the Gipps model, which means that it presents a good performance in the acceleration profile. It is a model that has 7 calibration parameters which implies an acceptable computational cost and presents better acceleration results at the input of the vehicle network.

1.3. Lane Changing Models

The limitations of the CFM models are that they only analyze longitudinal movement, therefore, in addition to the CFM models, lane change models were proposed to analyze lateral movement. Initially proposed lane-change models were based on decision rules [46, 56, 39], where the drivers compare the conditions on all antagonistic lanes using a hierarchy of considerations (e.g. downstream lane blockages, vehicle restrictions, obstructions, type of vehicle already using the lane, and speed gains). Other studies such as [57, 51, 58], use the random utility theory to describe the random decision of a driver to change lanes based on the maximization of his utility. These models are commonly estimated using the maximum likelihood approach based on vehicular trajectory data to describe lane selection behavior, and are able to capture trade-offs among various considerations. Several authors proposed discrete lane-change models similar to those used under homogeneous traffic conditions. In [59], a new approach for modeling mixed traffic flows with non-standard vehicles is proposed. The model allows the use of various types of vehicles; including motorcycles, bicycles, and three-wheelers on main streets. In order to take these aspects into account, the model adopts a detailed lateral motion modeling approach in which both longitudinal and lateral movements are covered.

In [60], a division of a lane into a large number of lane stripes, the sub-lanes, is proposed. In the sub-lane model where each vehicle occupies a number of sub-lanes depending on its lateral position and width. This means that a vehicle can have several immediate leaders and, therefore, the car-following model is applied to all leading vehicles and uses the minimum safety speed to ensure safe driving. Sub-lane model is used in mixed traffic conditions, in order to simulate the movement of two-wheeled vehicles more realistically. Results were validated with real data and show a good efficacy. The sub-lane model was implemented in the SUMO software under the label ’SL2015’.

The “sub lane” model, is a recent model that was proposed in [60], this model consists of laterally dividing the traditional lanes into a number of sub-lanes, with the objective of simulating a more realistic behavior for two-wheeled vehicles, so it is a model that can be used for PMDs. In this model, each vehicle occupies a number of sub-lanes depending on its lateral position and width. This means that a vehicle can have several immediate leaders. Therefore, the lane change model applies to all vehicles following a lead vehicle and the minimum safe speed is used to ensure safe driving.. For the case of the lane change model, the “sub lane” model, proposes the following modifications:

1. The number of possible maneuvers to be considered increases, since in the lane change models it is considered that the vehicle can change a maximum of 2 neighboring lanes, but in the case of the sub-lanes, all the sub-lanes that are within the two lanes are

considered, i.e. a higher number depending on the number of sub-lanes to be considered per lane.

2. The number of choices requires new exchanges: (e.g. should a vehicle try to find some space in the right sub-lane to increase its speed or should it move immediately to the left sub-lane when the speed is also higher, but not to the right)
3. When crossing multiple sub lanes in the same maneuver, each of the intervening sub lanes must be checked to avoid collisions.
4. The reasons for changing lanes are no longer mutually exclusive: a strategic change to the right lane does not exclude sub-lane changes in this lane in order to optimize travel speed

This model was initially developed to model mixed traffic behavior that includes motorcycles, and from this model, a more realistic simulation can be made for the following cases

1. For two-wheeled vehicles traveling in parallel in a single lane
2. Vehicles overtaking a bicycle in a single lane
3. Formation of virtual lanes in heavy traffic (3 vehicles running in parallel on 2 lanes)
4. Virtual lane formation for emergency traffic
5. Lateral behavior

Turning to our work, the lateral behavior PMDs within a traffic lane can be well described by the sub-lane model. We use the SL2015 SUMO component that has proven to successfully simulate lateral behavior of two-wheeled vehicles.

1.4. Artificial Neural Networks

Artificial neural networks are inspired by the functioning of biological neural networks. Biological neurons essentially have three components: the cell body, the dendrites that act as channels for receiving signals coming from other neurons, and the axon that is the signal emitting channel of a neuron. The junction point of a dendrite of one cell with the axon of another is called a synapse. At this junction point, which is between cell membranes, there is an exchange of chemical substances and therefore chemical reactions of electrical impulses, i.e. a complex process of transfer of information [53]. Based on this functionality, artificial neural networks are able to learn a phenomenon, even complex phenomena. This ability to learn even complex phenomena makes it possible to study phenomena such as transport. In the case of transport, neural networks was successfully used in user route choice modeling, in traffic volume modeling and prediction, for intersection delay prediction, in gas emission prediction, etc.

1.4.1. Basic neuronal network

Artificial Neural Networks receive a vector as input and, after some transformation, produce an output vector. Like any function they can represent a phenomenon if their parameters are chosen correctly [48]. Their main advantages are:

1. Neural networks do not have an a priori form for the function, which implies that the network, through a process called learning, takes the form of the phenomenon from the information of the input data.
2. Neural networks can have any complexity, the networks can in theory take any form however complex it may be.

A model of an artificial neuron includes the essential characteristics and is formulated by means of the following diagram:

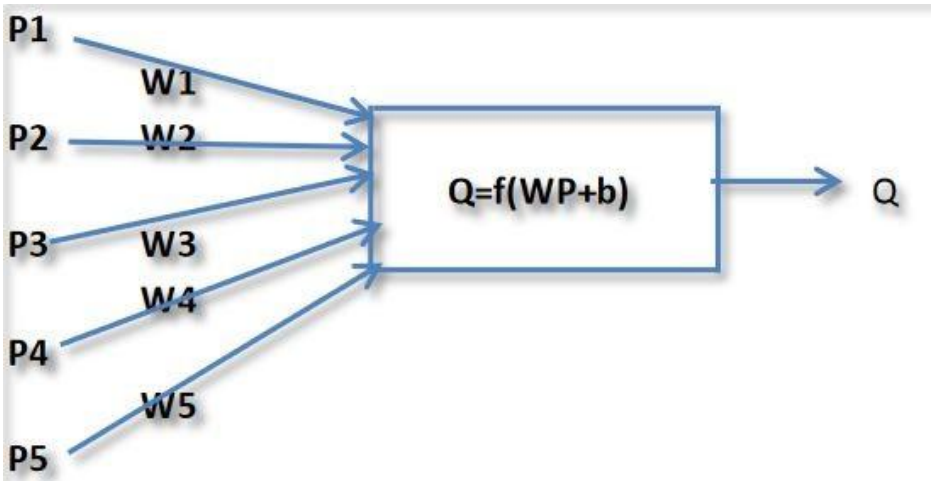

Figure 16. ANN Diagram

The vector $P = [P1, P2, \ldots, Pn]$ represents a set of n signals, where each of them inputs to the neuron through the corresponding dendrite; the associated number is w_k called weight. The set of dentrites corresponds to the vector of weights $W = [W1, W2, \ldots, Wn]$. When a P signal vector arrives to the neuron, the process that follows inside the cell body, it is represented by the sum of the products of each signal by its weight, added to a value called the gain or bias of the neuron. All this is represented by the following transformation:

$$WP + b = w_1 p_1 + w_2 p_2 + w_3 p_3 +, \ldots + b \qquad \text{Equation 9}$$

1.4.2. Activation functions

The activation function defines the relationship between the input and output signal of each network. In theory, all derivable functions can be activation functions. Among the most common transfer functions used in the design of neural networks are the following:

Table 3. Activation functions

Name	Function
Logistic, sigmoid	$\sigma(x) = \frac{1}{1+e^{-x}}$
Hyperbolic tangent (tanh)	$\tanh(x) = \frac{e^{x}-e^{-x}}{e^{x}+e^{-x}}$
Rectified linear unit (RELU)	$(x)^{+} = \begin{cases} 0 \; if \; x \leq 0 \\ x \; if \; x \leq 0 \end{cases}$ $= \max(0, x) = x1_{x>0}$
Softplus	$\ln(1+e^{x})$
Gaussian	$e^{-x^{2}}$

The processing of an input neuron through the activation function gives an output of each neuron. However, each neuron output in the network communication system between neurons has its own weight coefficient. Network training is a nonlinear minimization problem that iteratively changes the coefficients of the neuron weights in order to reduce the discrepancies between the desired and obtained values of output network results.

1.4.3. Deep Learning

Deep learning is among a larger family of machine learning methods based on artificial neural networks with rich representation learning. This learning can be supervised, semi-supervised or unsupervised [61].

The adjective "deep" in deep learning means the use of several layers in the network. Unlike non-deep neural networks where one has a linear perceptron that cannot be a universal classifier, but a network with a non-polynomial activation function and a hidden layer of unlimited width. Deep learning is a state-of-the-art variant that concerns itself with an unlimited number of layers of bounded size, which allows for practical application and optimized implementation, at the same time preserving theoretical universality under soft conditions. In deep learning, layers are also

permitted to be heterogeneous and deviate extensively from connectionist biologically informed models, for the sake of efficiency, trainability, and comprehensibility.

The main deep learning architectures of deep neural networks are deep reinforcement learning, recurrent neural networks and convolutional neural networks. These architectures have been applied to fields such as computer vision, speech recognition, etc. The literature review shows that deep recurrent neural networks were used for traffic simulation, specifically Long-Short Term Memory neural networks, since they are deep neural networks used for time series [61, 53].

1.4.3.1. Long Short Term Memory

Neural networks have been extensively used for traffic prediction and have been compared to conventional statistical models. Results indicate that neural networks can be more accurate predictors than classical time series models. Among deep neural networks of time series, one of the most commonly used is the Long Short Term Memory LSTM. [62] used LSTM to model the longitudinal behavior of a vehicle as an alternative to CFM. The model was estimated using the NGSIM dataset [63] and takes into consideration the asymmetric driving behavior to produce more realistic traffic simulations. The calibration was performed by comparing real to simulated trajectories. Results showed that the LSTM neural network can well reproduce traffic conditions. The use of LSTM is based on the fact that a driver makes a decision based on scenarios in which the driver has been subjected to before, i.e. the driver has a short and long term memory that allows the driver to make a new decision.

The impact of driving memory on longitudinal behavior, in particular historical driving memory, was analyzed by [50]. The authors employed an LSTM neural network to investigate the relationship between driving memory and car following behavior. Results show that LSTM neural network model can learn the driving memory information. The prediction accuracy was found to be higher compared to the Gipps model. The use of LSTM for lateral behavior modeling was also compared to lane-changing models in [64] and [61]. Again, LSTM neural network model showed higher performance compared to conventional lane change models. In [65] the authors proposed an LSTM neural network to model the two basic behaviors simultaneously (i.e. Car following and Lane Change) using the I-80 trajectory data of NGSIM dataset. The authors conclude that the neural network- based model is able to simulate the trajectory of a vehicle more realistically than classical models.

Regarding the case of PMDs, no model has been proposed for microscopic simulation. Since the LSTM neural network allows to model with high performance the longitudinal and lateral behavior in the case of other vehicles, in this article the input and output variables of the model are defined and the structure of a LSTM neural network is proposed to model both behaviors.

1.5. Conclusion

This chapter has provided an overview and comparative analysis of microscopic models used to describe and predict the behavior of drivers and pedestrians. The models used in the present thesis were presented in further detail, namely (i) the Social Force Model in continuous space, (ii) the Krauss model for longitudinal behavior, and (iii) the LSTM model for both lateral and longitudinal behavior. The implementation methodology, along with the datasets used, is presented in the following chapters. It is worth noting that the calibration of those models in the particular case of PMDs is a novelty introduced by the present thesis.

Chapter II

Data Collection

This chapter provides the different data collection technologies and databases used for the present research, as well as the traffic scenarios considered. The first part describes existing data collection technologies and justifies the choice of camera recordings as the main data collection technique. The second part describes thoroughly the data collection methodology. An initial overview of the methodology is shown in Fig. 6 and mixes existing and newly created databases, sites from 3 European countries, different experimental settings (on site or semi-controlled experiment), and diverse traffic scenarios from urban intersections to pedestrianized areas.

A database of data collected at intersections in Germany is available from this technology, which will allow validation of the vehicle-PMD interaction model. As for the other databases, they have been obtained using data processing tools as explained in the methodology. These obtained databases have been used both for calibration and to validate the model proposed in chapter 4.

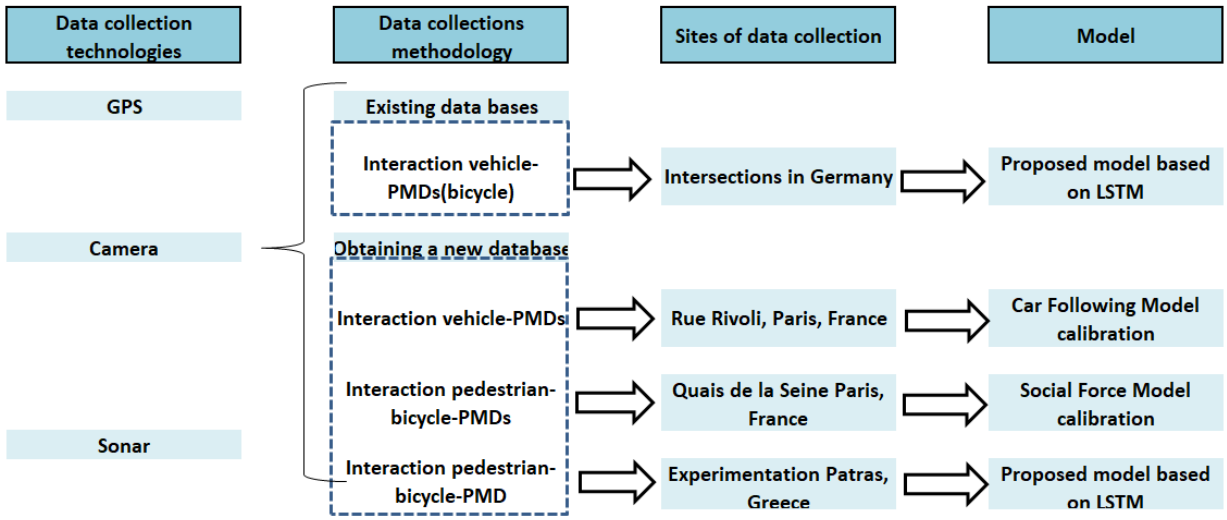

Figure 17. Data collection structure

2.1. Data collection technologies

Different methodologies for collecting data were evaluated in order to select the most relevant ones with the objective of simulating the interactions of PMDs with vehicles. In this context, we found three types of sensors that could achieve the objective: GPS, cameras and sonar. A comparative table with the advantages and weaknesses has been made, as shown below:

Table 4. Comparative of data collection technologies

Methodology	Advantages	Disadvantages
GPS	Easy installation. Low cost.	Metric precision, Not possible to measure interactions with other modes. Needs the approval of user.
Camera	Large database. Data from other modes/users. Centimeter accuracy. Methodology already applied in [51]	Local measure. Installation somewhat complicated, authorizations are necessary.
Sonar	More relevant for car following model. Database depends on the number of sensors in different vehicles. Possible model to analyze TTC. Adaptation to different scenarios.	Metric precision. Not possible to measure interactions with other modes

Between the different options, the collection of data through cameras was retained, because it allows us to have a centimetric precision for the trajectories and it is a methodology in the literature review that has been half-automated in [50] and that has been used to make adaptations of the microscopic simulation models of the bikes in [52]. This methodology that was selected consists of the installation of a camera, which allows filming of different movements in a determined place. Another important criterion is the fact that cameras capture all road users and their interactions which is one the thesis objectives.

2.2. Data collection methodology

To obtain the data, the image processing methodology was chosen. That is why in the thesis a software ”µ-scope” was developed to automate the acquisition of trajectories of vehicles, bicycles

and PMDs. The different functionalities and steps to be followed to obtain the trajectories are detailed below.

2.2.1. Preprocessing

Step 1: Create background from video In this step a random frame is obtained from the video, this frame will be used to determine the points corresponding to a plane image in real measurements.

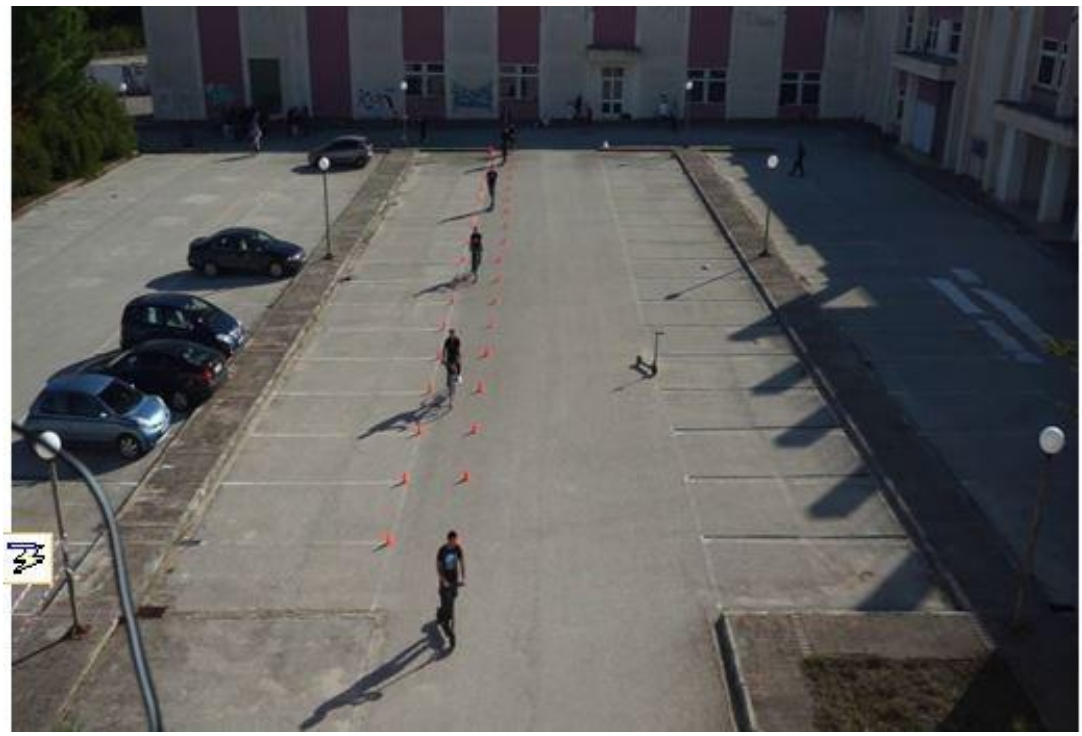

Figure 18. View of the camera

Step 2: Define analysis area this step consists of indicating the area from which the trajectories are to be obtained, i.e. a mask is defined that defines the analysis area.

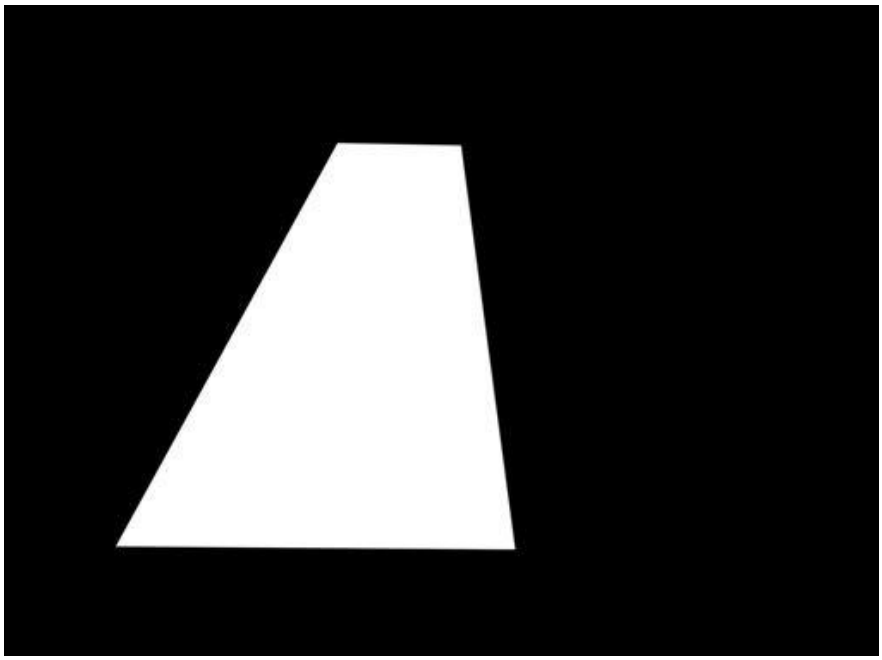

Figure 19. Mask to define the analysis area

Step 3: Get camera calibration file (.tcal) In order to transform the trajectories extracted from videos to trajectories with real measurements, the T-Analysis software developed by [35] was used. Specifically, the T-Calibration module was used to obtain the camera parameters in order to obtain the trajectory with real measurements. The trajectory transformation methodology is extensively explained by [53] and consists of defining some reference points in the camera view and the image with real measurements as shown below:

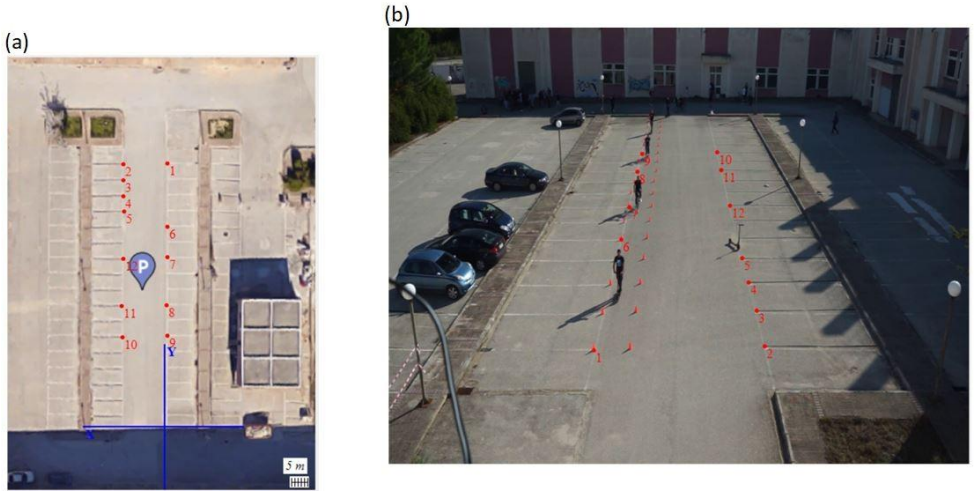

Figure 20. Calibration of camera

2.2.2. Processing: Trajectory extraction

The automated extraction of trajectories is divided into three parts, (1) object detection, which is represented by a frame border, (2) object tracking and (3) obtain trajectories with real measurements. Trajectory extraction in our work is based on yolo v5 (You Only Look Once) proposed by [54] for object detection and classification. YOLO models are able to detect objects with high accuracy, can be used in real time and are based on convolution neural networks-CNN. Yolo uses a single neural network to process the whole image, then the image is divided into equal parts and in each of these parts an object probability is calculated. Then a max-non suppression is performed to ensure that the object detection is not repeated. In our work we have used the pre-trained model YOLOv5m. This model is able to detect and classify cars, bicycles, pedestrians, buses, trucks. However, it is not able to identify a bicycle and bicycle rider as a single object nor an e-scooter and an e-scooter rider as a single object. That is why some algorithms were developed to detect the bicycle and its rider as a single object and similarly for e-scooters. In addition, an algorithm based on acceleration classification was developed to differentiate a bicycle from an e-scooter. The latter is one of the contributions of the thesis that could be used for further research and future PMD analyses.

For the object tracking process, i.e. to associate a bounding box detected in one frame of the video with another bounding box in another frame of the video, deep SORT (Simple Online and Real-time Tracking) proposed by [55] was used, which is an algorithm that has shown remarkable results in the Multiple Object Tracking (MOT) problem.

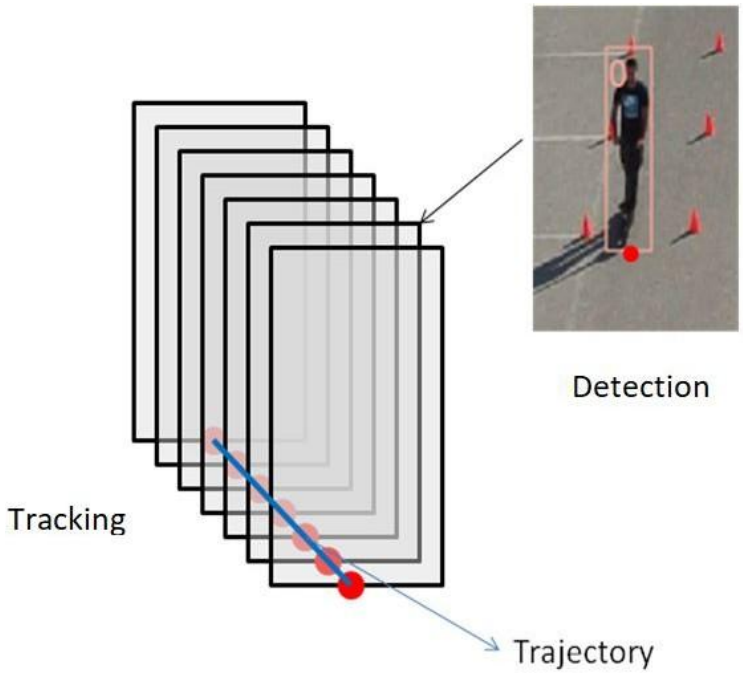

Figure 21. Methodology of detection/tracking

Finally, based on the .tcal file containing the camera calibration data and the trajectories of the tracking process, we can obtain the trajectories with real measurements and can perform statistics of velocities and accelerations of each detected object.

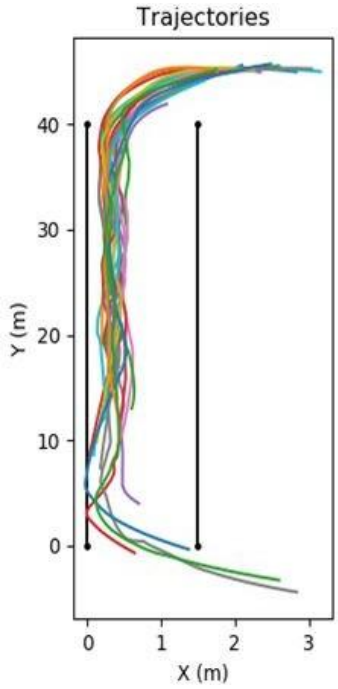

Figure 22. Results of trajectories

2.2.3. Validation of software "μ-scope"

The validation of the software developed during the thesis was studied in [56]. In which the acceleration results obtained through the μ-scope software and the acceleration results obtained through an application installed called Phyphox on the cell phones of the participants to the experiment were compared. The Phyphox app [57] is used to provide acceleration estimation of moving objects using the built-in sensors in every smartphone.

In the paper, the calculated acceleration rates of μ-scope and Phyphox were compared by error analysis and with the use of RMSE. The RMSE analysis was performed for different scenarios, explaining in which scenario the best performance of the u-scope software is obtained. The overall results validate the algorithm used by u-scope based on image analysis indicating that μ-scope is reliable in all micromobility configurations, both in unidirectional and bidirectional bicycle lanes.

For example, Figure 23 shows a comparison of the accelerations for one of the e-scooters in the experiment along with the corresponding velocity along time. Similar results can be observed for the acceleration curve with close values and following the same trend.

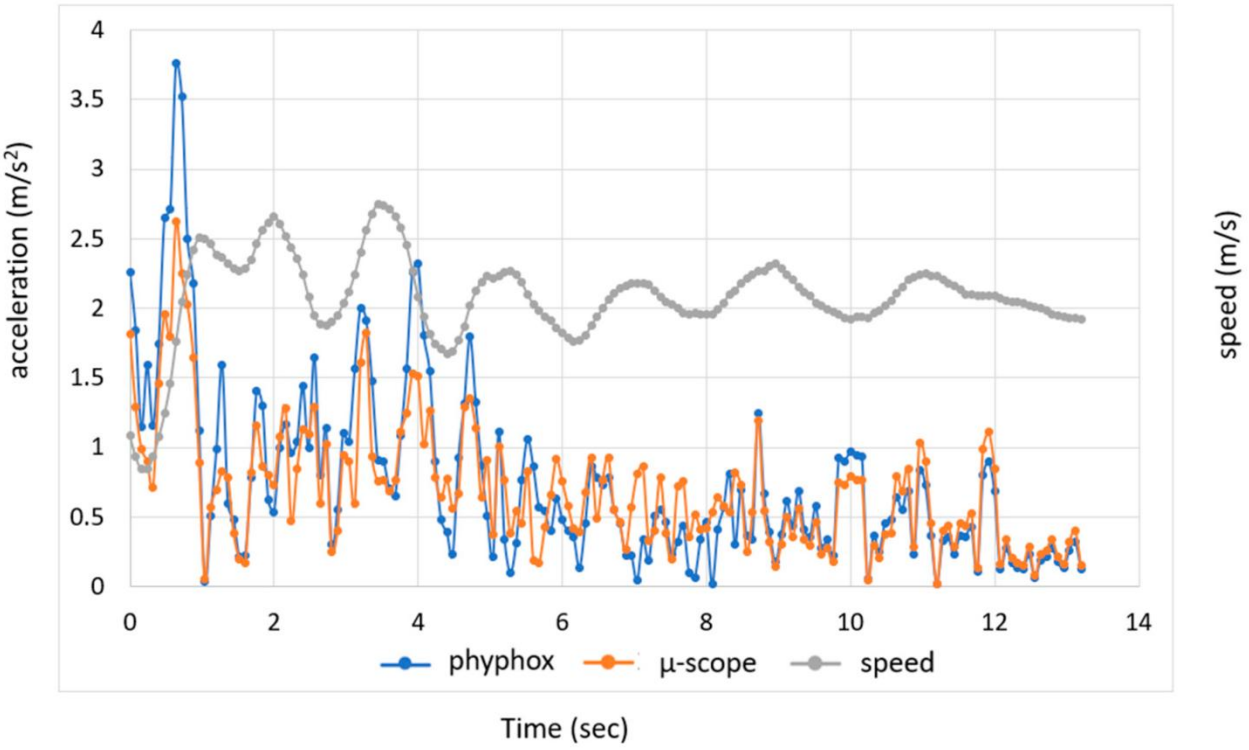

Figure 23. Comparison of μ-scope and phyphox software acceleration of an e-scooter

Consequently, the μ-scope can be considered reliable for all velocities in the 0-25 km/h range. It can also be observed that as the e-scooter approaches the camera the divergence decreases. Therefore, we can reasonably assume that the estimation accuracy decreases with distance, with a critical point at about 30 m from the camera, so a recommendation is also made regarding the camera location as a larger distance from the camera increases the estimation error.

2.3. Sites of data collection

In this section we present the different traffic scenarios considered along with the methodology of data acquisition for all cases.

2.3.1. Pedestrians and PMDs interactions

The study area is a large (approximately 60-meters) pedestrianized corridor along the river Seine "Quais de la Seine", in Paris (Figure 24). It was selected in the objective to observe a maximum number of interaction situations between e-scooters, two-wheelers, and pedestrians. It consists of an old expressway where motorized traffic was prohibited in 2016. Main travel purposes observed on the site are tourism, leisure and, secondarily, commuting.

The data collection methodology is presented in detail in [37] and [70]. It consists of 45 minutes camera recording totalizing 6,320 e-scooter position registrations. The level of analysis was at 20 frames per second and interactions were observable every 5-10 seconds.

Figure 24. Study area for pedestrian interactions (Quais de la Seine)

An ad hoc image analysis process was implemented to track the moving objects and extract their trajectories. The Urban Tracker software [67] was used to tag videos and label each object in the video recording. The results produced by the software were stored in a database, saving the position information at each period. Figure 25 shows a set of random trajectories after labeling the video with Urban Tracker software. Figure 26 shows the trajectories of the same video frame in plane after image processing.

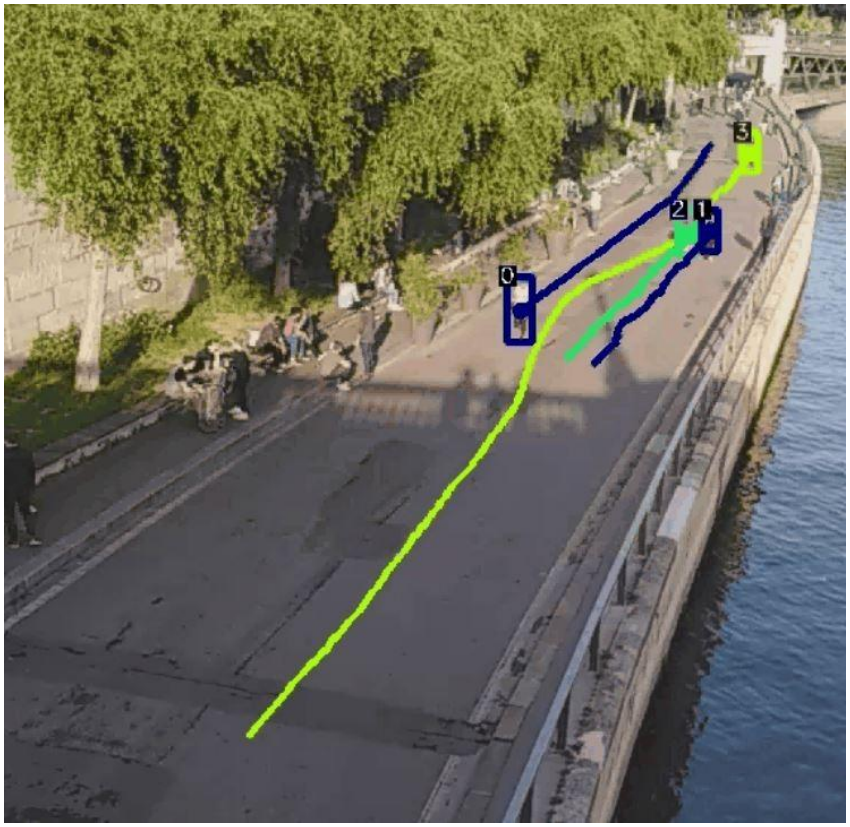

Figure 25. Trajectories in video frame: Greenyellow color = e-scooter; Blue and green = pedestrian.

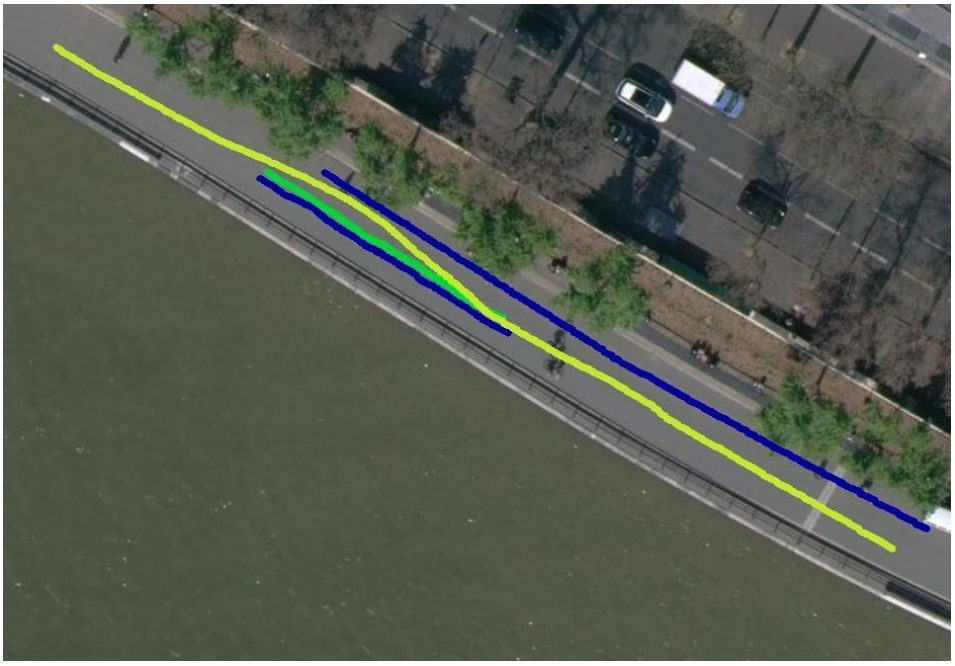

Figure 26. Trajectories in plane: Greenyellow color = e-scooter; Blue and green = pedestrian.

2.3.2. Vehicles and PMDs interactions

The study area is a 50-meter stretch of an urban street, the Rivoli Avenue in Paris, France (Figure 27). The right lane is a dedicated bus lane with permissive access to bicycles and taxis. The left lane is a two-directional cycle path. The central lane accommodates general traffic. A heavily used pedestrian crossing obliges vehicles to stop regularly. The site was selected in the objective to observe a maximum number of interactions among road users.

Figure 27. Study area and view of camera for interactions with vehicles (Rue Rivoli)

A recording of 30 minutes was made and provided 6,120 e-scooter position registrations.

The traffic composition is distributed as follows: 55% cars (595 veh/h), 16% bicycles (176 veh/h), 11% motorcycles (116 veh/h), 17% scooters (178 veh/h), and 1% buses (6 buses/h).

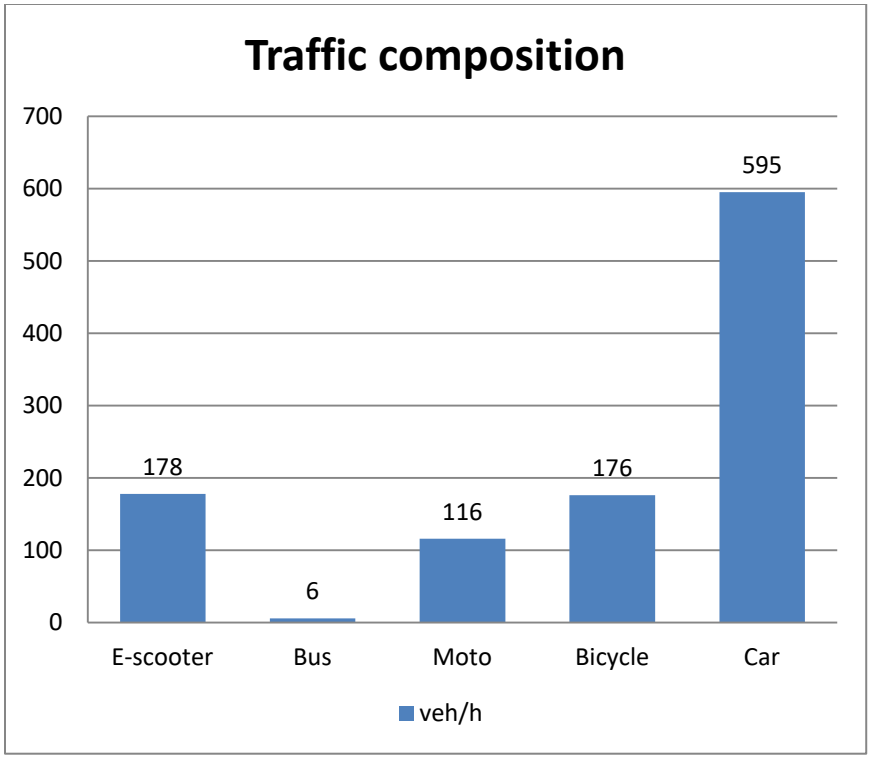

Figure 28 : Traffic composition for interactions with vehicles

2.3.3. PMDs behavior in cycle path

Neural networks need large databases for training and validation; and the previous record- ings were not sufficient for this purpose. Instead, we used inD database obtained by [58]. This database contains vehicle trajectories from urban and interurban intersections in Germany, captured from UAVs. We developed and implemented a suitable methodology for the extraction of the input data (i.e. mainly position in the X and Y directions) and the definition of the architecture of the neural network.

Our database includes 4 geometrical configurations (Figure 29) and 32 traffic scenarios, i.e. recordings at different times of the day. Configurations a and d are interurban, while configurations b and c are in urban contexts with important PMD (i.e. bicycle) flows.

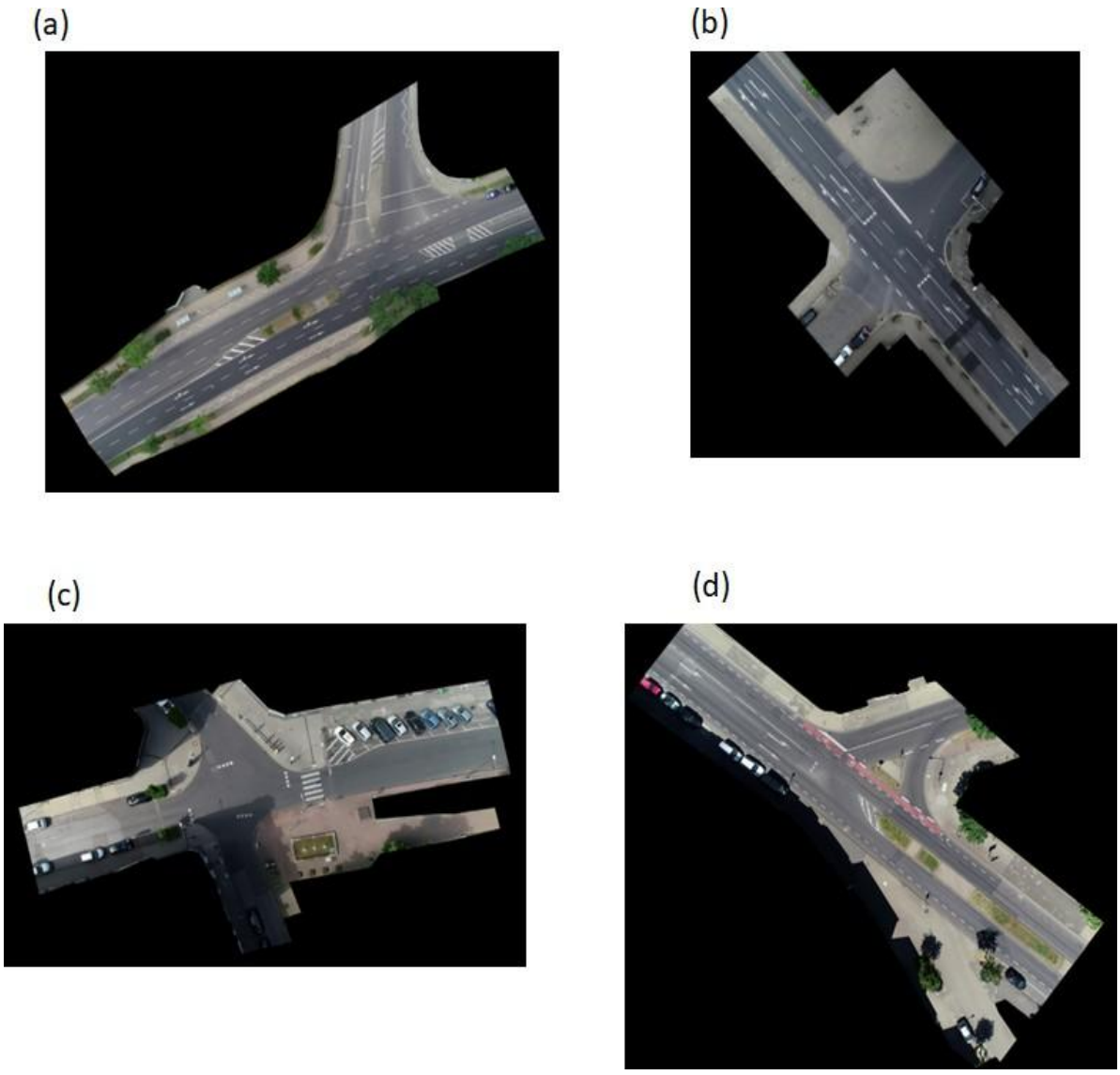

Figure 29. Scenarios of the InD (Intersections in Germany).

A preliminary analysis of the dataset gives the results of Figure 30. The duration of each video recording is in the Range of 10-22 minutes. We observe the dominant presence of private cars in all scenarios and particularly scenarios 1 and 4 (interurban intersections). As expected, a significant number of pedestrians and PMDs is observed in scenarios 2 and 3 (urban intersections).

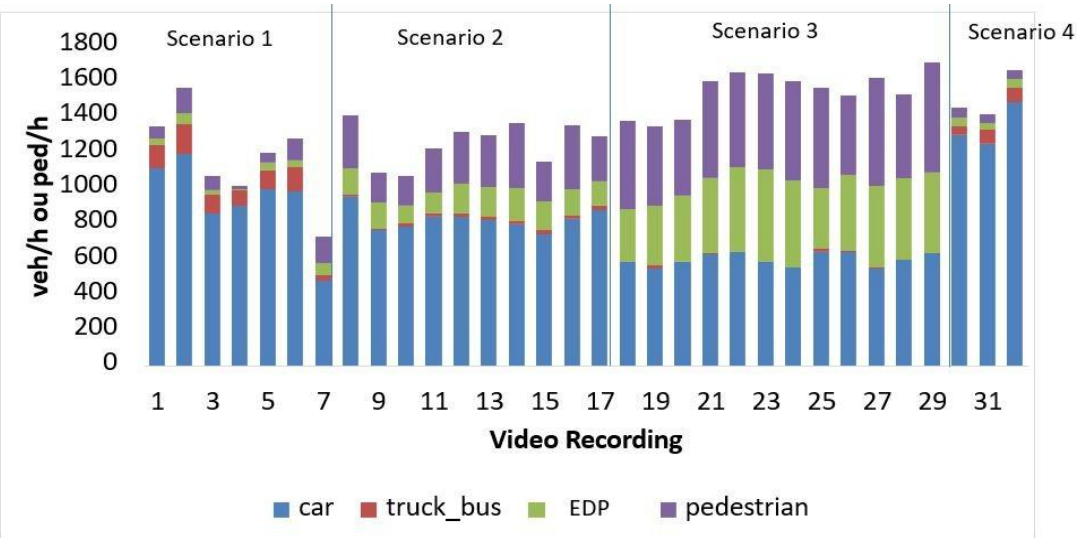

Figure 30. Traffic composition of each scenario from InD Dataset .

The InD dataset does not contain exact information about the lane number where the vehicle is located, therefore, a python-based algorithm was developed ad hoc to graphically represent the lane number and classify the position of vehicles in each lane number. This process was realized because this information is needed as an input variable to the neural network.

2.3.4. Semi-controlled scenario

A real-track experiment was designed and realized for the purposes of this research in a semi-controlled environment. The experiment was conducted in the campus of the University of Patras, Greece, with over 100 participants who received specific indications for the scenarios considered to simulate. In Figure 31, four(4) scenarios are observed and that have been conducted: (a) One-way bicycle path where interactions between bicycles and PMDs can be observed, (b) One-way bicycle path and a crosswalk where interactions between bicycles, PMD and pedestrians crossing the bicycle path can be observed, (c) shared road between pedestrians, bicycles and PMDs in the same direction where interactions between them can be observed, (d) shared road between pedestrians, bicycles and PMD in the same direction and with pedestrian crosswalks where interactions between them can be observed. Participants were asked to circulate freely on each shared space at the speed of their convenience and in low, medium, and high traffic conditions.

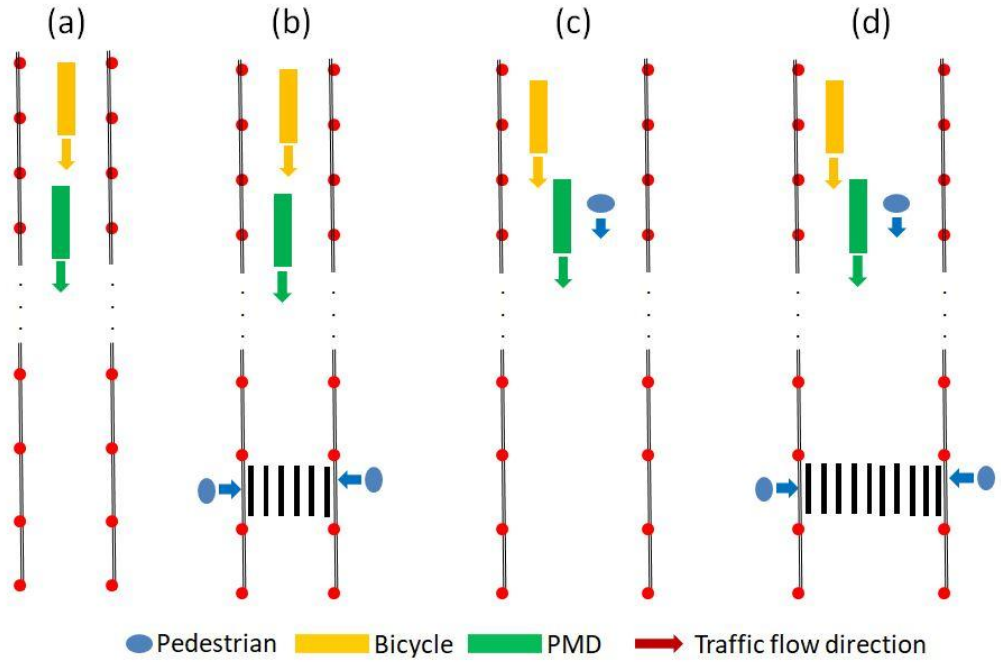

Figure 31. Scenarios: (a) bicycle lane, (b) bicycle lane with crosswalk, (c) road pedestrian, (d) road pedestrian with crosswalk

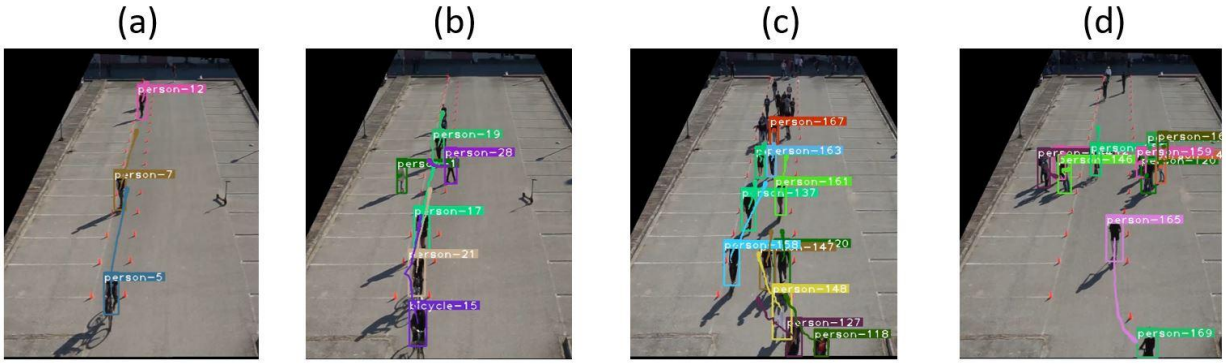

Figure 32. Camera view: (a) bicycle lane, (b) bicycle lane with crosswalk, (c) shared road, (d) shared road with crosswalk

Data was obtained through video recordings and view of each of the scenarios is presented in Figure 32}. Posterior automated methodology post-processing image processing was developed ad hoc and allows for the automatic extraction of all moving objects individual trajectories (see Figure 33 and, thus, positions, speeds, accelerations in each time step and travel time.

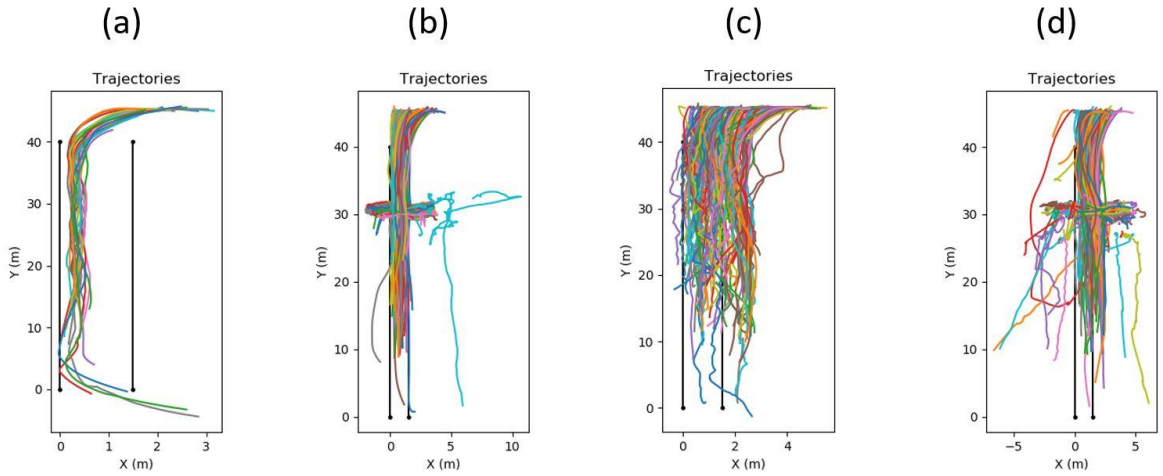

Figure 33. Trajectory extraction: (a) bicycle lane, (b) bicycle lane with crosswalk, (c) shared road, (d) shared road wit

2.4. Conclusion

In this chapter we analyzed the different data collection technologies, concluding that the most suitable technology to obtain the trajectories is by the use of cameras. To obtain the trajectories through cameras, image processing was used, in this context µ-scope software was developed that uses deep artificial neural network to detect and track vehicles including e-scooters.

This software has allowed to obtain the databases composed of positions, velocities and accelerations, which will allow us to calibrate and validate the different scenarios, will be obtained. The scenarios included are: (1) Pedestrian-PMDs interaction (Quais de la Seine), (2) vehicle-PMDs interaction (Rue Rivoli), (3) only PMDs behavior (InD dataset) and (4) pedestrian, bicycle and PMDs interaction (semi-controlled environment). Based on the data from each scenario, the next chapters analyze existing models and propose two new models.

Chapter III

Calibration of selected existing models

3.1. Interaction between pedestrians and PMDs

The idea of Social Force Model (SFM) is to consider that behavioral changes can be explained by force fields exerted on the moving object; i.e., the person varies his/her behavior due to external forces. This is the basic idea of microscopic pedestrian simulation. SFM is a continuous microscopic model of social forces proposed initially by [24], where pedestrian behavior is affected by the forces of the environment and other moving objects. These forces cause the pedestrian to make two levels of decision, the strategic decision that involves determining the minimum distance between his departure point and destination point and the tactic decision that is a consequence of his interaction with his environment. According to SFM, the movement of pedestrian i is driven by three forces as shown in (Fig 1):

1. term f_i^d describing the acceleration towards a destination d i.e. the object tries to reach its desired velocity by accelerating or decelerating,
2. repulsive forces exerted by j other individuals f_{ij} and w obstacles f_{iw}; and
3. a term f_i^amodeling attraction effects of a group of pedestrians a. The resultant of these forces $F_i(t)$ represents the motivation of a pedestrian to move with a specific orientation and magnitude of movement. This model was initially developed for low pedestrian densities, but posterior improvements were made to include diversified traffic contexts.

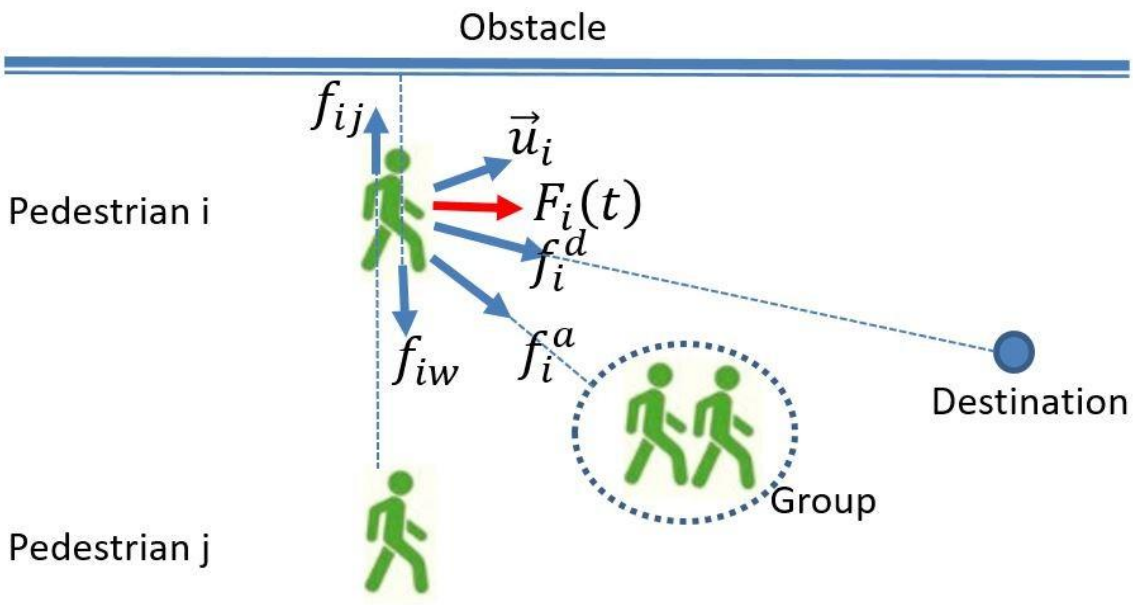

Figure 34. Forces exerted towards a pedestrian i(SFM).

It's means the movement of a particle i is a result of all the forces with which the pedestrian interacts. The resultant force $F_i(t)$ at time t, can be expressed as follows:

$$F_i(t) = f_i^d + \sum_{other\ particles\ j} f_{ij} + \sum_{obstacles\ w \to i} f_{iw} + \xi \qquad \text{Equation 10}$$

Where:

- f_i^d : the propelling force to conduct the object towards its objective;
- f_{ij} : the repulsive force from object j;
- f_{iw} : the repulsive force from obstacle w;
- ξ: the error of the model.

3.1.1. Strategic level: route choice

The propelling force is expressed as follows [24]:

$$f_i^d = \frac{\vec{v}_{i_{des}} - \vec{v}_i}{\tau_i} \qquad \text{Equation 11}$$

where:

- $\vec{v}_i$ is the observed speed of object i;

- $v_{i\,des}$ is the desired speed of particle j;
- τ_i is relaxation time (property of particle i), which determines the ability of the particle to follow its desired trajectory in case of disturbance.

Through $v_{i\,des}$, a will must be conferred to the objects. Several strategies have been proposed, including behavior rules or heuristics as in [23, 10, 72]. However, these rules presume knowledge about the interaction processes, or addition of new parameters to the model which requires a supplementary drive of calibration.

3.1.2. Tactical level: interaction with environment (obstacles, other particles)

As a first approach, a simple expression of repulsive force is proposed:

$$\vec{f}_{ij} = g(\theta_{ij}) A_{ij} \exp\left(-\frac{d(i,j)}{B_{ij}}\right) \vec{n}_{ij} \qquad \text{Equation 12}$$

where:

- $d(i,j)$is the distance between object i and j ;
- $\vec{n}_{ij}$ is the unit vector, oriented from i to j ;
- A_{ij} and B_{ij} are parameters that respectively adjust the amplitude of the strength, and the span;
- θ_{ij} is the angle between the direction of object j and object i.

We chose to make parameters A_{ij} and B_{ij} dependent upon both object i features and object j features. This allows us to distinguish interactions between (i) pedestrian and pedestrian, (ii) pedestrian and e-scooter, (iii) e-scooter and pedestrian, and (iv) e-scooter and e-scooter. These parameters will be determined in this article, by calibration methods.

$g(\theta_{ij})$ is a function to represent the anisotropy of the perception of the objects as humans are usually more attentive to the oncoming environment ahead than to the environment in the back. We propose here to use a commonly spread expression [24, 22, 23].

$$g(\theta_{ij}) = \left(\lambda_j + (1-\lambda_j)\frac{1+\cos(\theta_{ij})}{2}\right) \qquad \text{Equation 13}$$

Where λ_j is a parameter, so as that λ_j = 1 implies that the perception of object j is fully isotropic, and, on the contrary, λ_j = 0, that the perception is particularly anisotropic. A similar expression is used for repulsive forces from permanent obstacles.

The calibration process consists in determining the optimal parameters of the proposed model to obtain the lowest error between the simulated data and the real data i. e. a minimization process that depends on the simulated and real data, as follow:

$$min\ f(T_{obs}, T_{min}) \qquad \text{Equation 14}$$

The function f(.) is the metric of the error between real and simulated data.

In this work RMSE is used as an error metric to measure the performance of SFM, which allows to compare real to simulated pedestrian trajectories [22].

$$min\ f(T_{obs}, T_{min}) = min\ RMSE = \sum_n (T_{obs} - T_{min})^2 \qquad \text{Equation 15}$$

Where T_{obs} is pedestrian trajectory from the database and T_{min} is pedestrian simulated trajectory based on a vector $\vec{p}$ containing the parameters to calibrate SFM. Based on Equations, SFM parameters for pedestrians and PMDs (e-scooters) are calculated taking into account that parameters abide by log-normal law to avoid negative values.

- free speed V_0 for pedestrians and e-scooters;
- relaxation time τ for pedestrians and e-scooters;
- matrix of amplitude of repulsive forces $A_{i,j}$;
- matrix of spans of repulsive forces $B_{i,j}$

The λ_j parameter was calibrated in [35] for the case of pedestrians and found to be equal to 0.06. For the case of e-scooters in [22] λ_j was fixed to 0.56. These two values were introduced in the present analysis.

Different optimization algorithms exist to determine the minimum of Equation 18. Cross-Entropy method (CEM) is used following [22]. CEM is a general Monte-Carlo type optimization method and is composed of the following two phases:

Initialization. Initial value for the vector $\vec{p}$ of parameters

At each iteration:

1. we generate a set of values of the model parameters: free speed, relaxation time, amplitudes and spans of repulsive forces randomly taken following the probability distribution in accordance with current assessment of parameters ;
2. for each set of parameters generated in step 1,
3. we make simulations giving initial conditions from experimental data ;
4. we compare simulation outputs with experimental data thanks to the computation of RMSE; simulations are sorted in accordance with their RMSE;
5. we only keep ρ of the best simulations ;

6. we update $\vec{p}$ using unbiased estimators on the set of parameters associated with remaining simulations.

We stop when average RMSE of simulations stop decreasing and when the values of $\vec{p}$ are converging. Let us notice that simulations are made on selected configurations observed on the experimental site that are chosen in order to represent typical behaviors (frontal avoidance, overtaking.).

3.1.3. Results

The evolution of the RMSE is shown in Fig. 14 where we observe that convergence of the algorithm is reached. Likewise, Fig. 15 shows the parameters mean value and standard deviation for the first trajectory.

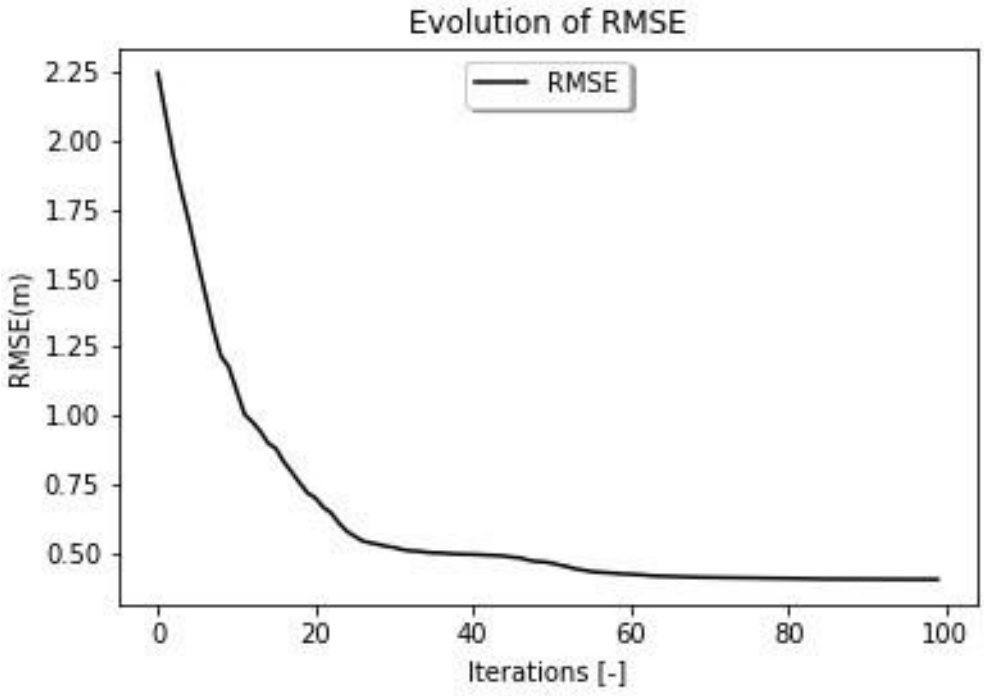

Figure 35. Calibration process: evolution of average error

At the end of calibration process for the 6320 e-scooter positions (20 trajectories), all parameters seem to converge towards a stable value.

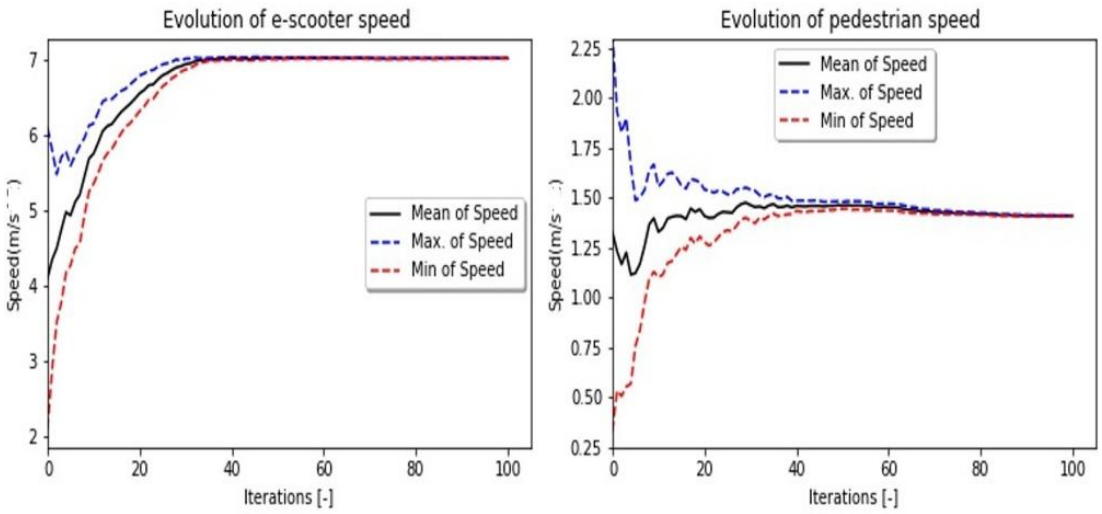

Figure 36. Calibration process for free speed of pedestrian and e-scooter

Calibration results for the 20 trajectories of pedestrians and e-scooters are presented in Table. 1

The free speed for pedestrians was estimated at 1.65m/s(±0.37SD), higher than the usual speed for pedestrians which has a range between 1.1m/s and 1.4m/s [7] The high value of the free speed can be explained by the lack of distinction between running and walking pedestrians. Indeed, many Parisians use the banks of River Seine for jogging and this was confirmed in the video footage.

Table 5. LSTM deep neural network-based model for the modeling of interaction between vehicles and PMDs- Parameters estimation results

Parameters	Pedestrian avoiding e-scooter	E-scooter avoiding pedestrian
$v_0(m/s)$	1.65($\pm$0.37)	5.34($\pm$0.89)
$A(kg.m/s^2)$	320($\pm$140)	414($\pm$256)
$B(m)$	0.44($\pm$0.15)	0.60($\pm$0.41)
$\tau(s)$	0.25($\pm$0.08)	0.19($\pm$0.08)

The free speed of e-scooters is estimated at 5.34m/s(±0.89SD), well below the maximum speed limit for e-scooters (i.e. 6.9 m/s) as determined by the French legislation (2019). This may be attributed to the site-specific geometric conditions and pedestrian affluence impeding speeding.

Parameters A and B are estimated (i) for the case of a pedestrian avoiding an e-scooter at 320kg.m/s2 (±140SD) and 0.44m (±0.15SD) respectively and (ii) for the case of an e-scooter avoiding a pedestrian at 414kg.m/s2(±256SD) and 0.60m(±0.41mSD) respectively. This shows that the repulsive force of an e-scooter to avoid a pedestrian is greater than the force of a pedestrian avoiding an e-scooter.

Likewise, the relaxation time was estimated equal to 0.25s (±0.08SD) for pedestrians and 0.19s (±0.08SD) for e-scooters. According to the estimated values for the relaxation time, we notice that the e-scooter drivers react faster than pedestrians.

3.2. Interaction vehicle - PMDs

In the literature review (Section 2), we presented different types of CFM. Their relative performance was evaluated by [49]. The authors concluded that implementing a correct calibration process leads to similar performance metrics for all models. In this work, we have used the Krauss model, implemented in SUMO software, which is essentially a stochastic version of the Gipps model [48]. The Krauss model allows considering two-wheeled vehicles, as explained in [54]. The model formulation for a single lane is given in [47]:

$$v_{safe} = v_l(t) + \frac{g(t) - v_l(t)\tau_r}{\frac{v_l(t) + v_f(t)}{2b} + \tau_r} \quad \text{Equation 16}$$

Where :

v_{safe}: is the safety speed (m/s);

$v_l(t)$: is velocity leader vehicle (m/s);

$g(t)$: is the gap (m);

τ_r : is the reaction time s;

$v_f(t)$: is velocity follower vehicle (m/s);

b : is the deceleration capabilities (m/s2).

If the v_{safe} is higher than the maximum speed allowed on the road or higher than the speed the vehicle is able to reach until the next pass owing to its acceleration capabilities, the minimum of these values is calculated as the resultant speed, called ”desired speed” v_{des}.

$$v_{des} = \min\left[v_{max}, v + at, v_{safe}\right] \quad \text{Equation 17}$$

Where:

v_{max}: is the maximum velocity (m/s);

a: is acceleration capabilities (m/s2);

t: is the step duration of the simulation (s);

Finally, there are two boundary parameters, the minimum gap value g_{min} and the maximum deceleration bemergency under emergency conditions.

The calibration methodology employed is the cross-entropy method (CEM). CEM was used as optimization algorithm and the RMSE as an error metric. Based on Equations 11 and 12 and boundary parameters, in this work we determine the parameters of the Krauss model for PMDs (in particular e-scooters and bicycles), taking into account that parameters abide by log-normal law to avoid negative values. The method is applied to determine the mean and standard deviation of each parameter:

- Acceleration capabilities a_j for e-scooter j;
- Deceleration capabilities b_j for e-scooter j;
- Emergency deceleration $b\_emergency_j$
- Reaction time τ_j for e-scooter j;
- Maximum velocity v_max_j for e-scooter j;
- Minimum gap min_gap_j for e-scooter j;

3.2.1. Results

A sample of 15 trajectories was used for calibration for each iteration that is to say in each iteration a sample of different combinations of parameters produce different trajectories. The results show that from iteration 8 the algorithm arrives at convergence Figure 37.

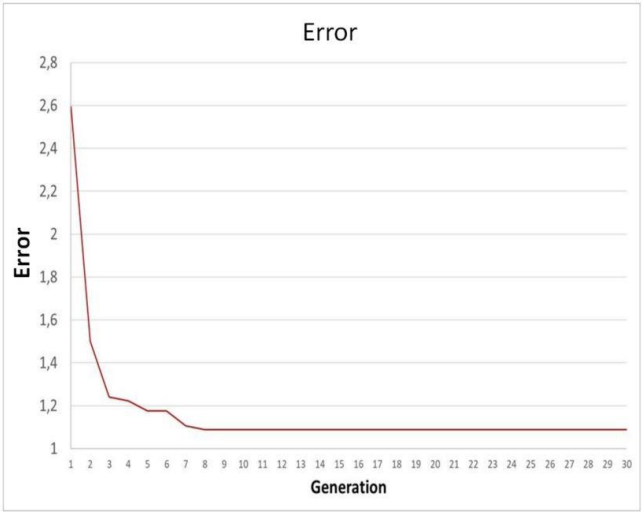

Figure 37. Model Interaction vehicle and PMDs - Calibration process

The six (6) calibration parameters of the car- following model (Krauss model) were thus calibrated. The optimal parameters show an intermediate behavior between a bicycle and a moped. The error of the real trajectory is of 1.08m with a standard deviation of 0.54. This value is high because the car- following model, cannot simulate the 'zig-zag' movement and lane-changing that e-scooters and bicycles make. This error can be reduced, if we consider a calibration for the lane change model and the sub-channel model. However, in this case, the number of parameters to be calibrated and optimization time would be greater. In Table 6, we provide the values of parameters for PMDs and other class of vehicles as given in SUMO software:

Table 6. Parameters estimation results

Vehicle Class	Bicycle	Moped	Motorcycle	E-scooter
maxSpeed (m/s)	20	45	200	28($\pm$1.5)
minGap (m)5	0.5	2.5	2.5	0.5($\pm$0.11)
accel (m/s)	1.2	1.1	6	3.5($\pm$0.59)
decel (m/s2)	3	7	10	7.5($\pm$0.8)
emergencydecel (m/s2)	7	10	10	9.6($\pm$1.2)
τ (s)	–	–	–	0.3($\pm$0.1)

Results show that in terms of maximum speed, PMDs are similar to bicycles. Standard deviation is only provided for e-scooters in the software. In relation to minimum gap, PMDs have same behavior as a bicycle, probably because of similar average speed. In terms of average acceleration and deceleration however, PMDs are closer to a moped and a motorcycle, while emergency acceleration is practically equal to the one of moped and motorcycle. This is an intuitive finding due to the electric assistance of e-scooters and comes to verify our initial hypothesis on the hybrid nature of e-scooters.

Chapter IV

Proposed novel models

In the previous chapter, adaptations of car and pedestrian traffic simulation models were studied. High values of the error rate were found between the comparison of the real trajectory and the simulated trajectory. Although high error rates were found, estimating calibration parameters allowed to better determine the behavior of the PMDs and their interaction with pedestrians and vehicles. In this chapter, two novel models are proposed to ameliorate the descriptive force of the existing models: (1) First model combines particle dynamics, social force modeling and LSTM deep neural network-based model for the simulation of interaction between pedestrians and PMDs and (2) LSTM deep neural network-based model for the modeling of interaction between vehicles and PMDs. The choice of deep neural networks is based on the literature review, where it was observed that artificial neural network-based models, mainly deep recurrent neural networks of the LSTM type, performed better than classical traffic simulation models.

4.1. Interaction pedestrians - PMDs

In this part, a new model based on artificial neural networks is presented, specifically in the type of LSTM neural networks. The PMD type considered are bicycles and e-scooters, but the modeled behavior concerns exclusively the e-scooter rider.

The database was generated in a semi-controlled experiment at the campus of University of Patras, Greece and was used for model training and validation. The database is composed of 285 pedestrians (51.5%), 113 e-scooters (20,4%) and 155(28%) bicycles, totalizing 80 451 registers of position, instant speed and acceleration data.

Table 7. Composition of database of semi controlled environment

	Number of pedestrians	Number of e-scooters	Number of bicycles	Number of positions
One-way bicycle path	0	11	12	2088
One-way bicycle path with crosswalk	17	32	31	13325
Shared road	101	28	29	26258
Shared road with crosswalk	167	42	83	38780
Total	285	113	155	80451
Percentage	51,5%	20,4%	28,0%	

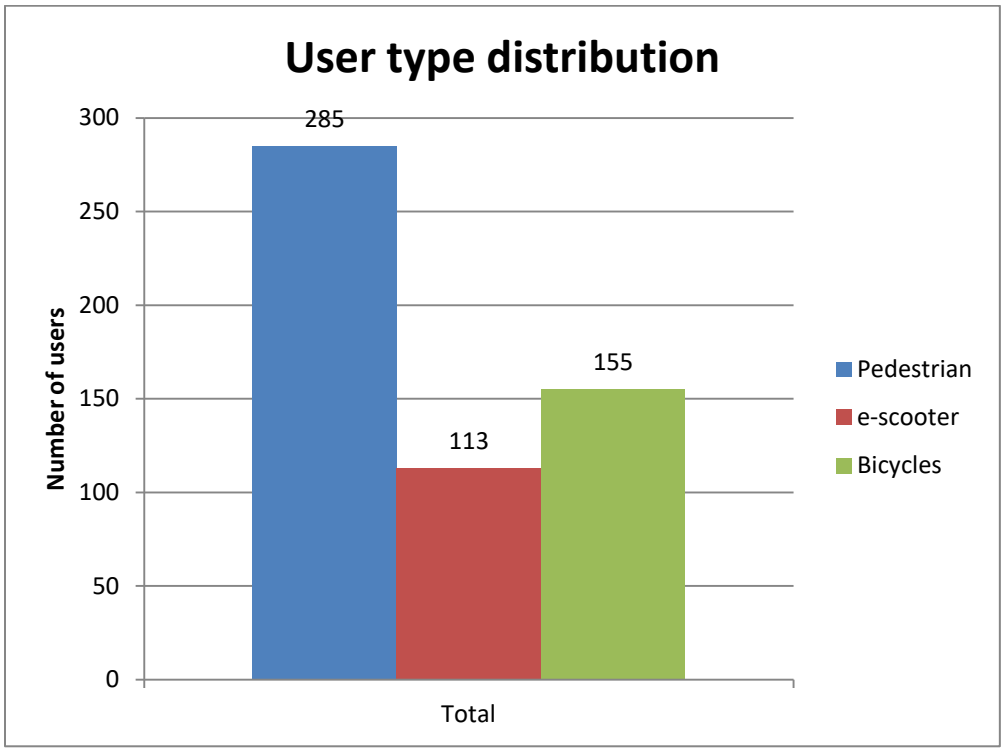

Figure 38. User type distribution in semi-controlled experiment

Based on the database, 75% was used for training and 25% for testing, This chapter presents the proposed model and the results obtained.

4.1.1. Model principle

The model principle combines particle dynamics, social force modeling and neural networks and is detailed below. First, the particle dynamics equation is presented. Then, the space discretization methodology is described and justified.

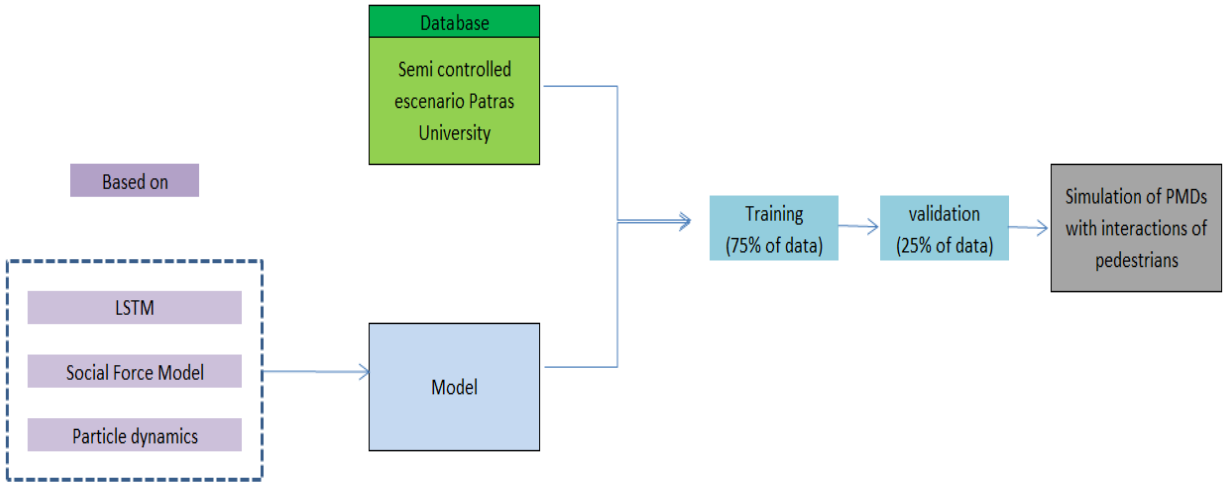

Figure 39. Scheme of new model for simulation interaction PMDs with pedestrian an bicycles

4.1.2. Particle dynamics

The quantity of motion (or linear momentum) of the system is the sum of the quantities of motion of each of the particles. In the proposed model we consider as each particle a pedestrian, a bicycle or a PMD.

Figure 40 shows a general scheme of a scenario in which a shared space between pedestrians, bicycles and PMDs is observed. Each of these road users has a position xi,yi, mass m_i and speed v_i.

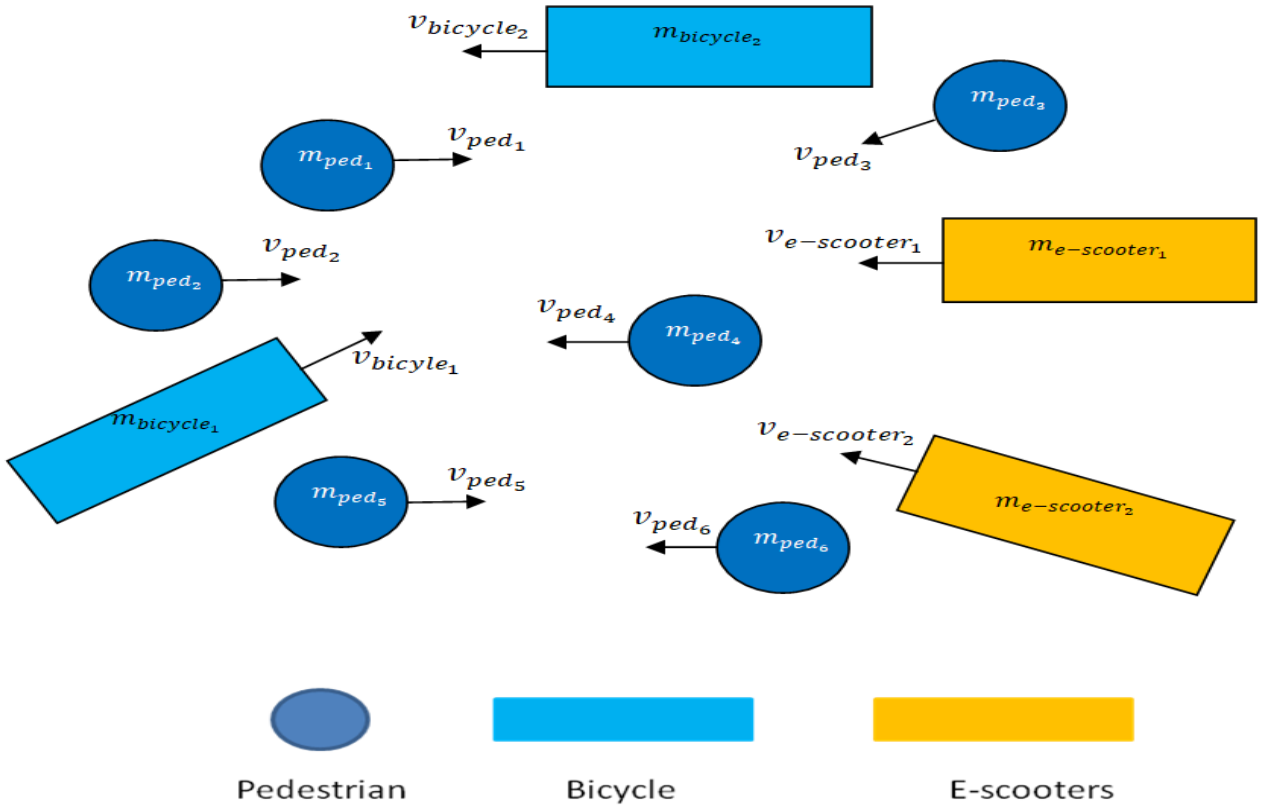

Figure 40. General scheme of quantity of motion

From mass and velocity, the quantity of motion of the center of mass pi can be calculated for each type of user, as shown below:

$$\vec{p}_{user\_type} = \sum_i m_{user\_type\ i}\vec{v}_{usert\_type\ i} = \vec{p}_{user\_type\ 1} + \vec{p}_{user\_type\ 2} + \cdots + \vec{p}_{usert\_type\ n} = m_{usert\_type\ 1}\vec{v}_{user\_type\ 1} + m_{user\_type\ 2}\vec{v}_{user\_type\ 2} + \cdots + m_{user\_type\ n}\vec{v}_{user\_type\ n}$$

Equation 18

Where:

$\vec{p}_{user\_type}$: Quantity of motion of user type (pedestrian, bicycle or e-scooter).

$m_{user\_type\ i}$: Mass of user type (pedestrian i, bicycle i or e-scooter i).

$\vec{v}_{user_{type}i}$: velocity of user_type (pedestrian i, bicycle i or e-scooter i).

Using Eq. 19 we can calculate the velocity of the center of mass of a set of particles, which in this case are divided into pedestrians, bicycles and PMDs.

$$\overrightarrow{v}_{cm_{user\_type}} = \frac{\vec{p}_{user\_type}}{M_{user\_type}} \qquad \textit{Equation 19}$$

Where $user\_type$ = (pedestrians, bicycles or PMDs) and $M = m_1 + m_2 + \cdots + m_n$ is the total mass.

If we consider that all pedestrians have equal mass and equally for bicycles and e-scooters, we can reduce Equation 19 to the following expression:

$$\overrightarrow{v}_{cm_{user\_type}} = \frac{\sum_i \vec{v}_{user\_type\ i}}{n} \qquad \textit{Equation 20}$$

Where n is the number of pedestrians, bicycles or e-scooters.

A system of particles has a center of mass, the position vector of center of mass is determined by the weighted sum of their positions:

$$\vec{r}_{cm_{user\_type}} = \frac{m_1 r_1 + m_2 r_2 + \cdots + m_n r_n}{m_1 + m_2 + \cdots + m_n} = \frac{\sum_i \vec{r}_{user\_type\ i}}{n} \qquad \textit{Equation 21}$$

Where $\vec{r}_{cm_{user\_type}}$ is the position vector of center of mass by user type (pedestrian, bicycle or PMDs)

Finally, to summarize, based on the quantity of motion, the location $\vec{r}_{cm_{user\_type}}$ and velocity $\overrightarrow{v}_{cm_{user\_type}}$ of the center of mass can be determined by type of user. These variables will be calculated from a discretized space and then used as input variables for the training of a LSTM neural network as is explained in the following chapters.

4.1.3. Space discretization

In [61], an adaptation of the social force model for vehicles is proposed including a discretization of space used by private cars into 3 zones (1) Front area, (2) Body area and (3) Rear area as shown in the following figure.

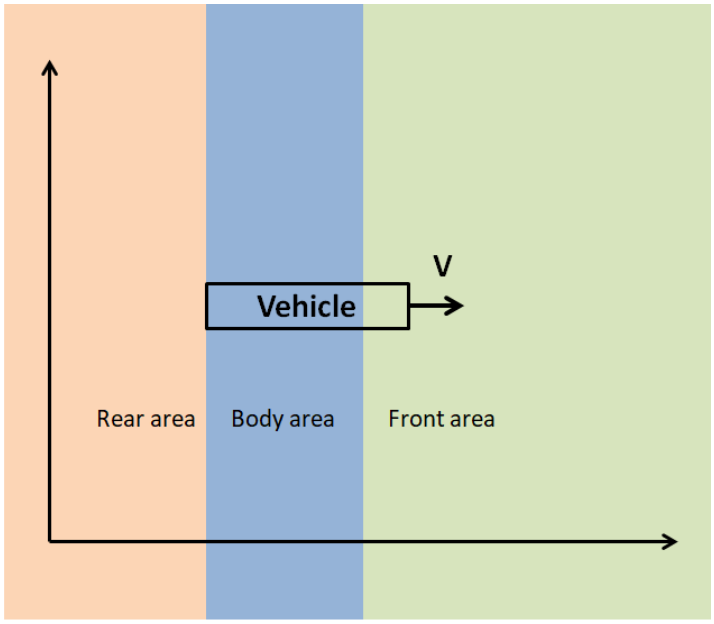

Figure 41. Discretization for simulation of vehicle proposed in [61]

The results show a great performance in reproducing the behavior of vehicles in the side and rear area of the vehicle.

Another proposal of spatial discretization can be found in [62]. Here a discretization is proposed in the zone delimited by the angle of view of a pedestrian. The proposed zones are (1) Intimate space, (2) Personal space, (3) Social space and (4) Public space as follow in Figure 42 .

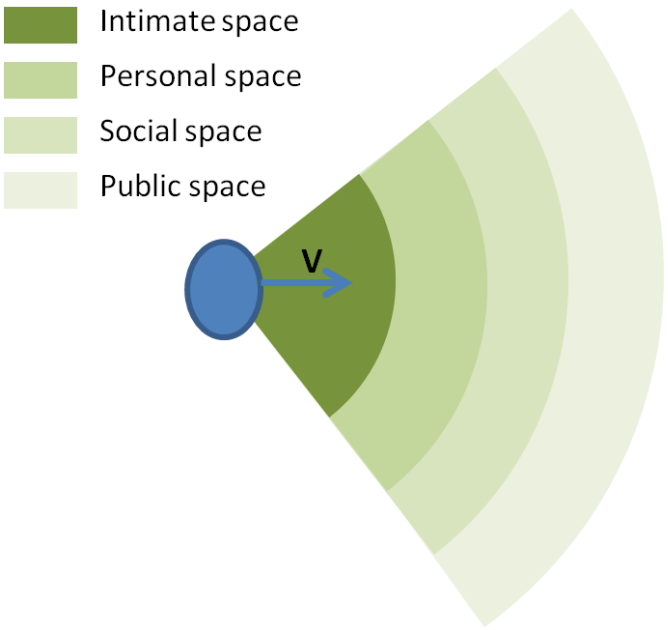

Figure 42. Discretization for simulation of pedestrian proposed in [62].

Based on [61] and [62], a discretization of the combination is proposed and explained below:

- Divide space into right and left zone of the road user to be modeled.
- Divide space into 3 zones (1) Front area, (2) Body area and (3) Rear area. Unlike that proposed in 5, the frontal area proposed for the model is bounded by the road user's angle of view.
- Divide the Front area into 4 zones (1) Intimate space, (2) Personal space, (3) Social space and (4) Public space.

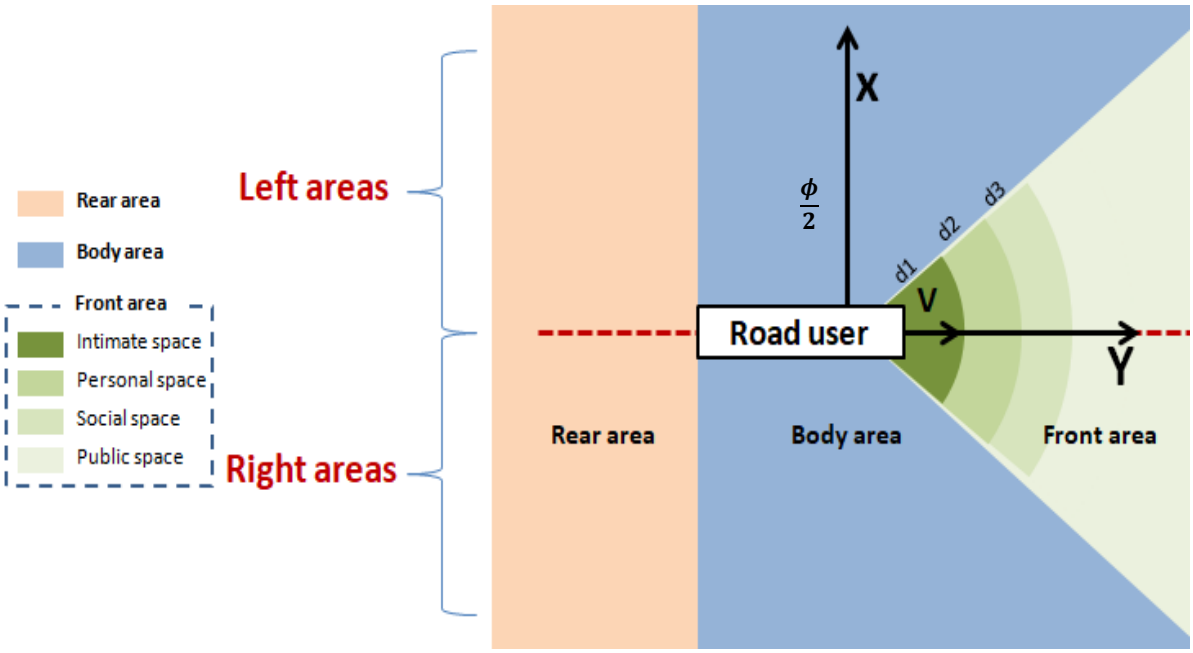

Figure 43. Discretization proposed

Figure 43 shows the proposed discretization of the space. The equations describing the proposed zoning are shown below. The origin for all coordinates is considered to be the eye of the rider of the non-controlled vehicle. The x-axis is considered parallel to the body of the vehicle to simplify calculations.

$$Rear\ area = \begin{cases} \xi_x < -d_r \\ \xi_y > 0, left\ area \\ \xi_y < 0,\ right\ area \end{cases} \qquad Equation\ 22$$

$$Body\ area = \begin{cases} -d_r < \xi_x < 0 \ \ if\ \xi_x < 0 \\ \frac{\xi_y}{\xi_x} > tan\left(\frac{\phi}{2}\right) \ if\ \xi_x > 0 \\ \xi_y > 0, \ left\ area \\ \xi_y < 0, \ right\ area \end{cases} \quad Equation\ 23$$

$$Intimate\ space = \begin{cases} \xi_x > 0 \\ \frac{\xi_y}{\xi_x} < tan\left(\frac{\phi}{2}\right) \\ 0 < \sqrt{{\xi_x}^2 + {\xi_y}^2} < d_1 \\ \xi_y > 0, \ left\ area \\ \xi_y < 0, \ right\ area \end{cases} \quad Equation\ 24$$

$$Personal\ space = \begin{cases} \xi_x > 0 \\ \frac{\xi_y}{\xi_x} < tan\left(\frac{\phi}{2}\right) \\ d1 \leq \sqrt{{\xi_x}^2 + {\xi_y}^2} < d_2 \\ \xi_y > 0, \ left\ area \\ \xi_y < 0, \ right\ area \end{cases} \quad Equation\ 25$$

$$Social\ space = \begin{cases} \xi_x > 0 \\ \frac{\xi_y}{\xi_x} < tan\left(\frac{\phi}{2}\right) \\ d_2 \leq \sqrt{{\xi_x}^2 + {\xi_y}^2} < d_3 \\ \xi_y > 0, \ left\ area \\ \xi_y < 0, \ right\ area \end{cases} \quad Equation\ 26$$

$$Public\ space = \begin{cases} \xi_x > 0 \\ \frac{\xi_y}{\xi_x} < tan\left(\frac{\phi}{2}\right) \\ d_3 \leq \sqrt{{\xi_x}^2 + {\xi_y}^2} \\ \xi_y > 0, \ left\ area \\ \xi_y < 0, \ right\ area \end{cases} \quad Equation\ 27$$

Where (ξ_x, ξ_y) is the coordinates of space discretization, d_r is the distance of the origin of coordinates to the rear end of the vehicle ϕ is the angle of view, $d_1, d_2\ and\ d_3$ are unknown parameters concerning the delimitation of the front area .

d_r is a parameter that can be obtained from observations, the values considered can be seen in Table 10. In the case of the distances, $d_1, d_2\ and\ d_3$ some values are shown in [62], but in the

present thesis, these distances were determined and adjusted from the optimal architecture of the neural network. The horizontal field of view ϕ of a person is 120°; however this field decreases as the person has a certain speed, that is why a value of 120° was initially assumed for the case of bicycles and e-scooters. This is a starting value to be confirmed by future analyses.

In addition, in each area portion shown in Figure 43, two subclasses are defined according to the direction of the road user:

- Subclass A, comprises all road users who have the same direction of traffic as the vehicle under analysis. In other words, the angle of the velocity vectors is less than 90°.
- Subclass B, comprises all road users who have the opposite direction of traffic compared to the vehicle under analysis. In other words, the angle of the velocity vectors is over 90°.

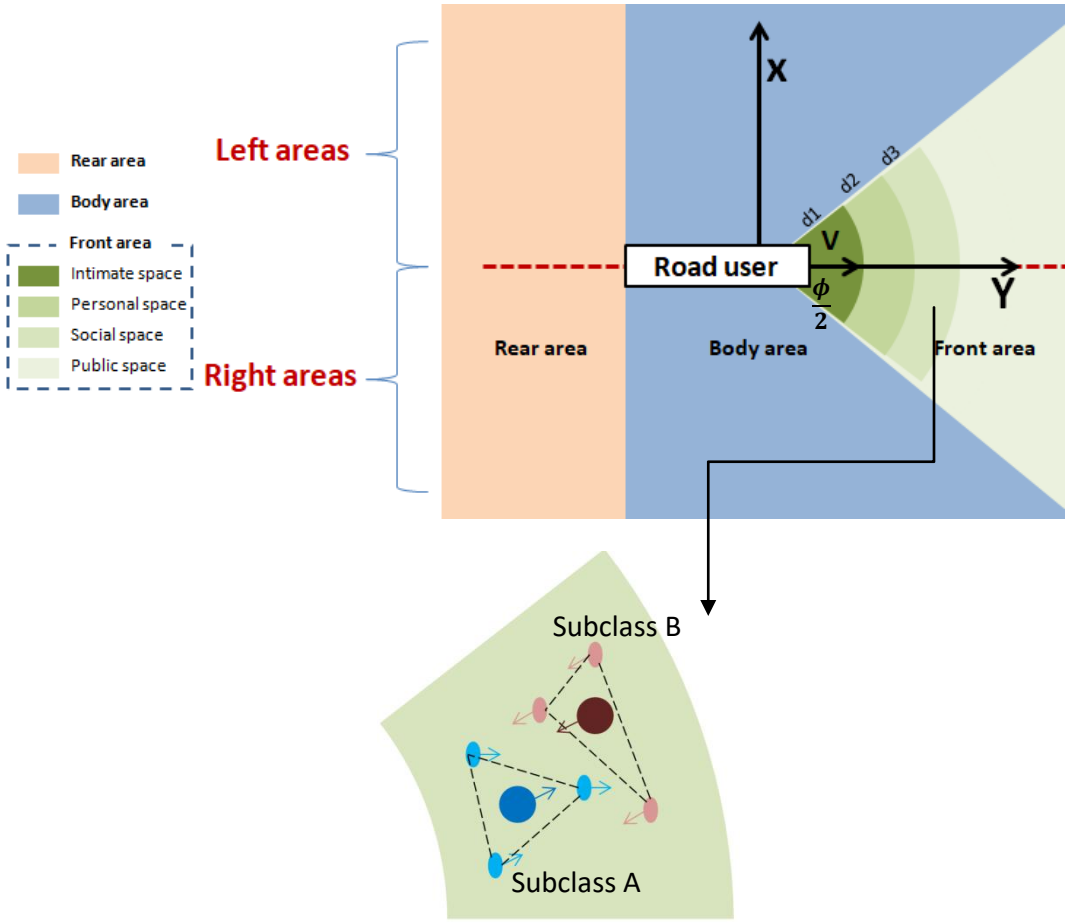

Figure 44. Sub-classification in each area with respect to velocity direction

4.1.4. Long Short Term Memory

The estimation of the proposed model was made using again an LSTM model. The neural network of type LSTM is a time series neural network, this means that from data of a state t, the neural network is able to predict a new state in $t+1$. Additionally, since this neural network has a short and long term memory at the training, it is possible to predict from n state sequences $t, t+1, \dots t+(n-1)$ the state $t+n$. In the proposed model, acceleration a at instant $t+n$ is predicted from accelerations of n-1 sequences. In addition, at each sequence variables are added to explain the different interactions to which the road user is exposed. The position at instant t+n is deduced from acceleration and previous position at instant t+n-1.

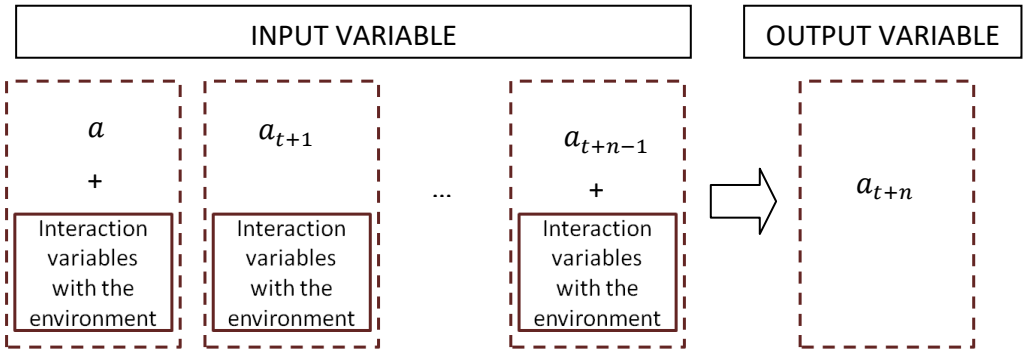

Figure 45. LSTM architecture

4.1.4.1. Input Variables

The variables with the interaction of the environment are calculated (i) for each type of road user (ii) in each area and (iii) at the center of mass. In each of the areas the following variables are generated:

Table 8. Input variables of LSTM

Nomenclature	Description
$X_{A_{S_{D_{rut}}}}$	X-Position of the center of mass of area A, side S, direction D and road user type rut.
$Y_{A_{S_{D_{rut}}}}$	Y-Position of the center of mass of area A, side S, direction D and road user type rut.
$Vx_{A_{S_{D_{rut}}}}$	X-Velocity of the center of mass of area A, side S, direction D and road user type (RUT).
$Vy_{A_{S_{D_{rut}}}}$	Y-Velocity of the center of mass of area A, side S, direction D and road user type (RUT).

Where:

$$A = \{Rear\ area, Body\ area,\ Intimate\ space,\ Personal\ space, Social\ Space, Public\ space\}$$

$$S = \{Left, Right\}$$

$$D = \{Same\ direction\ speed, Opposite\ direction\ speed\}$$

$$user\ type = \{pedestrian, bicycle, e-scooter\}$$

Depending on the number of combinations between the different options, a total of 288 input variables are obtained. However, to this number of variables it is necessary to add the variables of the road user to be modeled, that is, the road user $\{pedestrian, bicycle, e-scooter\}$, the velocity (Vx, Vy) and the acceleration (ax, ay) . There are then a total of 292 input variables.

4.1.4.2. Output Variables

The proposed output variable is the acceleration; this means that the acceleration (ax, ay) will be calculated from n data sequences containing the acceleration and variables that explain the interaction with the environment. From the acceleration it will be possible to calculate the velocity and the predicted position. There are then a total of 2 output variables.

4.1.4.3. Training and Architecture of LSTM

To determine the best architecture, the following values have been considered for each type of road user.

The distance sight could only concern the pubic space and is neglected here because it can be supposed not to influence immediate acceleration decisions as low speeds make it possible to react slower.

Table 9. Values of parameters of road user types in novel interaction pedestrian and PMDs model

Road user type	d_r	ϕ
Pedestrian	0.15 m	120 °
Bicycle	0.8 m	120 ° (starting value)
E-scooter	0.6 m	120 ° (starting value)

In Table 10, different architectures for the neural network are tested and based on the error results obtained for training process (75% of data) and validation (25% of data), the best architecture can be determined.

Table 10. Tested architectures with Root Mean Squared Error

Number of sequences	Architecture	RMSE of acceleration in training process (m/s2)	RMSE of acceleration in validation process (m/s2)
4	128 tanh 128 tanh 2 tanh	0,3828	0,4899
4	32 sigmoid 32 sigmoid 2 sigmoid	0,25	0,2975
4	64 tanh 64 tanh 2 tanh	0,3720	0,4092
4	32 tanh 32 tanh 2 tanh	0,28	0,3416
4	48 tanh 48 tanh 2 tanh	0,2731	0,3495
4	60 tanh 60 tanh 6 tanh 2 tanh	0,2598	0,3195
4	**128 tanh 128 tanh 6 tanh 2 tanh**	**0,2023**	**0,2629**
3	32 tanh 32 tanh 2 tanh	0,2635	0,2951
3	18 tanh 18 tanh 2 tanh	0,4155	0,4902
3	18 relu 18 tanh 2 tanh	0,4740	0,5830
3	18 relu 18 relu 2 relu	0,2478	0,3072
3	36 tanh 36 tanh 2 tanh	0,3134	0,3635
3	36 relu 36 relu 2 relu	0,3282	0,3938
1	16 tanh 16 tanh 2 tanh	0,3903	0,5073
1	18 relu 18 relu 2 relu	0,2478	0,3072

The best architecture is composed of 4 sequences with 292 neurons in the first layer (input variables), 128 neurons in the second layer with a tanh activation function, 128 neurons in the third layer with a tanh activation function, 6 neurons in the fourth layer with a tanh activation function and 2 neurons in the last layer with a tanh activation function. The value of RMSE of the acceleration in determined in 0.2023.

Once the best neural network architecture was determined, different boundaries for intimate space, personal space, social space and public space were tested to determine the best performance for each of the road users as shown in Table 11.

Table 11. Determination of range in meters? of each area

Road user type	Intimate space (m)	Personal space (m)	Social space (m)	Public space (m)	RMSE acceleration (m/s2)
Pedestrian	0 - 0,4	0,4 - 3	3 - 6	> 6	0,23
	0 - 0,4	**0,4 - 1,5**	**1,5 - 5**	**> 5**	**0,19**
	0 - 0,4	0,4 - 1,3	1,3 - 4,5	> 4,5	0,2
	0 - 0,4	0,4 - 1	1 - 4	> 4	0,21
Bicycle	0 - 0,4	0,4 - 3	3 - 6	> 6	0,41
	0 - 0,4	0,4 - 1,5	1,5 - 5	> 5	0,55
	0 - 0,4	0,4 - 2	2 - 6	> 6	0,39
	0 - 0,4	**0,4 - 2,2**	**2,2 - 7**	**> 7**	**0,38**
E-scooters	0 - 0,4	0,4 - 3	3 - 6	> 6	0,44
	0 - 0,4	0,4 - 1,5	1,5 - 5	> 5	0,56
	0 - 0,4	0,4 - 2	2 - 7	> 7	0,43
	0 - 0,4	**0,4 - 2,5**	**2,5 - 8**	**> 8**	**0,42**

Based on the values determined for pedestrians, we can compare with the values in [63] as shown in the table.

Table 12. Comparaison of values of areas

	Values suggest by [62] for pedestrian	Values finding with LSTM for pedestrian
Intimate space	0 to 0,46 m	0 to 0,40 m
Personal space	0,46 to 1,2 m	0,4 to 1,5 m
Social space	1,2 to 5,7 m	1,5 to 5,0 m
Public space	> 5,7 m	> 5,0 m

The suggested values show similar values to those found with the neural networks with a small difference in the personal space. However, only values similar to those suggested in [62] were tested, therefore, in future works optimization algorithms can be developed to determine these values more accurately. Additionally, values for bicycles and e-scooters were determined.

A variation of the angle of sight for e-scooters and bicycles was also obtained, giving the following results for the training process (75% of the data) and for the testing process (25% of the data)

Table 13. Determination of the most appropriate angle of sight for e-scooters and bicycles

Angle of sight	RMES of acceleration (m/s2) for e-scooter		RMES of acceleration (m/s2) for bicycle	
	Training	Testing	Training	Testing
120° (Initially angle)	0,38	0,42	0,45	0,51
110°	0,36	0,44	0,44	0,56
100°	**0,34**	**0,43**	0,44	0,56
90°	0,36	0,45	**0,43**	**0,52**
80°	0,36	0,43	0,44	0,55

The best performing angle for e-scooters has been determined to be 100° and for bicycles 90°. Of course, this topic needs to be further explored in order to obtain more robust conclusions.

Finally, the following table shows the values of the error rate for both acceleration and trajectories.

Table 14. RMSE for training and test

	RMSE of training process		RMSE of testing process	
	Acceleration(m/s2)	Trajectory(m)	Acceleration(m/s2)	Trajectory(m)
Pedestrian	0,19	0,034	0,24	0,043
E-scooter	0,34	0,031	0,43	0,041
Bicycle	0,43	0,033	0,52	0,038

4.1.5. Comparison with the social force model

Based on social force model and the neural network model, the following table was elaborated to compare the two models.

Table 15. Comparison of Social Force Model and LSTM model

	Social Force Model	LSTM Model for interactions between pedestrians and PMDs
Database	• Small, medium and large databases can be used. • Database from camera can be used.	• Large database model is needed. • Database from camera can be used
Model	• Model based on physics, so it is a general model that can be applied to different scenarios. • Simple to understand	• Model based on the database, after a training process; therefore, it is possible that the model can only be used in a specific case. • Complex to find the architecture of the neural network
Performance	• RMSE of the real and simulated trajectory in training process of 0,4 for pedestrian, 0,88 for e-scooters and 0,93 for bicycles. • RMSE of the real and simulated trajectory in test of 0,44 for pedestrian, 0,98 for e-scooters and 1,19 for bicycles	• RMSE of the real and simulated trajectory in training process of 0,134 for pedestrian, 0,131 for e-scooters and 0,133 for bicycles. • RMSE of the real and simulated trajectory in test of 0,143 for pedestrian, 0,141 for e-scooters and 0,138 for bicycles

The choice of which model to use for PMDs simulation in interactions with pedestrians depends on different aspects. LSTM seems to clearly outperform SFM as the RMSE is significantly lower for both training and testing. However, LSTM requires large datasets that are not always available and has not been tested in as many contexts and scenarios as the SFM and provides acceptable results in terms of coherence and error. In the case of the thesis, the model developed is in the context of an eco-neighborhood in which it is possible to install cameras and obtain a large database.

Consequently, neural networks based on LSTM are the best option because they offer better performance.

4.2. Interaction vehicle - PMDs

We propose a recurrent neural network (RNN), and more specifically a long and short term memory network (LSTM), to model the trajectory of a PMD. In this case the PMD type considered is bicycle. LSTM has connection and feedback and can process entire sequences of data (such as vehicle trajectories). LSTM networks are well suited to classify, process and make predictions based on time series data, because there can be shifts of unknown duration between important events.

4.2.1. Input variables

The proposed model is able to learn the displacement in the x and y direction of a vehicle (orange color in Figure 46 and Figure 47), interacting with other vehicles (blue color in Fig. 17 and 18). The InD dataset [58] was used to train the model. Each of the input variables are explained below :

- Gap distance between vehicles in the x-direction, (Figure 46). In case the vehicle does not exist, the entered gap x-distances takes the value of zero.

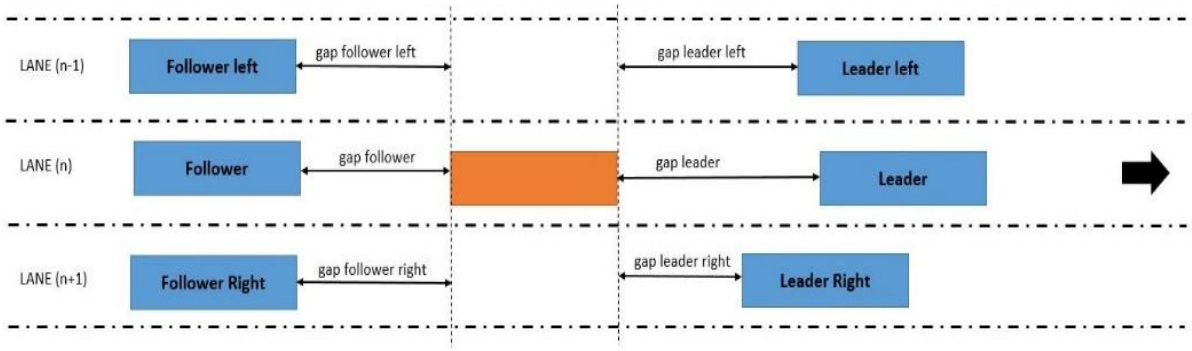

Figure 46. Gap distance in direction X. (1) Orange: Vehicle to be analyzed (2) Blue: Vehicles around.

.

- Gap distance between vehicles in the y-direction, (Figure 47). Similarly, if a second vehicle does not exist, a value of zero is assumed.

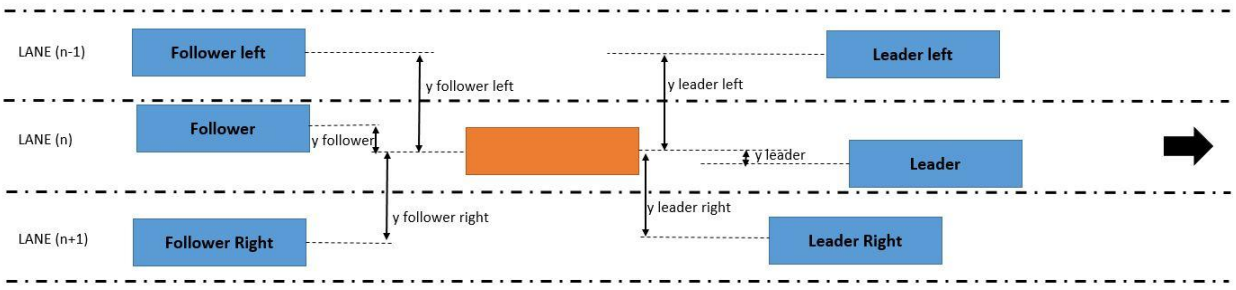

Figure 47. Gap distance in direction Y. (1) Orange: Vehicle to be analyzed (2) Blue: Vehicles around.

- The other variables used are the length and width of all vehicles and their speeds in x and y directions. Table 4 provides the notations used in the sub-indexes for each of the variables and Table 5 provides the necessary input variables for the model.

Table 16. Notation of the sub-indexes of the input variables

Notation	Description
fl	Vehicle in front and on the left side of the analyzed vehicle.
f	Vehicle in front of the analyzed vehicle.
fr	Vehicle in front and on the right side of the analyzed vehicle.
bl	Vehicle behind and on the left side of the analyzed vehicle.
b	Vehicle behind of the analyzed vehicle.
br	Vehicle behind and on the right side of the analyzed vehicle

Table 17. LSTM - Input variables

Name	Notation	Description
Vehicle exists	$b_{i_{fl}}, b_{i_f}, b_{i_{rl}}, b_{i_{bl}}, b_{i_b}, b_{i_{br}}$	Presence of the vehicle at instant i. 1 if the vehicle exist, 0 otherwise.
Vehicle length	$l_{i_{fl}}, l_{i_f}, l_{i_{rl}}, l_{i_{bl}}, l_{i_b}, l_{i_{br}}$	Length of each vehicle at instant i, including the vehicle to be modeled.
Vehicle width	$w_{i_{fl}}, w_{i_f}, w_{i_{rl}}, w_{i_{bl}}, w_{i_b}, w_{i_{br}}$	Width of each vehicle at instant i, including the vehicle to be modeled.

Gap distance x-axis	$gx_{i_{fl}}, gx_{i_f}, gx_{i_{rl}}, gx_{i_{bl}}, gx_{i_b}, gx_{i_{br}}$	Gap x-distance at instant i in relation to each vehicle. 0 if the vehicle does not exist.
Gap distance y-axis	$gy_{i_{fl}}, gy_{i_f}, gy_{i_{rl}}, gy_{i_{bl}}, gy_{i_b}, gy_{i_{br}}$	Gap y-distance at instant i in rela- tion to each vehicle. 0 if the vehicle does not exist.
Speed direction x-axis	$sx_{i_{fl}}, sx_{i_f}, sx_{i_{rl}}, sx_{i_{bl}}, sx_{i_b}, sx_{i_{br}}$	Speed in x direction at instant i for be modeled. 0 if the vehicle does not exist.
Speed direction y-axis	$sy_{i_{fl}}, sy_{i_f}, sy_{i_{rl}}, sy_{i_{bl}}, sy_{i_b}, sy_{i_{br}}$	Speed in y direction at instant i for be modeled. 0 if the vehicle does not exist.
Relative position	$Xi, Y\ i$	Relative position of the vehicle at instant i.

4.2.2. Outputs

The objective is to predict the trajectory in the next time step as a function of p previous scenarios, which we can express as follows:

$$f(E\ , E, E\&, \ldots, E) = XY, \quad where \quad k \in 1, 2, \ldots, N - 1\ ;$$

Where:

E_i : Scenario in frame i, which is composed of all the variables in Table 5

N : Number of frames

p : Number of previous scenarios

XY_i : Position x and y at the frame i

4.2.3. Architecture of LSTM

The architecture of an LSTM is composed of 3 parts (Figure 48): the forget gate, the update gate and the output gate. Each of these parts consists of a neural network, a sigmoid function and a

multiplier. The sigmoid function gives the balloon effect, i.e. the balloon is more ”open” for values closer to 1, and more ”closed” for values closer to 0.

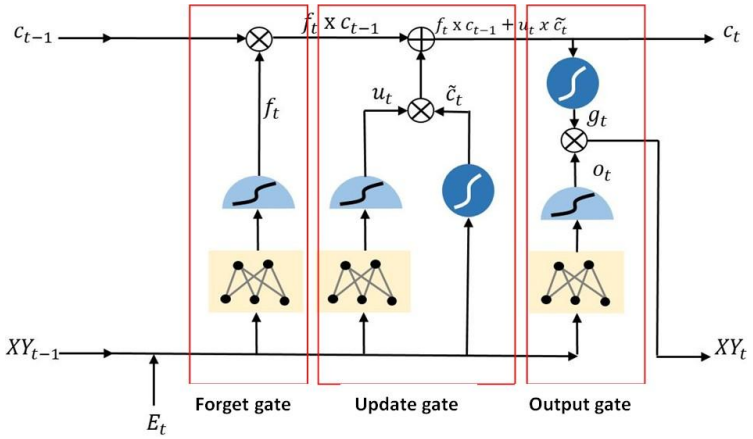

Figure 48. Architecture of the LSTM network.

The forget gate allows to decide which information to delete and therefore not to transmit. The output of this part is expressed in Eq. (11), where coefficients wf and bf are learned during the training process.

$$ft = sigmoidal(w_f\,[E_t, (x,y)_{(t-1)}] + bf\,), \qquad \text{Equation 28}$$

The update gate allow to update information. An initial process gives in Eq.

(12). Coefficients w_u and b_u are learned during training.

$$u_t = sigmoidal(w_u[E_t, (x,y)_{(t-1)}] + b_u) \qquad \text{Equation 29}$$

Once we have vector u_t, we generate a candidate vector in $c\tilde{}t = tanh[w_c[E_t, (x,y)_{(t-1)}] + b_c]$ Equation 30, where the coefficients w_c et b_c are learned during neural network training.

$$c\tilde{}t = tanh[w_c[E_t, (x,y)_{(t-1)}] + b_c] \qquad \text{Equation 30}$$

Then, we filter values $u_t * \vec{c}_t$, and the output of the update gate is added to the values of the forget gate partition. This allows us to generate the updated memory ct. To scale the values between 0 and 1, we use the $tanh(c_t)$ function.

$$c_t = f_t * c_{(t-1)} + u_t * \vec{c}_t \qquad \text{Equation 31}$$

The output gate is a filtered version of the cell, where coefficients w_0 and b_0 are learned during the training process.

$$o_t = sigmoidal(w_0[E(t-1), (x,y)_t] + b_0) \quad \text{Equation 32}$$

Finally, to calculate the new position of vehicle, we use the following equation:

$$(x,y)_t = o_t * tanh(c_t) \quad \text{Equation 33}$$

4.2.4. LSTM Training

For training we used the ”Adam” algorithm which is an optimization algorithm that can be applied instead of the classic stochastic gradient descent procedure to update iterative network weights based on training data. The interesting advantages of using Adam on non-convex optimization problems are explained by [75] and are shown below:

- Easy to implement.
- Computer efficient.
- Low memory requirements.
- Well suited for problems that are important in terms of data and/or parameters.
- Suitable for non-stationary objectives.
- Suitable for problems with very noisy and/or few gradients.

4.2.5. Training results and testing

In this part, we show the comparison of real trajectories to simulated trajectories with the neural network model (Figure 49). We observe that the Neural Network Model can describe the lateral behavior of a PMD. In addition, the error is very small (approximately 0,03 m), indicating that the model is capable of modeling the behavior of a PMD with respect to the vehicle’s surrounding conditions.

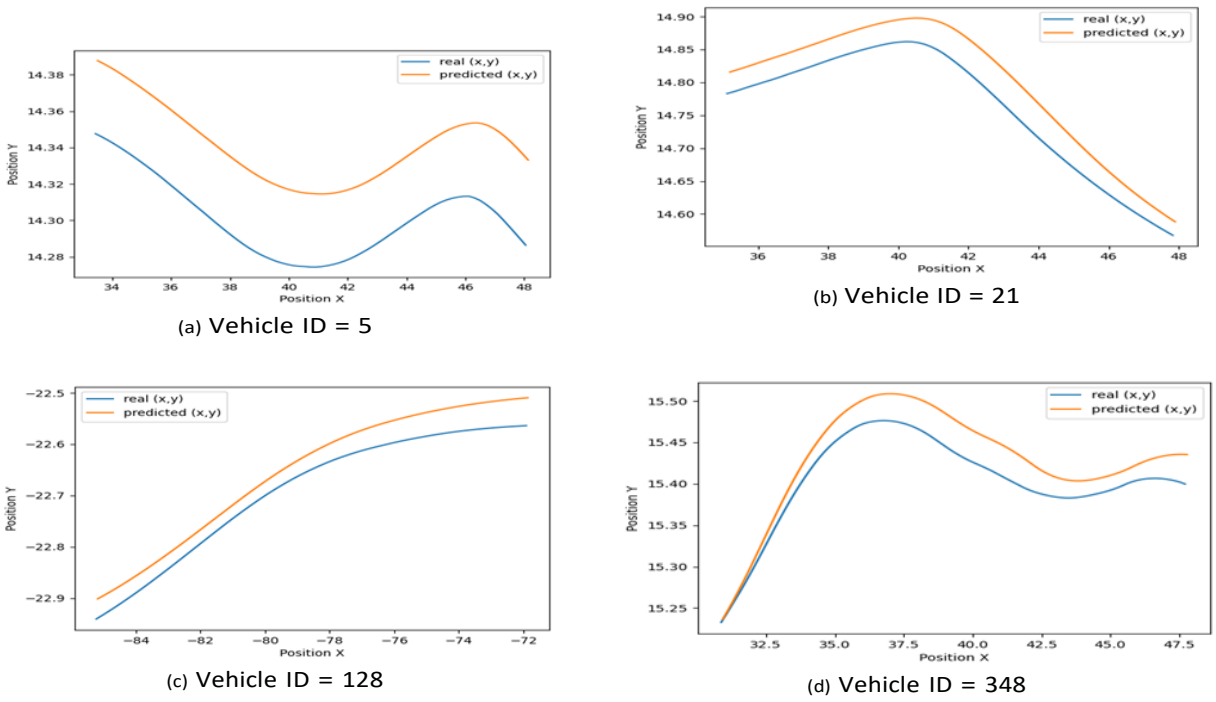

(a) Vehicle ID = 5

(b) Vehicle ID = 21

(c) Vehicle ID = 128

(d) Vehicle ID = 348

Figure 49. Real and predicted trajectories

We used 75% of the available 22,653 input data for training and the remaining 25% for testing. The function to be optimized in the training was RMSE, which was found at 0.03 m. Considering that obtaining the trajectories by image processing has an error of 0.10 m, we can conclude that the overall RMSE is of 0.13 m.

For the test the RMSE was found to be of 0.04 m. Considering that methodology by image processing has an error of 0.10 m, we can conclude that the RMSE is 0.14 m, for the test. RMSE is very low in both cases and slightly higher in the test case. We can thus conclude that the RNN can well describe PMD traffic at the microscopic level.

4.2.6. Comparison to car following model

Based on the car following model and the neural network model, the following table was elaborated to compare the two models.

Table 18. Comparison of Car Following Model and LSTM model

	Car Following	LSTM Model for interaction between vehicles and PMDs
Database	• Small, medium and large databases can be used. • Database from camera can be used.	• Large database model is needed. • Database from camera can be used
Model	• Model based on physics, so it is a general model that can be applied to different scenarios. • Simple to understand	• Model based on the database, after a training process; therefore, it is possible that the model can only be used in a specific case. • Complex to find the architecture of the neural network
Performance	RMSE of the real and simulated trajectory of 1.08m for the calibration process and 1.2m for the validation process.	RMSE of the real and simulated trajectory of 0.13m for the training process and 0.14m for the validation process.

The choice of which model to use for PMDs simulation in interactions with pedestrians depends on different aspects. LSTM seems to clearly outperform CFM as the RMSE is significantly lower for both training and testing. Additionally, in contrast to the CFM, the LSTM in this thesis have been trained to provide longitudinal and lateral behavior. However, LSTM requires large datasets that are not always available and has not been tested in as many contexts and scenarios as the CFM and provides acceptable results in terms of coherence and error. In the case of the thesis, the model developed is in the context of an eco-neighborhood in which it is possible to install cameras and obtain a large database. Consequently, neural networks based on LSTM are the best option because they offer better performance.

Chapter V

Conclusions and recommendations

5.1. Summary of findings

The present thesis aims to contribute in the analysis of the movement of PMDs in urban contexts in order to gain new insight into PMD characteristics and, thus, be capable of quantifying their impact on traffic flow and safety as well as on the environment. The main research questions concerned (i) the extent to which current traffic models are able to reproduce PMD movement and (ii) the possibilities of model enhancement. The research perimeter includes all PMDs but focuses on e-scooters and regular bikes. The scope of the analysis covers all urban infrastructure from pedestrianized areas and shared spaces to cycle paths and mixed traffic lanes. However, particular attention is given to the particularities of the LaVallée Eco-neighborhood in Southern Paris where a sustainable micromobility system is being designed for future residents and visitors. The scope of the thesis also addresses without differentiation all travel purposes, as well as free-floating and privately owned vehicles. The objective of the thesis was to develop and test a modeling framework suitable for PMD particularities going from (O1) literature review to comparative assessment (O2) and calibration of models (O3), and developments for enhancement (O4).

Chapter 1 addressed O1 and O2 where most popular traffic models were presented and assessed as to their suitability for PMDs. Among all microscopic models reviewed above, SFM seems to be the most prominent to use as a starting point for modeling the interactions between PMDs and pedestrians. The literature on microscopic traffic modeling for cars is more voluminous and well-established under different contexts and scenarios. The comparative assessment showed that the Krauss model seems to be more prominent for the modeling of interactions between PMDs and motorized vehicles for longitudinal behavior. In fact, it is an enhanced version of the Gipps model as it presents a better performance in the acceleration profile. It has seven calibration parameters which implies an acceptable computational cost. Nevertheless, more recent neural network models present important advantages that have not yet been considered for PMD modeling.

Chapter 3 addressed thesis objective O3. The models identified as most prominent through the literature review were calibrated for the case of PMDs. The Cross-Entropy method, a general Monte-Carlo type optimization technique, was used in this purpose. Results show acceptable errors in reproducing the dynamics of PMDs. When interacting with pedestrians, PMDs seem to have low

speeds (5.34 ±0.89 m/s), well below the legal limit of 6.9 m/s determined by French legislation. This finding indicates that PMDs can coexist in the same space with pedestrians. Also, the repulsive force of a PMD avoiding a pedestrian is greater than the force of a pedestrian avoiding a PMD. This finding suggests that PMD users are more careful in the presence of pedestrians. Turning to interactions with general traffic, it was found that maximum speed (28km/h) and minimum gap for e-scooters are close to the one of bicycles (20km/h). However, in terms of average acceleration and deceleration, e-scooters are closer to a motorcycle and a moped; probably due to electric propulsion. Overall, results suggest a certain hybrid behavior for PMDs in all cases.

Chapters 2 and 4 addressed O4. The former proposes new methodologies for data acquisition while the latter proposes new models for the representation of their movement at the microscopic scale. In the former case, various technologies were assessed and trajectory extraction from camera recordings was found to be the most suitable for immediate application. However, existing software tools do not cover PMDs. An ad hoc software, μ-scope, was developed and used for the purposes of the thesis. It is worth noting that essentially different databases were used in the analyses: 3 different countries, real world data from drones and from fixed point cameras, semi-controlled experiment on vehicle track. The diversity of case studies and fields ensures a significant level of generality of findings. Turning to new models, the thesis proposes two models: a first for the interactions between pedestrians and PMDs and a second for the interactions between general traffic and PMDs. The first model combines particle dynamics, social force modeling and neural networks for parameter estimation. Space is discretized and intimate, personal, social, public space are geometrically defined. The second model is an RNN with 8 input variables and the trajectories as output. In both cases, calibration and test were performed. The findings suggest that the novel models outperform the previous models as they provide more precise estimations and RMSE is significantly lower (by a factor of 7 to 10).

5.2. Recommendations

The comparative analysis of all models can provide a roadmap for future micromobility analysts from the academia or the industry. Table 17 presents a comparative table for all models analyzed in the present thesis.

Table 19. Comparison of all models

Advantage	Depends on the scenario	Disadvantage

Criteria	Interaction between pedestrians and PMD		Interaction between pedestrians and PMD	
	Social Force Model	**LSTM deep neural network-based model**	**Car Following Model Krauss**	**LSTM deep neural network-based model**
Database	• Small, medium and large databases can be used. • Database from camera can be used.	• Large database model is needed. • Database from camera can be used	• Small, medium and large databases can be used. • Database from camera can be used.	• Large database model is needed. • Database from camera can be used
Model	• Model based on physics, so it is a general model that can be applied to different scenarios. • Simple to understand	• Model based on the database, after a training process; therefore, it is possible that the model can only be used in a specific case. • Easy to find the architecture of the neural network	• Model based on physics, so it is a general model that can be applied to different scenarios. • Simple to understand	• Model based on the database, after a training process; therefore, it is possible that the model can only be used in a specific case. • Complex to find the architecture of the neural network
Calibration o training process	• Easy calibration process when there is not a large database. • Complex calibration process when the database is medium or large.	• Easy training even with a large database	• Easy calibration process when there is not a large database. • Complex calibration process when the database is medium or large.	Easy training even with a large database
Performance	• RMSE of the	• RMSE of the	RMSE of the real	RMSE of the real

	real and simulated trajectory in training process of 0,4 for pedestrian, 0,88 for e-scooters and 0,93 for bicycles. • RMSE of the real and simulated trajectory in test of 0,44 for pedestrian, 0,98 for e-scooters and 1,19 for bicycles	real and simulated trajectory in training process of 0,19 for pedestrian, 0,38 for e-scooters and 0,42 for bicycles. • RMSE of the real and simulated trajectory in test of 0,24 for pedestrian, 0,45 for e-scooters and 0,51 for bicycles	and simulated trajectory of 1.08m for the calibration process and 1.2m for the validation process.	and simulated trajectory of 0.13m for the training process and 0.14m for the validation process.

As can be seen in the table above, each model has its advantages and disadvantages. For our particular case at the scale of an eco-neighborhood in which it is planned to install cameras and through them obtain a large database, it is concluded that the most appropriate model is the LSTM models based on neural networks due to the following main reasons: (1) There is a particular case of behavior, i.e. the study area is delimited to an eco-neighborhood with particular behavioral characteristics. (2) The installation of cameras in the eco-neighborhood is planned, which will provide a large database. (3) The performance of LSTM models based on deep neural networks is better in relation to classical vehicular and pedestrian traffic models and (4) The database acquisition methodology using the µ-scope software was validated.

5.3. Main Contributions

The main contributions of this dissertation are listed as follows:

- Contribution 1: Development of a methodology to obtain data such as trajectories, speeds, accelerations of scenarios that include interaction of vehicles, pedestrians and PMDs through image processing techniques.

- Contribution 2. Development of a simulation methodology in free software that includes PMDs and with interaction of vehicles and pedestrians.
- Contribution 3. Determination of the Car Following Model parameters for PMDs
- Contribution 4. Determination of the Social Force Model parameters for PMDs
- Contribution 5. New traffic microsimulation model based on neural networks to simulate the interaction between PMDs and vehicles.
- Contribution 6. New traffic microsimulation model based on neural networks to simulate the interaction between PMDs and pedestrian.

5.4. Perspectives and further research

In the present thesis, different databases were used and the acquisition of a database in the eco neighborhood LaVallée was planned, however, this was not possible due to the extension of the deadlines for the implementation of the project and the arrival of the first residents. This is why one of the shortcomings of the proposed model and the proposed neuronal network architecture is based on data other than those of an eco neighborhood, but the methodology remains the same as that proposed in the thesis. That is why the following perspectives are proposed to extend this research work:

1. Through the proposed methodology, verify if the neural network architecture proposed in this thesis shows satisfactory results for the simulation of a database collected in an eco-neighborhood. This database can be acquired once the La Valle project is operational.
2. In the present work two models are presented separately, one for the simulation with vehicle interaction and the second model with pedestrian interaction, that is why future work could focus on the connection and integration of both models in open source traffic simulation software such as SUMO. This will allow simulating the behavior of PMDs in different scenarios under the same framework.

Further research works are currently in progress for submission, which are listed along:

1. Valero, Y., Christoforou, Zhao, Z., Farhi, N. Long Short-Term Memory Neural Networks for modeling shared spaces between pedestrians, vehicles and PMDS.

Bibliography

[1] K. Heineke, B. Kloss et D. Scurtu, «Micromobility: Industry progress, and a closer look at the case of Munich,» *McKinsey & Company,* 2019.

[2] Z. Christoforou, A. de Bortoli, C. Gioldasis et R. Seidowsky, «Who is using e-scooters and how? Evidence from Paris,» *Transportation Research Part D: Transport and Environment,* vol. 92, p. 102708, 2021.

[3] C. Gioldasis, Z. Christoforou et R. Seidowsky, «Risk-taking behaviors of e-scooter users: A survey in Paris,» *Accident Analysis & Prevention,* vol. 163, p. 106427, 2021.

[4] A. de Bortoli et Z. Christoforou, «Consequential LCA for territorial and multimodal transportation policies: Method and application to the free-floating e-scooter disruption in Paris,» *Journal of Cleaner Production,* vol. 273, p. 122898, 2020.

[5] A. M. P. Kalakoni, Z. Christoforou et N. Farhi, «A novel methodology for micromobility system assessment using multi-criteria analysis,» *Case Studies on Transport Policy,* 2022.

[6] N. Foissaud, C. Gioldasis, S. Tamura, Z. Christoforou et N. Farhi, «Free-floating e-scooter usage in urban areas: A spatiotemporal analysis,» *Journal of transport geography,* vol. 100, p. 103335, 2022.

[7] S. Bozzani-Franc, T. Leysens, A. l'Hostis, C. Soulas et B. Vulturescu, *Un Urbanisme orienté vers le rail illustré par le projet Bahn. Ville,* 2010.

[8] J. Bodgi, «Synchronisation piétons-structure: Application aux vibrations des passerelles souples,» 2008.

[9] S. Lemercier, «Simulation du comportement de suivi dans une foule de piétons à travers l'expérience, l'analyse et la modélisation,» 2012.

[10] C. W. Reynolds, «Flocks, herds and schools: A distributed behavioral model,» chez *Proceedings of the 14th annual conference on Computer graphics and interactive techniques*, 1987.

[11] G. Antonini, M. Bierlaire et M. Weber, «Discrete choice models of pedestrian walking

behavior,» *Transportation Research Part B: Methodological,* vol. 40, p. 667–687, 2006.

[12] T. Robin, G. Antonini, M. Bierlaire et J. Cruz, «Specification, estimation and validation of a pedestrian walking behavior model,» *Transportation Research Part B: Methodological,* vol. 43, p. 36–56, 2009.

[13] K. Nagel et M. Schreckenberg, «A cellular automaton model for freeway traffic,» *Journal de physique I,* vol. 2, p. 2221–2229, 1992.

[14] C. Burstedde, K. Klauck, A. Schadschneider et J. Zittartz, «Simulation of pedestrian dynamics using a two-dimensional cellular automaton,» *Physica A: Statistical Mechanics and its Applications,* vol. 295, p. 507–525, 2001.

[15] M. Schultz, S. Lehmann et H. Fricke, «A discrete microscopic model for pedestrian dynamics to manage emergency situations in airport terminals,» chez *Pedestrian and evacuation dynamics 2005*, Springer, 2007, p. 369–375.

[16] R.-Y. Guo et H.-J. Huang, «A modified floor field cellular automata model for pedestrian evacuation simulation,» *Journal of Physics A: Mathematical and Theoretical,* vol. 41, p. 385104, 2008.

[17] J. Van den Berg, M. Lin et D. Manocha, «Reciprocal velocity obstacles for real-time multi-agent navigation,» chez *2008 IEEE International Conference on Robotics and Automation*, 2008.

[18] S. J. Guy, J. Chhugani, C. Kim, N. Satish, M. Lin, D. Manocha et P. Dubey, «Clearpath: highly parallel collision avoidance for multi-agent simulation,» chez *Proceedings of the 2009 ACM SIGGRAPH/Eurographics Symposium on Computer Animation*, 2009.

[19] S. Paris, J. Pettré et S. Donikian, «Pedestrian reactive navigation for crowd simulation: a predictive approach,» chez *Computer Graphics Forum*, 2007.

[20] K. H. Lee, M. G. Choi, Q. Hong et J. Lee, «Group behavior from video: a data-driven approach to crowd simulation,» chez *Proceedings of the 2007 ACM SIGGRAPH/Eurographics symposium on Computer animation*, 2007.

[21] E. Ju, M. G. Choi, M. Park, J. Lee, K. H. Lee et S. Takahashi, «Morphable crowds,» *ACM Transactions on Graphics (TOG),* vol. 29, p. 1–10, 2010.

[22] C. Dias, M. Iryo-Asano, H. Nishiuchi et T. Todoroki, «Calibrating a social force based model for simulating personal mobility vehicles and pedestrian mixed traffic,» *Simulation Modelling*

Practice and Theory, vol. 87, p. 395–411, 2018.

[23] B. Kabalan, «Crowd dynamics: modeling pedestrian movement and associated generated forces,» 2016.

[24] D. Helbing et P. Molnar, «Social force model for pedestrian dynamics,» *Physical review E,* vol. 51, p. 4282, 1995.

[25] J. Erdmann, «SUMO's lane-changing model,» chez *Modeling Mobility with Open Data*, Springer, 2015, p. 105–123.

[26] S. Hochreiter et J. Schmidhuber, «Long Short-Term Memory,» *Neural Computation,* vol. 9, pp. 1735-1780, 1997.

[27] D. P. Kingma et J. Ba, «Adam: A method for stochastic optimization,» *arXiv preprint arXiv:1412.6980,* 2014.

[28] X. Huang, J. Sun et J. Sun, «A car-following model considering asymmetric driving behavior based on long short-term memory neural networks,» *Transportation research part C: emerging technologies,* vol. 95, p. 346–362, 2018.

[29] X. Chen, M. Treiber, V. Kanagaraj et H. Li, «Social force models for pedestrian traffic–state of the art,» *Transport reviews,* vol. 38, p. 625–653, 2018.

[30] D. Helbing, I. Farkas et T. Vicsek, «Simulating dynamical features of escape panic,» *Nature,* vol. 407, p. 487–490, 2000.

[31] R. Mah'd Alsaleh, «Development of a multi-agent based simulation model for cyclist-pedestrian interactions in shared spaces,» 2021.

[32] F. Zanlungo, T. Ikeda et T. Kanda, «Social force model with explicit collision prediction,» *EPL (Europhysics Letters),* vol. 93, p. 68005, 2011.

[33] J. Laufer et P. T. Planner, «Passenger and pedestrian modelling at transport facilities,» chez *2008 Annual AIPTM Conference. Perth, Australia*, 2008.

[34] X. Zhang, J. Sun, X. Qi et J. Sun, «Simultaneous modeling of car-following and lane-changing behaviors using deep learning,» *Transportation research part C: emerging technologies,* vol. 104, p. 287–304, 2019.

[35] A. Johansson, D. Helbing et P. K. Shukla, «Specification of the social force pedestrian model by evolutionary adjustment to video tracking data,» *Advances in complex systems,* vol. 10, p. 271–288, 2007.

[36] T.-C. Lee, J. W. Polak et M. G. H. Bell, «New approach to modeling mixed traffic containing motorcycles in urban areas,» *Transportation Research Record,* vol. 2140, p. 195–205, 2009.

[37] P. Hidas, «Modelling lane changing and merging in microscopic traffic simulation,» *Transportation Research Part C: Emerging Technologies,* vol. 10, p. 351–371, 2002.

[38] R. E. Chandler, R. Herman et E. W. Montroll, «Traffic dynamics: studies in car following,» *Operations research,* vol. 6, p. 165–184, 1958.

[39] Z. Christoforou, N. Farhi et Y. Valero, «Is the car-following model appropriate for the simulation of mixed traffic considering e-scooters?,» *Transport Research Arena 2020(Conference accepted),* 2020.

[40] V. Kanagaraj, G. Asaithambi, C. N. Kumar, K. K. Srinivasan et R. Sivanandan, «Evaluation of different vehicle following models under mixed traffic conditions,» *Procedia-Social and Behavioral Sciences,* vol. 104, p. 390–401, 2013.

[41] P. G. Gipps, «A behavioural car-following model for computer simulation,» *Transportation Research Part B: Methodological,* vol. 15, p. 105–111, 1981.

[42] P. Fan, J. Guo, H. Zhao, J. S. Wijnands et Y. Wang, «Car-Following Modeling Incorporating Driving Memory Based on Autoencoder and Long Short-Term Memory Neural Networks,» *Sustainability,* vol. 11, p. 6755, 2019.

[43] M. Li, F. Shi et D. Chen, «Analyze bicycle-car mixed flow by social force model for collision risk evaluation,» chez *3rd International Conference on Road Safety and Simulation*, 2011.

[44] K. I. Ahmed, «Modeling drivers' acceleration and lane changing behavior,» 1999.

[45] P.-T. De Boer, D. P. Kroese, S. Mannor et R. Y. Rubinstein, «A tutorial on the cross-entropy method,» *Annals of operations research,* vol. 134, p. 19–67, 2005.

[46] S. Krauß, «Microscopic modeling of traffic flow: Investigation of collision free vehicle dynamics,» 1998.

[47] U. Chattaraj, A. Seyfried et P. Chakroborty, «Comparison of pedestrian fundamental diagram

across cultures,» *Advances in complex systems,* vol. 12, p. 393–405, 2009.

[48] P. Fafoutellis, E. I. Vlahogianni et J. Del Ser, «Dilated LSTM Networks for Short-Term Traffic Forecasting using Network-Wide Vehicle Trajectory Data,» chez *2020 IEEE 23rd International Conference on Intelligent Transportation Systems (ITSC)*, 2020.

[49] J. Zhang, W. Klingsch, A. Schadschneider et A. Seyfried, «Ordering in bidirectional pedestrian flows and its influence on the fundamental diagram,» *Journal of Statistical Mechanics: Theory and Experiment,* vol. 2012, p. P02002, 2012.

[50] T. Toledo, H. N. Koutsopoulos et M. Ben-Akiva, «Integrated driving behavior modeling,» *Transportation Research Part C: Emerging Technologies,* vol. 15, p. 96–112, 2007.

[51] M. Treiber et A. Kesting, «Traffic flow dynamics,» *Traffic Flow Dynamics: Data, Models and Simulation, Springer-Verlag Berlin Heidelberg,* 2013.

[52] F. Li, S. Chen, X. Wang et F. Feng, «Pedestrian evacuation modeling and simulation on metro platforms considering panic impacts,» *Procedia-social and behavioral sciences,* vol. 138, p. 314–322, 2014.

[53] T.-Q. Tang, H.-J. Huang et H.-Y. Shang, «A dynamic model for the heterogeneous traffic flow consisting of car, bicycle and pedestrian,» *International Journal of Modern Physics C,* vol. 21, p. 159–176, 2010.

[54] J.-P. Jodoin, G.-A. Bilodeau et N. Saunier, «Urban tracker: Multiple object tracking in urban mixed traffic,» chez *IEEE Winter Conference on Applications of Computer Vision*, 2014.

[55] Y. Weng et T. Wu, «Car-following model of vehicular traffic,» chez *2001 International Conferences on Info-Tech and Info-Net. Proceedings (Cat. No.01EX479)*, 2001.

[56] Z. Christoforou, C. Gioldasis, Y. Valero et G. Vasileiou-Voudouris, «Smart Traffic Data for the Analysis of Sustainable Travel Modes,» *Sustainability,* vol. 14, 2022.

[57] S. Staacks, S. Hütz, H. Heinke et C. Stampfer, «Advanced tools for smartphone-based experiments: phyphox,» *Physics education,* vol. 53, p. 045009, 2018.

[58] J. Bock, R. Krajewski, T. Moers, S. Runde, L. Vater et L. Eckstein, «The inD Dataset: A Drone Dataset of Naturalistic Road User Trajectories at German Intersections,» chez *2020 IEEE Intelligent Vehicles Symposium (IV)*, 2020.

[59] R. Kimmel, «Fast marching methods for computing distance maps and shortest paths,» 1996.

[60] P. A. Lopez, M. Behrisch, L. Bieker-Walz, J. Erdmann, Y.-P. Flötteröd, R. Hilbrich, L. Lücken, J. Rummel, P. Wagner et E. Wießner, «Microscopic traffic simulation using sumo,» chez *2018 21st International Conference on Intelligent Transportation Systems (ITSC)*, 2018.

[61] Q. Yang, H. N. Koutsopoulos et M. E. Ben-Akiva, «Simulation laboratory for evaluating dynamic traffic management systems,» *Transportation Research Record,* vol. 1710, p. 122–130, 2000.

[62] P. Wang, «Understanding social-force model in psychological principles of collective behavior,» *arXiv preprint arXiv:1605.05146,* 2016.

[63] H. Wei, J. Lee, Q. Li et C. J. Li, «Observation-based lane-vehicle assignment hierarchy: microscopic simulation on urban street network,» *Transportation research record,* vol. 1710, p. 96–103, 2000.

[64] S. Wei-Guo, Y. Yan-Fei, W. Bing-Hong et F. Wei-Cheng, «Evacuation behaviors at exit in CA model with force essentials: A comparison with social force model,» *Physica A: Statistical Mechanics and its Applications,* vol. 371, p. 658–666, 2006.

[65] E. I. Vlahogianni et M. G. Karlaftis, «Testing and comparing neural network and statistical approaches for predicting transportation time series,» *Transportation research record,* vol. 2399, p. 9–22, 2013.

[66] F. Viti, B. Wolput, C. M. J. Tampère et P. Vandervelden, «Dynamic modeling of VISSIM's critical gap parameter at unsignalized intersections,» *Transportation Research Record,* vol. 2395, p. 12–20, 2013.

[67] Y. Valero, A. Antonelli, Z. Christoforou, N. Farhi, B. Kabalan, C. Gioldasis et N. Foissaud, «Adaptation and calibration of a social force based model to study interactions between electric scooters and pedestrians,» chez *2020 IEEE 23rd International Conference on Intelligent Transportation Systems (ITSC)*, 2020.

[68] (. U.S. Federal Highway Administration, «The Next Generation Simulation (NGSIM),» 2008.

[69] J. Treiterer et J. Myers, «The hysteresis phenomenon in traffic flow,» *Transportation and traffic theory,* vol. 6, p. 13–38, 1974.

[70] A. Smith, C. James, R. Jones, P. Langston, E. Lester et J. Drury, «Modelling contra-flow in crowd

dynamics DEM simulation,» *Safety Science,* vol. 47, p. 395–404, 2009.

[71] A. B. Siddique et others, «Modeling drivers' lateral movement behavior under weak-lane disciplined traffic conditions,» 2013.

[72] A. Seyfried, B. Steffen, W. Klingsch et M. Boltes, «The fundamental diagram of pedestrian movement revisited,» *Journal of Statistical Mechanics: Theory and Experiment,* vol. 2005, p. P10002, 2005.

[73] L. X. Nguyen, S. Hanaoka et T. Kawasaki, «Describing Non–Lane-Based Motorcycle Movements in Motorcycle-Only Traffic Flow,» *Transportation Research Record,* vol. 2281, pp. 76-82, 2012.

[74] T. V. Mathew, C. R. Munigety et A. Bajpai, «Strip-based approach for the simulation of mixed traffic conditions,» *Journal of Computing in Civil Engineering,* vol. 29, p. 04014069, 2015.

[75] T. V. Mathew, «Car following models,» *Transportation Systems Engineering,* vol. 14, p. 1–8, 2014.

[76] T. Lochrane, «A new multidimensional psycho-physical framework for modeling car-following in a freeway work zone,» 2014.

[77] Q. Liu, «A social force model for the crowd evacuation in a terrorist attack,» *Physica A: Statistical Mechanics and its Applications,* vol. 502, p. 315–330, 2018.

[78] C. Li, X. Jiang, W. Wang, Q. Cheng et Y. Shen, «A simplified car-following model based on the artificial potential field,» *Procedia engineering,* vol. 137, p. 13–20, 2016.

[79] J.-P. Lebacque, «First-order macroscopic traffic flow models: Intersection modeling, network modeling,» chez *Transportation and Traffic Theory. Flow, Dynamics and Human Interaction. 16th International Symposium on Transportation and Traffic TheoryUniversity of Maryland, College Park*, 2005.

[80] P. A. Langston, R. Masling et B. N. Asmar, «Crowd dynamics discrete element multi-circle model,» *Safety Science,* vol. 44, p. 395–417, 2006.

[81] T. I. Lakoba, D. J. Kaup et N. M. Finkelstein, «Modifications of the Helbing-Molnar-Farkas-Vicsek social force model for pedestrian evolution,» *Simulation,* vol. 81, p. 339–352, 2005.

[82] S. Krauß, P. Wagner et C. Gawron, «Metastable states in a microscopic model of traffic flow,» *Physical Review E,* vol. 55, p. 5597, 1997.

[83] S. Jackson, L. F. Miranda-Moreno, P. St-Aubin et N. Saunier, «Flexible, mobile video camera system and open source video analysis software for road safety and behavioral analysis,» *Transportation research record,* vol. 2365, p. 90–98, 2013.

[84] W. Huang, M. Fellendorf et R. Schönauer, «Social force-based vehicle model for two-dimensional spaces,» chez *TRB Annual Meeting*, 2012.

[85] R. Herman et R. B. Potts, «Single lane traffic theory and experiment,» 1959.

[86] W. Helly, «Simulation of bottlenecks in single-lane traffic flow,» 1959.

[87] T. George Oketch, «New modeling approach for mixed-traffic streams with nonmotorized vehicles,» *Transportation research record,* vol. 1705, p. 61–69, 2000.

[88] M. de la Transition écologique et solidaire, «LOI n° 2019-1428 du 24 décembre 2019 d'orientation des mobilités.,» *Journal Officiel de la République Française,* vol. 0299, 2019.

[89] M. Aron, «Car following in an urban network: simulation and experiment,» chez *Proceedings of Seminar D, 16ˆ< th> PTRC Meeting, 1988*, 1988.

Annex:

Test of µ-scope with CEREMA[4] data

In the present thesis, a test of the u-scope software was realized with CEREMA. The results interface as well as the validation realized by CEREMA is presented below.

Figure 50, shows the u-scope software interface where the location of the project under analysis can be observed.

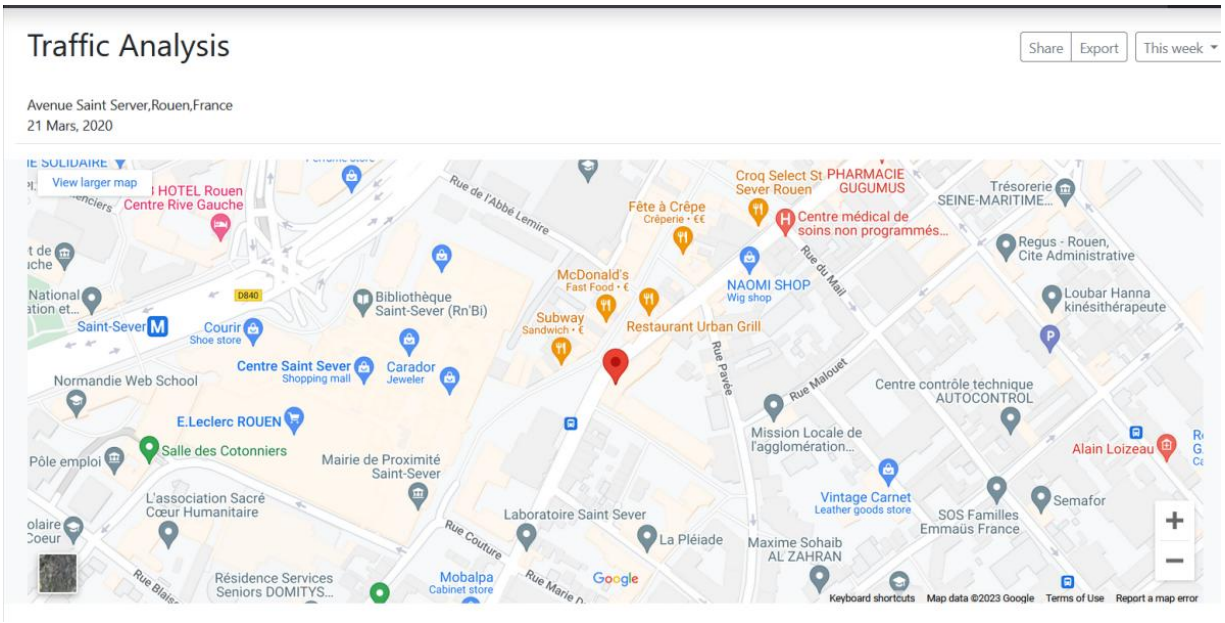

Figure 50. µ-scope software, localization of the project under analysis

Figure 51, shows the u-scope software interface where a frame of the video under analysis can be observed on the left and on the right an orthophoto with real measurements of the area under analysis.

[4] is the major French public agency for developing public expertise in the fields of urban planning, regional cohesion and ecological and energy transition

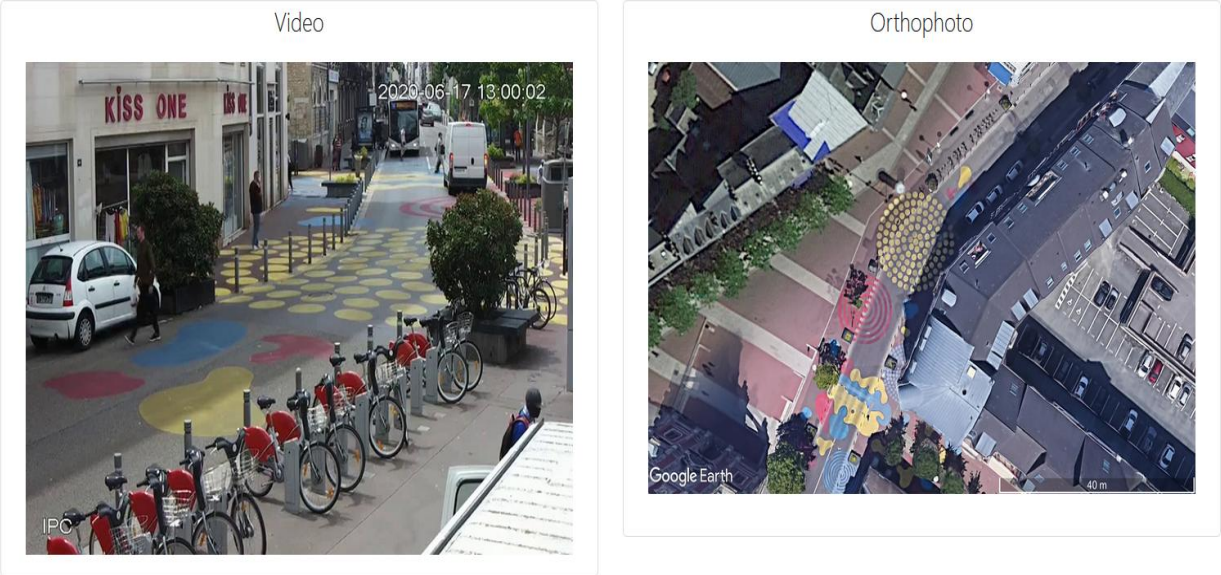

Figure 51. µ-scope software, video frame and orthophoto of the analysis area

Figure 52 shows the u-scope software interface where the vehicle counts classified every 5 minutes during a half-hour period are observed. It is important to note that the counting interval is configurable, i.e. the counts can be displayed at any desired time interval. The types of vehicles counted are: bicycle, bus, car, e-scooter, motorcycle, pedestrian and truck.

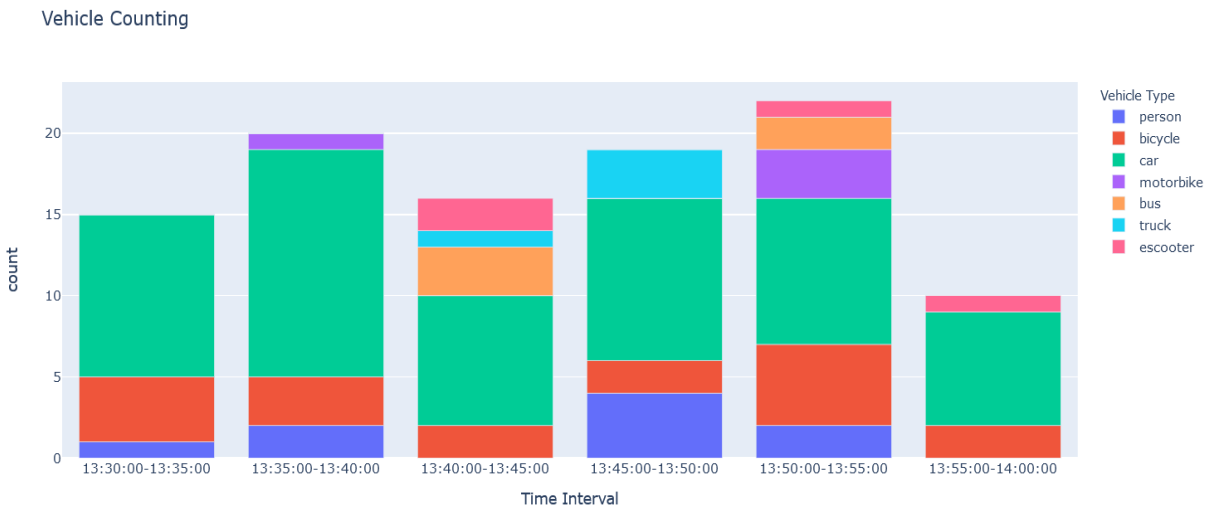

Figure 52. µ-scope software, Vehicle counts each 5 minutes

Figure 53, show the u-scope software interface where the vehicle counts classified every 5 minutes during a half-hour period are observed in format of table.

Traffic Count

Time Interval	bicycle	bus	car	escooter	motorbike	person	truck
13:30:00-13:35:00	4	0	10	0	0	1	0
13:35:00-13:40:00	3	0	14	0	1	2	0
13:40:00-13:45:00	2	3	8	2	0	0	1
13:45:00-13:50:00	2	0	10	0	0	4	3
13:50:00-13:55:00	5	2	9	1	3	2	0
13:55:00-14:00:00	2	0	7	1	0	0	0

Figure 53. µ-scope software, Vehicle counts each 5 minutes in table

Figure 54, shows the u-scope software interface where the trajectories of the vehicles after processing can be observed.

Figure 54. µ-scope software, Vehicle trajectories after processing

Figure 55, shows the real speed measured by vehicle type. The graphic allows us to observe the mean speed, and the standard deviation.

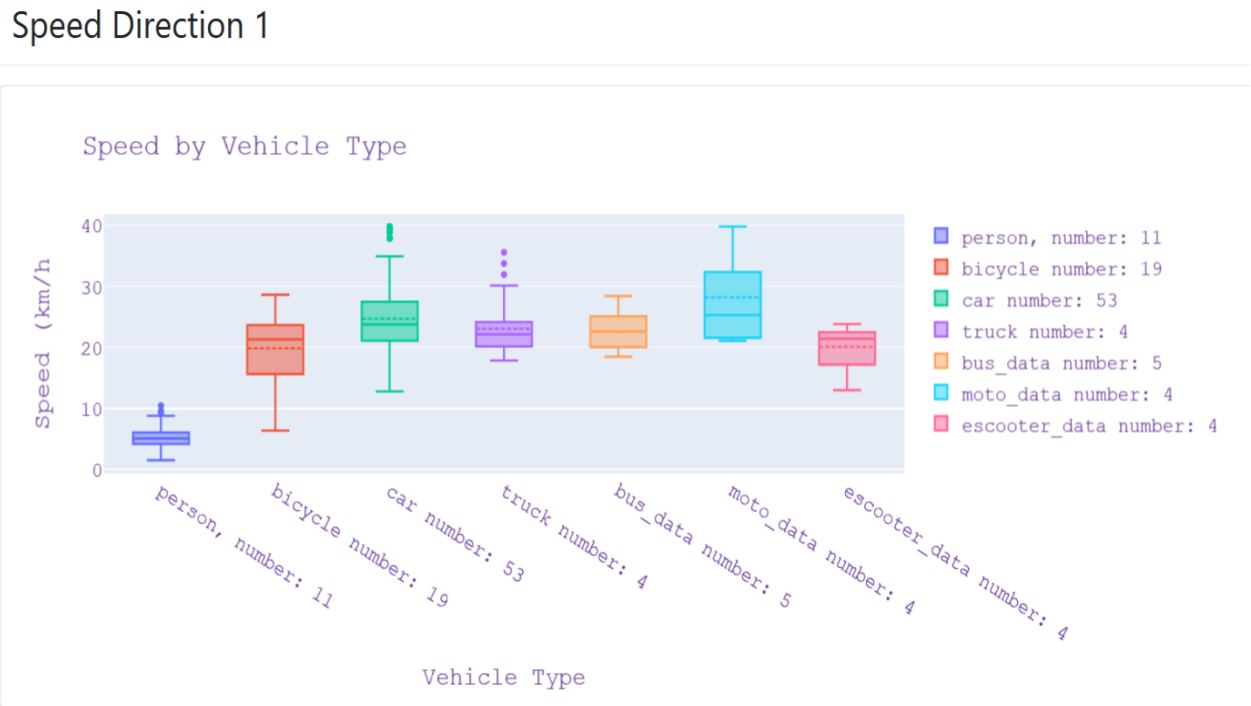

Figure 55. µ-scope software, Speed results, by vehicle type

In Figure 56 the results of detection and tracking by type of vehicle are shown. As can be seen in the Figure, each road user is represented by an ID and is classified as car, pedestrian, bicycle, e-scooter, bus, truck, bus, truck and bus.

The results are exported in the form of a video and a sql database, which contains the following information: position, velocity, acceleration and typology at each time instant.

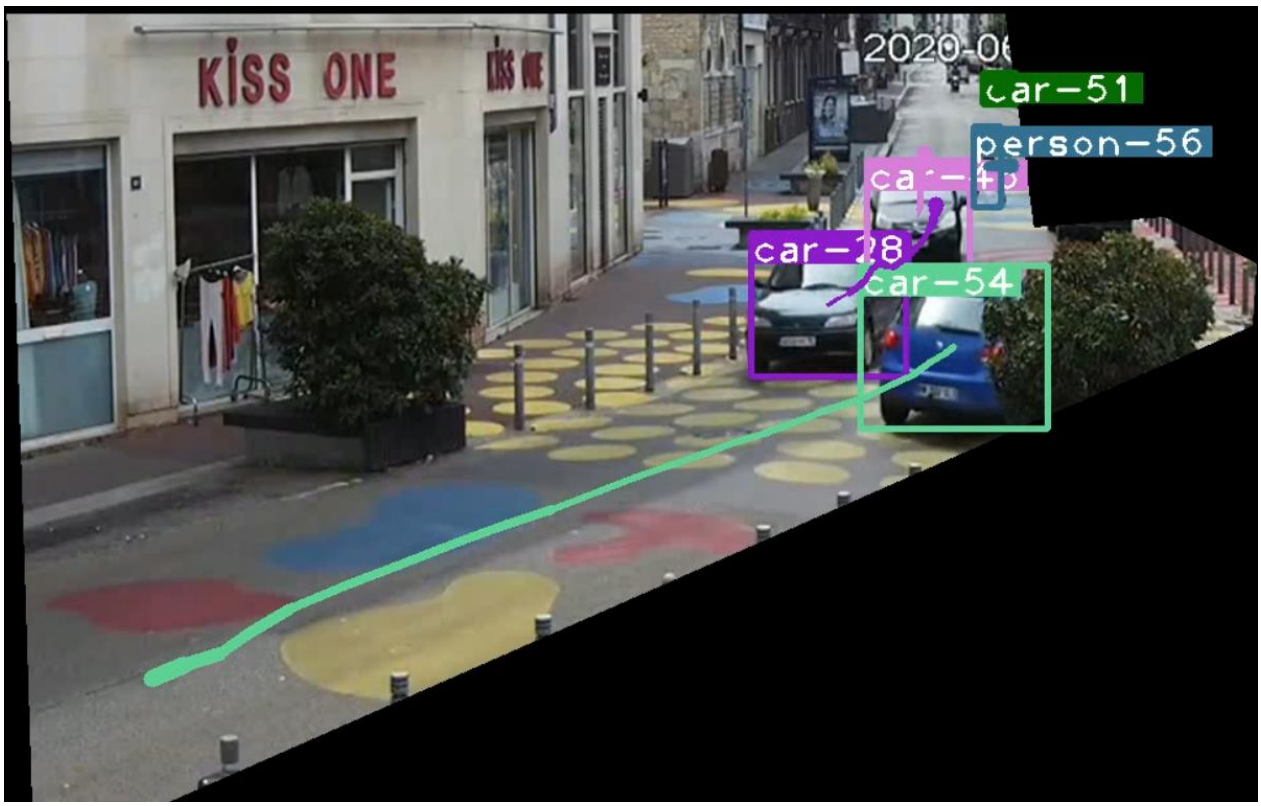

Figure 56. u-scope software detection and tracking results

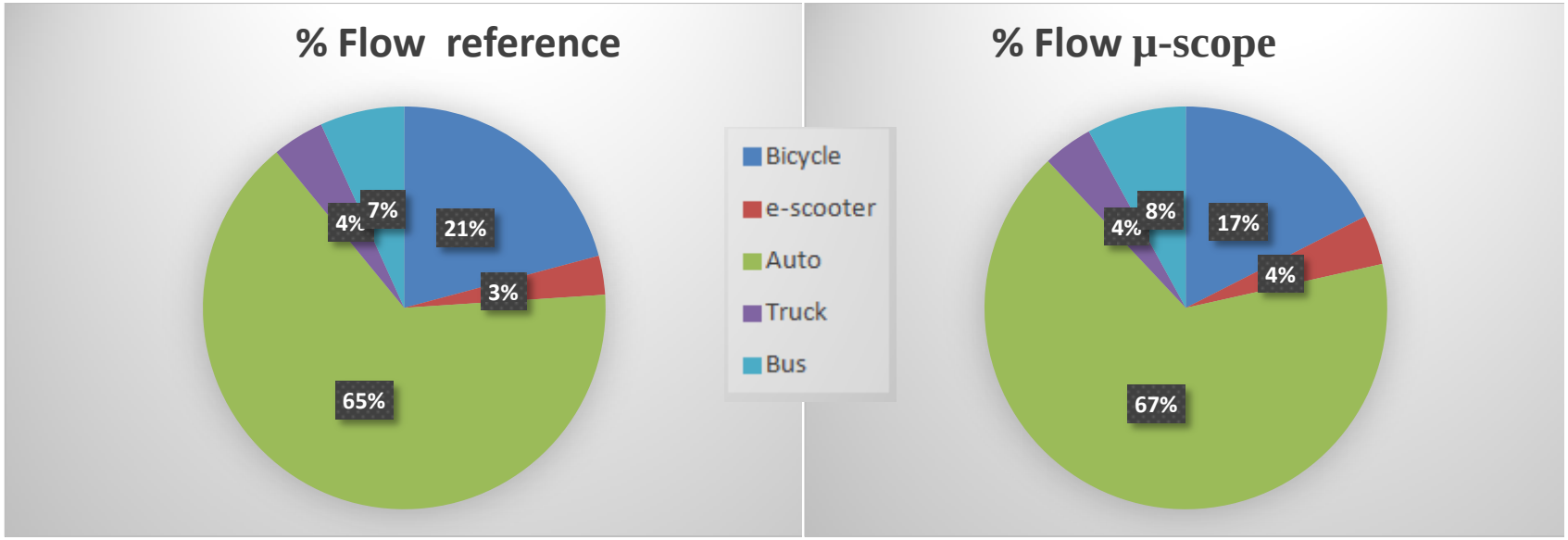

Figure 57. Comparison of u-scope with real data

The Figure 57, shows a comparison of the percentage of flow by vehicle type from the µ-scope results and real results. The results clearly show a good performance of the µ-scope software.

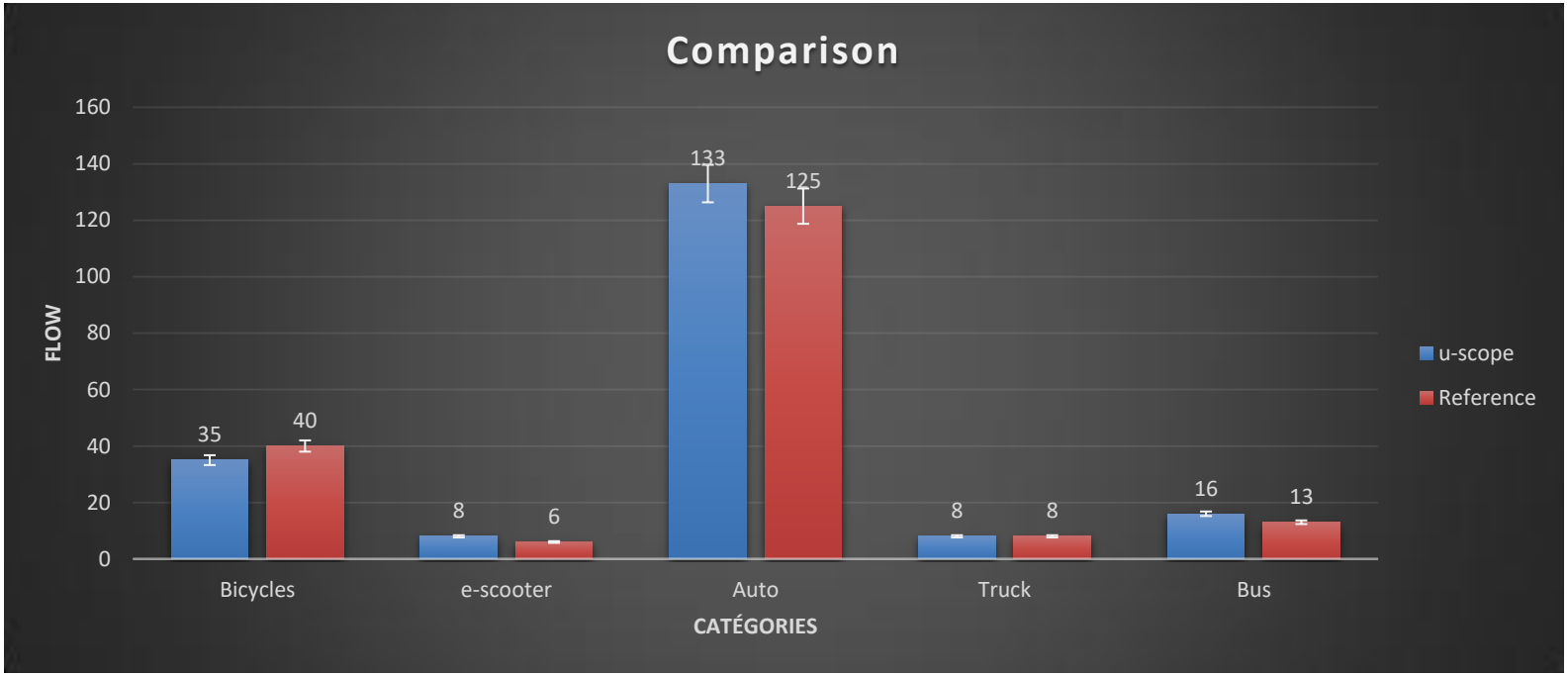

Figure 58. Comparison bar of u-scope with real data

The Figure 58, shows a comparison of the flow by vehicle type from the µ-scope results and real results. The results clearly show a good performance of the µ-scope software. This performance has allowed the use of the software in this thesis.